Universidade de São Paulo
Instituto de Física

Deformações: no espaço de configuração, no espaço de gauge e algébricas

Celso L. Lima

Submetido ao Instituto de Física da Universidade de São Paulo como parte dos requisitos para obtenção do título de Livre Docente

São Paulo - 1999

Deformações: no espaço de configuração, no espaço de gauge e algébricas

Celso L. Lima

ERRATA:

Pag.	Parágr.[1)]	Linha[2)]	Consta	Deveria ser
1	2	5↓	elemento de ligação a minha	elemento de ligação era a minha
1	3	2↑	contém	contêm
2	1	2↓	ao fim	no fim
2	2	1↓	reportado aqui, não constitue	reportado aqui não constitui
2	2	7↓	não foram incluidos [6,7,8]	não foram incluídos [6,7,8]
2	nota	3↑	núcleon-núcleon, fez-se	núcleon-núcleon fez-se
4	1	7↑	deformaç ão	deformação
4	2	3↓	tem se	tem-se
5	4	3↓	atrativos motivadores do motivaram seu	atrativos motivadores do seu
6	2	2↑	premio	prêmio
6	nota	1↑	nuclear coletiva, pode ser	nuclear coletiva pode ser
9	1	2↓	pode ser consertado	pode ser consertada
13	3	4↑	esperado do op- (erador)	esperado do ope- (rador)
13	2	2↓	pode a alterar funções	pode alterar as funções
16	6	1↓	sucesso, tem uma	sucesso, têm uma
16	6	2↓	não contém os	não contêm os
21	1	3↓	vale de estabil- (idade)	vale de estabi- (lidade)
21	1	2↓	campo médo	campo médio
30	3	1↓	interessante para a de- (scrição)	interessante para a des- (crição)
30	4	4↑	modelos e aprox- (imações)	modelos e aproxi- (mações)
32	4	2↑	Nambu-jona-Lasinio	Nambu-Jona-Lasinio
34	nota	1↓	refer- (ência)	referên- (cia)
34	nota	1↑	mas	mais
35	2	2↓	fermionico com dois apenas	fermiônico com apenas dois
37	1	1↓	ex- (igem)	exi- (gem)
37	1	1↑	sistema levando, neste caso,	sistema, levando, neste caso,
40	1	1↓	Pessoalmente porém, creio o modo	Pessoalmente porém, creio que o modo

[1)] Os parágrafos são contados sempre de cima para baixo; parágrafos que têm início na página anterior são incluídos na contagem.

[2)] O símbolo ↑ (↓) indica contagem, em um dado parágrafo, de baixo para cima (cima para baixo).

ÍNDICE

1 Introdução 1

2 Deformação nuclear 4
- 2.1 Introdução . . . 4
- 2.2 Motivação científica . . . 5
- 2.3 Partícula independente em potenciais esféricos ou deformados . . . 6
  - 2.3.1 Correlações de emparelhamento . . . 7
- 2.4 Modelo de partícula(s) + caroço coletivo . . . 9
- 2.5 Movimento de partícula independente em um potencial em rotação 13
- 2.6 Modelo com projeção em momento angular e a transição de forma prolato-oblato . . . 16
- 2.7 Sumário . . . 18

3 BCS e núcleos exóticos 21
- 3.1 Introdução . . . 21
- 3.2 Motivação Científica . . . 22
- 3.3 Emparelhamento e BCS . . . 22
- 3.4 Movimento coletivo de emparelhamento . . . 24
- 3.5 ^{11}Li e BCS . . . 26
- 3.6 Sumário . . . 27

4 Álgebras e deformações 29
- 4.1 Introdução . . . 29
- 4.2 Motivação científica . . . 30
- 4.3 Álgebras deformadas: algumas aplicações . . . 30
  - 4.3.1 Física nuclear e molecular . . . 31
  - 4.3.2 Transições de fase: Lipkin, BCS e Nambu-Jona-Lasinio . . . 32
- 4.4 Sumário . . . 36

5 Comentários finais 39

Resumo

É apresentada uma revisão dos diversos contextos em que o conceito de deformação aparece em física nuclear. Propriedades de núcleos em rotação, de núcleos exóticos leves e de sistemas na região de transição de fase serão discutidos tendo como fio condutor a idéia de deformação em diversas manifestações: no espaço de configuração, no espaço de gauge e na álgebra.

Abstract

A review is presented on the different contexts the deformation concept appears in nuclear physics. Properties of rotational nuclei, light exotic nuclei and systems undergoing phase transition are discussed having the idea of deformation as a conducting line, in its different manifestations: in the configuration space, in the gauge space, and in the algebra.

1. Introdução

O que se pretende neste texto é colocar em perspectiva minha contribuição científica ao longo dos últimos anos. A escolha de um tema comum a esses trabalhos foi difícil[1], pois a linha conectando-os é por vezes tênue e espero ter tido sucesso ao explicitá-la. Visando simplificar a tarefa, achei conveniente limitar a cinco anos o período a ser revisado.

Definido o período, resta o problema de encontrar a linha diretriz que deveria servir de guia para a apresentação; o uso do "encontrar" é adequado, na medida em que não houve, na minha carreira, uma linha pré-determinada de atuação, mas sim, os diversos trabalhos foram se sucedendo, em temas de pesquisa distintos, onde o elemento de ligação a minha experiência prévia, não havendo um problema central que norteasse a atuação. Ocorreu-me, entretanto, algo que talvez pudesse servir de fio condutor: o recorrente aparecimento, por vezes fugaz, por vezes explícito, da idéia de deformação ao longo da minha carreira científica.

Na verdade, meu doutoramento foi sobre a descrição do fenômeno do *back-bending* em núcleos transicionais, significando que a física de sistemas nucleares deformados acompanha-me desde então. Pareceu-me portanto bastante adequado colocar como primeiro capítulo desta revisão, aquele contendo uma discussão dos fenômenos ligados à alteração da forma nuclear devido à rotação e reportar os dois trabalhos nesse assunto que ficaram contidos no período de cinco anos escolhido. Em seguida, no Capítulo 3, passo à apresentação das minhas contribuições ao problema da estrutura de núcleos exóticos leves; aqui, alguma ginástica teve que ser feita para inserir esses trabalhos no tema escolhido. É discutida no Capítulo 4 a aplicação de álgebras deformadas à física de muitos corpos; finalmente, no Capítulo 5, alguns comentários encerram esta revisão. Os três apêndices colocados no fim do texto contém cópias dos meus trabalhos que serviram de referência para a elaboração de cada um dos capítulos.

Tentei escrever os diversos capítulos de modo que cada um deles fosse o mais independente possível dos demais, mesmo que o preço a ser pago fosse o de rea-

[1]Na XXI Reunião de Trabalho sobre Física Nuclear no Brasil, fui convidado a apresentar um relato das atividades dos teóricos do IFUSP. Dei à minha palestra um sub-título, "Missão Impossível", e devo confessar que, guardadas as devidas proporções, em alguns momentos senti-me tentado a apensar o mesmo sub-título a este trabalho de revisão.

presentar a discussão de certos tópicos; consistentemente, optei por incluir a bibliografia pertinente ao fim de cada um deles, ainda que pudessem ocorrer repetições.

O que está reportado aqui, não constitue a totalidade da minha atividade científica mais recente. Tivessem sido escolhidos os últimos dez anos para relatar, meus trabalhos sobre forças de van der Waals de cor [1, 2], flutuações estatísticas na transição caos-ordem [3, 4] ou efeitos da troca de dois píons no espalhamento αN periférico [5] seriam deixados de lado por não se enquadrarem no tema escolhido[2]; limitando a "janela observacional" aos cinco anos mais recentes, vários trabalhos também não foram incluidos [6, 7, 8], ainda que pudessem ser considerados como representantes adequados da minha contribuição ao tema da tese, pois sua discussão demandaria várias páginas adicionais, mas, inevitavelmente, referências acabaram sendo feitas a eles ao longo do texto. Optei também por concentrar a revisão apenas em trabalhos já publicados; não obstante, serão encontradas citações incidentais a trabalhos que estão ainda em fase final de elaboração.

Os trabalhos sumarizados foram fruto de proveitosas colaborações com vários outros pesquisadores; por isso, algumas palavras específicas de agradecimento são adequadas.

A retomada do meu envolvimento com a física de altos spins, ocorrida alguns anos após o doutoramento, deveu-se essencialmente à interação com o Grupo de Espectroscopia γ do Laboratório Pelletron. À demanda e ao continuado estímulo dos meus colegas experimentais devo a manutenção do meu trabalho nesse assunto; espero que essa colaboração tenha sido para eles tão frutífera e interessante quanto foi para mim. Cabe aqui um agradecimento todo especial à Ewa Cybulska, coração e alma do Grupo γ.

Ao meu amigo de longa data Mauro Kyotoku, pelas conversas estimulantes, pelo entusiasmo e por dividir generosamente comigo sua forma não convencional de ver problemas científicos.

Aos meus "cúmplices" no assunto de álgebras deformadas, Diógenes Galetti e Bruto Pimentel, ambos também amigos antigos, pelo muito que aprendemos juntos e pelas longas conversas sobre os mais diversos assuntos que tive a oportunidade de entabular com eles.

E não seria completo e muito menos justo, se não estendesse os agradecimentos aos meus estudantes. Ettore Baldini Neto, Varese S. Timóteo e Leandro Tripodi; bastante deles está também contido nas páginas seguintes.

[2] É interessante que, mesmo em trabalhos que exclui, o conceito de deformação aparece, implícita ou explicitamente. Minha contribuição ao estudo da transição caos-ordem, deu-se no contexto do DGOE (Deformed Gaussian Orthogonal Ensemble) e minha única contribuição relacionada ao tema interação núcleon-nucleon, fez-se no estudo da contribuição da troca de dois píons ao espalhamento $N\alpha$ periférico; ora, píons aparecem como partículas massivas por que a simetria quiral é violada.

BIBLIOGRAFIA

[1] M.S. Hussein, C.L. Lima, M.P. Pato, and C.A. Bertulani, Phys. Rev. Lett. **65** (1990) 839.

[2] A.C.C. Villari, W. Mittig, A. Lépine-Szily, R. Lichtenthaler Filho, G. Auger, L. Bianchi, R. Bernard, J.N. Casadjian, J.L. Ciffre, A. Cunsolo, A. Foti, L. Gaudard, C.L. Lima, E. Plagnol, Y. Schutz, R.H. Siemsen, and J.P. Weleczka, Phys. Rev. Lett. **71** (1993) 2551.

[3] M.P. Pato, C.A. Nunes, C.L. Lima, M.S. Hussein, and Y. Alhassid, Phys. Rev. **C49** (1994) 2919.

[4] C.I. Barbosa, C.L. Lima, M.S. Hussein, and M.P. Pato, Phys. Rev. **E59** (1999) 321.

[5] L.A. Barreiro, C.L. Lima, and M.R. Robilotta, Phys. Rev. **C57** (1998) 2142.

[6] M. Kyotoku, C.L. Lima, and Hsi-Tseng Chen, Phys. Rev. **C53** (1996) 2243.

[7] D. Galetti, B.M. Pimentel, C.L. Lima, and J.T. Lunardi, An. Acad. Bras. Ci. **70** (1998) 1.

[8] D. Galetti, B.M. Pimentel, C.L. Lima, and M. Kyotoku, Physica A **262** (1999) 428.

2. Deformação nuclear

2.1. Introdução

O embate entre as correlações nucleares de longo alcance, que levam à deformação, e as de emparelhamento, que privilegiam a esfericidade, é em grande parte responsável pela riqueza estrutural do espectro de baixas energias dos sistemas nucleares. Com o aumento da energia disponível nas colisões entre íons pesados, vários novos fenômenos emergiram dessa arena, o mais saliente dos quais é o fenômeno do *back-bending*, que se caracteriza por um desvio marcante do comportamento rotacional puro como resultado da quebra, induzida pela rotação, de pares de partículas estrategicamente localizadas nos níveis intrusos, migrantes extraídos da camada de oscilador imediatamente acima pela interação spin-órbita (por exemplo, nêutron $i_{13/2}$, próton $h_{11/2}$, etc); esses estados intrusos caracterizam-se por terem um valor elevado do momento angular j e paridade oposta à dos seus vizinhos, sendo portanto pouco acessíveis a correlações. Vale mencionar também, como um exemplo mais recente de fenômenos interessantes ligados a aspectos da deformaç ão nuclear, a descoberta de bandas rotacionais super-deformadas em meados da década passada, uma magnífica manifestação da persistência da forma nuclear a grandes momentos angulares ($\sim 60\hbar$). Em qualquer caso, uma descrição fenomenológica do espectro rotacional pode ser obtida a partir de expansões em série de potências de $I(I+1)$, onde I é o momento angular[1] [1]. Expansões mais exóticas podem ser encontradas na literatura mais recente [2, 3, 4, 5] mas nos ocuparemos apenas da última delas no Capítulo 4.

A retomada do meu envolvimento nesse tipo de física deu-se essencialmente através da colaboração com o Grupo de Espectroscopia γ do Laboratório Pelletron que, desde 1985. tem se dedicado ao estudo de estados de momento angular intermediário ($\sim 14\hbar$) e realizado estudos sistemáticos em núcleos ímpar-ímpar na região de massa em torno de $A \approx 130$, identificando e analisando bandas rotacionais, obtendo dessa forma informações acerca da natureza do esquema de acoplamento e da forma desses núcleos. Estão ainda particularmente vívidas na minha mente as conversas que tive com membros do grupo, e em particular com

[1] Ou, de modo alternativo, através da mais rapidamente convergente expansão em termos da freqüência de rotação ω.

a Profa. Ewa W. Cybulska, logo após meu retorno a São Paulo em 1985, época em que o ingresso do grupo nesse tipo de física estava sendo discutido.

Como resultado dessa colaboração, alguns trabalhos foram publicados [6, 7, 8, 9] (e algumas teses experimentais foram defendidas), nos quais minha participação deve ser devidamente qualificada: fui o "teórico de plantão", auxiliando na discussão dos resultados, tentando trazer luz a aspectos mais confusos do ferramental teórico e apontando novos desenvolvimentos que poderiam ser úteis (a "revisita" do Prof. K. Hara (Technische Universität - Munique) à USP após longos anos, pode ser assim enquadrada).

Neste capítulo[2] farei uma breve revisão de alguns aspectos dos fenômenos e modelos relacionados com a deformação e os fenômenos ligados à rotação nuclear, tentando desenhar um quadro onde se insira minha contribuição mais recente ao problema. Eventualmente, plantarei aqui e acolá algumas sementes que talvez produzam frutos em capítulos posteriores.

2.2. Motivação científica

Núcleos transicionais duplamente ímpares na região de massa $A \approx 130$, além de serem acessíveis nas condições experimentais existentes no Laboratório Pelletron, têm uma série de outros atrativos motivadores do motivaram seu estudo. Núcleos nessa região são deformados mas apresentam a característica de não manterem uma forma axialmente simétrica definida, podendo alterá-la com o aumento do momento angular, sendo também facilmente polarizáveis à medida que novas partículas são agregadas. Esses núcleos têm ambas as partículas de valência ocupando o orbital $h_{11/2}$, porém em uma situação de competição: os nêutrons estão na parte superior desse orbital (e portanto privilegiando a forma prolata) enquanto os prótons estão na parte mais baixa (favorecendo dessa maneira a forma oblata); a forma nuclear resultante pode então ser a de um elipsoide triaxial.

Uma das perguntas básicas que nos fizemos era como os efeitos polarizadores das partículas de valência refletiam-se na forma nuclear e nas bandas rotacionais e qual a influência das interações residuais entre essas quase-partículas; essas perguntas foram atacadas durante nossa colaboração e algumas respostas parciais foram obtidas ao longo desses anos[3].

[2] Baseado parcialmente em palestra apresentada na XV Reunião de Trabalho sobre Física Nuclear no Brasil (1992); não publicada.

[3] Vale ressaltar que o problema da interação residual entre as quase-partículas aparece apenas marginalmente nos trabalhos desse período.

2.3. Partícula independente em potenciais esféricos ou deformados

Nas proximidades de uma camada fechada, os núcleos são essencialmente esféricos, sendo os diversos estados de momento angular construidos através do reacoplamento das partículas de valência e de excitações partícula-buraco formadas a partir do estado fundamental. Um cálculo usando o modelo de camadas esférico reproduz o espectro experimental com boa precisão, mas torna-se numericamente impraticável à medida que o número de partículas fora da camada fechada cresce, devido à necessidade de se levar em conta a interação residual [10].

Por outro lado, com o aumento de número de partículas de valência, a simetria esférica deixa de ser energeticamente favorável. O núcleo sofre então uma quebra espontânea de simetria. Sendo o núcleo um sistema isolado cuja hamiltoniana deve ser explicitamente invariante sob rotações. entra em cena o conceito de deformação intrínseca. A. Bohr [11], em palestra ministrada quando da outorga do premio Nobel, expressou essas idéias claramente:

> "De fato, a ocorrência do grau de liberdade rotacional coletivo pode ser encarada como oriunda da quebra da invariância rotacional, que introduz uma "deformação" que torna possível especificar a orientação do sistema. A rotação representa o modo coletivo associado a essa quebra espontânea de simetria (bóson de Goldstone)."

Poderia, sem dúvida, ser objetado que conceitos como esse são aplicáveis apenas a sistemas com um número infinito de graus de liberdade; o conspícuo aparecimento da rotação nuclear serve provavelmente para calar discordâncias[4].

As deformações típicas dos sistemas nucleares, obtidas a partir de medidas de momentos de quadrupolo, são da ordem de $\delta \sim 0,2 - 0,3$. Potenciais deformados (Nilsson ou Woods-Saxon) surgem então como substitutos adequados do modelo de camadas esférico; a interpretação bem sucedida do espectro de baixa energia dos núcleos ímpares como resultado do acoplamento de uma partícula de valência movendo-se no potencial gerado por um caroço par-par deformado, é um indicador inequívoco da adequação dessa idéia.

O sucesso no uso de um potencial deformado pode ser atribuido ao fato de que a maior parte das interações de dois corpos no potencial esférico é absorvida em um campo médio deformado[5], restando então apenas fracas interações residuais

[4]Uma discussão extremamente interessante do mecanismo de Higgs e do aparecimento do modo de Nambu-Goldstone em conexão com a descrição de Bohr e Mottelson para a rotação nuclear coletiva, pode ser encontrada no artigo de Fujikawa e Ui [12].

[5]Esta idéia é recorrente e aparecerá várias vezes ao longo do texto; ver, por exemplo, as seções (2.3.1) e (2.5).

de dois corpos a serem consideradas[6]. Entretanto, como resultado da quebra da invariância rotacional, os níveis de partícula independente deixam de poder ser rotulados pelo momento angular, permanecendo apenas a projeção no eixo de simetria como um bom número quântico[7]. Uma molesta decorrência do uso de campos médios deformados é a necessidade de técnicas adequadas de projeção a fim de restaurar a simetria quebrada.

2.3.1. Correlações de emparelhamento

Este parece ser um bom momento para abordar alguns aspectos da interação residual e fazer uma primeira discussão das correlações de emparelhamento[8]; teremos oportunidade de retomá-la outras vezes ao longo deste texto.

O entendimento da importância do emparelhamento remonta aos primórdios da física nuclear; já no modelo da gota líquida, foi necessária a inclusão de uma contribuição adicional capaz de dar conta da sistemática variação da energia de ligação de acordo com a parilidade[9] do número de prótons ou de nêutrons. O efeito de emparelhamento, apareceu também no desenvolvimento do modelo de camadas permitindo a interpretação de muitas propriedades dos núcleos ímpares em termos dos estados ligados da partícula ímpar de valência.

O trabalho pioneiro de Bohr, Mottelson e Pines [17] trouxe ao cenário da física nuclear correlações de emparelhamento similares às da teoria microscópica da supercondutividade em sólidos formulada por Bardeen, Cooper e Schrieffer [18]; desde então, elas têm sido um dos elementos fundamentais para a descrição das propriedades do núcleo atômico e em particular daquelas ligadas à forma nuclear e aos fenômenos de rotação.

A idéia subjacente a essa abordagem consiste numa extensão do conceito de campo médio; é sem dúvida fascinante que correlações de dois corpos, responsáveis pela criação e aniquilação de pares de partículas, possam ser incorporadas em um novo campo médio onde quase-partículas, formadas a partir de partículas e buracos definidas no campo médio antigo, comportam-se como objetos independentes. Na verdade, essa redefinição do campo médio, através da incorporação

[6] Um bom exemplo desse procedimento, pode ser encontrado na Ref. [13], onde estudamos o papel das vibrações γ (que distorcem a simetria axial do elipsoide nuclear) como um mecanismo para a formação dos *yrast traps*, estados que têm longa vida por serem estruturalmente distintos dos seus vizinhos.

[7] Ou nem mesmo ela se a deformação for triaxial; neste caso, a invariância por rotações de π em torno de um dos eixos principais do sistema, provê o necessário número quântico

[8] No plural, pois, mesmo considerando que vou basicamente descrever correlações envolvendo partículas acopladas com momento angular total zero, pares de partículas com momento angular dois desempenham também algum papel na física das rotações.

[9] Uso esta palavra um tanto rara apenas para não utilizar seu sinônimo paridade, que tem também a acepção de número par ou número ímpar

de remanescentes escolhidos da interação residual, constituiu-se numa filosofia no tratamento do problema nuclear de muitos corpos, irradiada a partir de Copenhague (o potencial de Nilsson mencionado acima, é um representante emblemático dessa abordagem).

Passando rapidamente pelos aspectos técnicos envolvidos, a hamiltoniana de emparelhamento tem a seguinte forma,

$$H = \sum_{\nu} \varepsilon_{\nu} c_{\nu}^{\dagger} c_{\nu} - G P_0^{\dagger} P_0 \tag{2.1}$$

$$P_0^{\dagger} = \frac{1}{2} \sum_{\nu} c_{\nu}^{\dagger} c_{\bar{\nu}}^{\dagger}, \tag{2.2}$$

onde ν rotula os estados de partícula independente e $\bar{\nu}$ seu conjugado por reversão temporal[10].

O primeiro termo em (2.1), $H_{sp} = \sum_{\nu} \varepsilon_{\nu} c_{\nu}^{\dagger} c_{\nu}$, descreve partículas independentes em um campo médio e o segundo a criação e aniquilação de pares de partículas em órbitas conjugadas (se o campo médio em questão for o modelo de camadas esférico, tratam-se de pares de partículas acopladas com momento angular total zero); G é a intensidade dessa interação.

Através da transformação de quase-partícula,

$$\begin{aligned} \alpha_{\nu}^{\dagger} &= u_{\nu} c_{\nu}^{\dagger} + v_{\nu} c_{\bar{\nu}} \\ \alpha_{\bar{\nu}}^{\dagger} &= u_{\nu} c_{\bar{\nu}}^{\dagger} - v_{\nu} c_{\nu}, \end{aligned} \tag{2.3}$$

canônica pois $u_{\nu}^2 + v_{\nu}^2 = 1$, a hamiltoniana (2.1) torna-se,

$$H = \mathcal{E}_0 + \sum_{\nu} E_{\nu} \alpha_{\nu}^{\dagger} \alpha_{\nu}. \tag{2.4}$$

Contribuições devidas à interação entre as quase-partículas foram desconsideradas, em consonância com a idéia de que essa "renormalização" das partículas incorporou parcela considerável da interação de emparelhamento à própria definição desses novos objetos, os quais têm agora

$$|BCS\rangle = \prod_{\nu>0} \left(u_{\nu} + v_{\nu} c_{\nu}^{\dagger} c_{\bar{\nu}}^{\dagger} \right) |0\rangle \tag{2.5}$$

como vácuo; o preço pago para termos quase-partículas independentes ou, de forma equivalente, uma aproximação de campo médio, é que este novo vácuo

[10] $c_{\bar{\nu}}^{\dagger} = \mathcal{T} c_{\nu}^{\dagger} \mathcal{T}^{-1}$, onde $\mathcal{T}$ é o operador de reversão temporal. A forma explícita do operador conjugado por reversão temporal passa por uma adequada definição das fases: vou passar ao largo dessa "eterna dor de cabeça" e mencionar que, na base do modelo de camadas esférico, a ser utilizada futuramente, e na convenção de fase de Condon e Shortley, temos: $c_{\bar{\nu}}^{\dagger} \rightarrow (-1)^{j-m} c_{j-m}^{\dagger}$

não tem mais o número de partículas, N, como um bom número quântico; essa "moléstia" pode ser consertado, ainda que em média, incluindo-se na hamiltoniana (2.1) um termo adicional, $-\lambda\hat{N}$ ($\hat{N}$ é o operador número de partículas), onde o multiplicador de Lagrange λ é escolhido tal que $N = 2\sum_{\nu>0} v_\nu^2$.

$\mathcal{E}_0$ em (2.4) é o valor esperado de $H - \lambda\hat{N}$ no vácuo de BCS, $\mathcal{E}_0 = \langle BCS|\, H - \lambda\hat{N}\,|BCS\rangle$, e

$$E_\nu = \sqrt{(\varepsilon_\nu - \lambda)^2 + \Delta^2}, \tag{2.6}$$

é a energia das quase-partículas, onde $\Delta = G\sum_{\nu>0} u_\nu v_\nu$, o *gap* de emparelhamento, pode ser encarado como a contribuição da interação de emparelhamento à energia de quase-partícula independente no novo campo médio.

2.4. Modelo de partícula(s) + caroço coletivo

Muitos dos fenômenos que aparecem na física de momentos angulares elevados, podem ser mais facilmente entendidos no contexto de modelos híbridos; por isso, vou fazer um *detour* para discutir com algum detalhe uma velha história [14]: núcleos podem ser descritos como constituidos por um caroço coletivo, com todo o apelo clássico que ele carrega, acoplado ao movimento de partículas de valência (ou, mais adequadamente, quase-partículas de valência). Adiabaticidade é assumida, significando que o movimento das partículas é muito mais rápido que o do caroço coletivo.

Mesmo considerando que a maior parte da discussão nesta seção será feita para o caso em que o caroço coletivo é um rotor rígido, é útil discutir brevemente a situação em que uma partícula de valência com um grande momento angular intrínseco j é acoplada a vibrações quadrupolares harmônicas [15]; j grande significa que sua direção não é alterada substancialmente pelo acoplamento às vibrações, restando como efeito mais importante apenas o aparecimento de uma deformação estática. Para valores pequenos da constante de acoplamento, o quintupleto $I = j-2, j-1, j, j+1, j+2$ é ligeiramente separado pela interação; entretanto, com o aumento do acoplamento, um comportamento rotacional típico desenvolve-se, caracterizado pelo aparecimento de uma banda de estados com momentos angulares $I = j+1, j+2, j+3, \ldots$ A deformação de equilíbrio de tal sistema, que é função da constante de acoplamento e de j, cresce correspondentemente. Esse modelo singelo, mostra claramente os efeitos de polarização da partícula de valência com grande j, que são de importância fundamental em núcleos transicionais.

No caso de um caroço rígido, a hamiltoniana que descreve um sistema com-

posto por partículas a ele acopladas pode ser escrita como

$$H = \sum_{i=1,3} \frac{\hbar^2}{2\Im_i} R_i^2 + \sum_{\substack{partículas \\ de\ valência}} (H_{sp} + H_{pair}) + H_{res}. \tag{2.7}$$

Na expressão acima, o primeiro termo descreve a contribuição puramente coletiva para a dinâmica do problema onde R_i, a $i^{ésima}$ componente do momento angular do rotor, e $\Im_i$, o momento de inércia em relação ao eixo i, são expressos em termos de um sistema fixo no corpo (sistema intrínseco). H_{sp} e H_{pair} representam respectivamente o campo médio deformado (em geral, um potencial de Nilsson) e a contribuição da interação de emparelhamento, que poderiam ter sido combinados em um campo médio de quase-partículas, H_{qp}; H_{res} representa a interação remanescente entre as partículas de valência. A anisotropia do potencial é responsável pelo acoplamento entre os movimentos da(s) partícula(s) e do rotor.

O momento angular total ($\vec{I}$) do sistema composto é dado por

$$\vec{I} = \vec{R} + \sum_{\substack{partículas \\ de \\ valência}} \vec{j}, \tag{2.8}$$

onde $\vec{R}$ é o momento angular do rotor; reescrevendo a parte coletiva da equação (2.7) em termos dos momentos angulares total e das partículas de valência, obtém-se

$$H_{coletivo} = \sum_{i=1,3} \frac{\hbar^2}{2\Im_i} (I_i - j_i)^2 . \tag{2.9}$$

Os termos cruzados do tipo $\frac{\hbar^2}{\Im_i} I_i j_i$ constituem o acoplamento de Coriolis e descrevem as contribuições não inerciais (centrífugas e de Coriolis) que aparecem por estarmos descrevendo a dinâmica do sistema no referencial intrínseco; mais especificamente, a interação de Coriolis representa as perturbações ao movimento das partículas devido ao movimento rotacional do sistema, manifestando-se através do acoplamento entre estados intrínsecos distintos. As contribuições quadráticas em j constituem o termo de recuo e dependem apenas das variáveis intrínsecas (i.e. das partículas de valência); no caso geral, ele contém um termo de dois corpos, mas quando há apenas uma partícula de valência esse termo é freqüentemente incorporado ao próprio campo médio.

As forças não inerciais, que levam ao desacoplamento entre o movimento da partícula e do caroço, competem com as que privilegiam o acoplamento forte entre ambos; vencendo as primeiras, temos o chamado limite desacoplado e vencendo as outras, o limite de acoplamento forte. Em núcleos muito deformados, o acoplamento forte é a regra, mas, na região de núcleos transicionais, o decréscimo da

deformação nuclear (e com ela do momento de inércia) e a presença de estados intrusos de momento angular elevado, contribuem para que a interação de Coriolis seja privilegiada. Nesse caso, a(s) partícula(s) de valência move(m)-se independentemente do caroço coletivo, com seu momento angular intrínseco, j, paralelo ao momento angular total, I. Uma boa parcela dos fenômenos que aparecem na física dos estados de momento angular elevado tem sua origem no embate aludido acima.

A base de acoplamento forte é a mais usada na diagonalização dessa hamiltoniana[11],

$$\Psi^I_{MK} = \sqrt{\frac{2I+1}{16\pi^2\left(1+\delta_{K0}\right)}}\left(\mathcal{D}^I_{MK}\left(\Omega\right)\varphi_K^{valência} + \left(-1\right)^{I+K}\mathcal{D}^I_{M-K}\left(\Omega\right)\varphi_{\bar{K}}^{valência}\right), \tag{2.10}$$

onde $\varphi_K^{valência}$ representa a função de onda das partículas de valência (próton, nêutron, próton-próton, nêutron-nêutron, nêutron-próton, etc) e $\mathcal{D}^I_{MK}$, a função de onda rotacional. A função de onda (2.10) descreve bandas rotacionais com

$$I = K, K+1, K+2, \ldots . \tag{2.11}$$

A fase $(-1)^{I+K}$, usualmente chamada de *signature*, está ligada à invariância sob rotações de π em torno de um eixo perpendicular ao eixo de simetria z, geradas por $\mathcal{R}_x(\pi) = \exp\left(-i\pi I_x\right)$[12]. Esse número quântico tem enorme importância na classificação de estados do espectro rotacional, bem como das órbitas nucleônicas em potenciais nucleares em rotação (ver sec. 2.5).

A discussão a seguir será restrita ao caso de apenas uma partícula acoplada ao caroço rígido axialmente simétrico ($\mathfrak{I}_1 = \mathfrak{I}_2 \equiv \mathfrak{I}$), visando explicitar o conteúdo físico de grandezas que serão relevantes mais adiante. O valor esperado da hamiltoniana é

$$E_K\left(I\right) = \frac{\hbar^2}{2\mathfrak{I}}\left[I\left(I+1\right) - K^2 + a\left(-1\right)^{I+K}\left(I+\frac{1}{2}\right)\delta_{K,1/2}\right] + E_K, \tag{2.12}$$

onde o parâmetro de desacoplamento a é dado por

$$a = -\left\langle\varphi^{valência}_{K=1/2}\right| j_+ \left|\varphi^{valência}_{K=1/2}\right\rangle = -\sum_{nj}\left|\eta_{nj}\right|^2\left(-1\right)^{j+1/2}\left(j+\frac{1}{2}\right). \tag{2.13}$$

[11] Sem prejuizo do fato de que, no caso de duas partículas de valência, truncamentos são mais facilmente efetuados na base de acoplamento quase-fraco [16].

[12] Na verdade, uma classe importante de potenciais nucleares tem sua hamiltoniana invariante sob rotações de π em torno dos tres eixos principais do sistema. Os operadores correspondentes são $\mathcal{R}_k(\pi) = \exp\left(-i\pi I_k\right)$ $(k = x, y, z)$. Essa invariância implica, por exemplo, que não existem multipolos ímpares na expansão do campo nuclear deformado. Ainda como decorrência dessa invariância, os estados intrísecos com $K \neq 0$ são duplamente degenerados.

Na expressão acima, se as funções de onda intrínsecas forem descritas pelo modelo de Nilsson, os η_{nj} são as amplitudes da expansão dos orbitais de Nilsson na base esférica.

Se $\varphi_K^{valência}$ tem uma forte mistura em j (como é o caso de núcleos muito deformados), o fator de desacoplamento é pequeno devido a cancelamentos causados pela fase $(-1)^{j+1/2}$; entretanto, se os estados de partícula relevantes forem intrusos, a soma em (2.13) reduz-se a um único termo e a dependência no momento angular de $E_K(I)$ tem a estrutura $I(I+1)+(-1)^{I-j}\left(I+\frac{1}{2}\right)\left(j+\frac{1}{2}\right)$, apresentando um comportamento em ziguezague devido à fase $(-1)^{I-j}$. Os diversos estados de momento angular separam-se em dois ramos distintos: favorecido, quando a diferença $I-j$ for par, e não favorecido, quando essa diferença for ímpar. Tecnicamente, essa separação recebe o nome de *signature splitting*.

Núcleos ímpar-ímpar também apresentam no seu espectro um ziguezague devido à fase $(-1)^{I-j}$, onde $j=j_p+j_n$; em alguns casos, porém, quando $I-j$ é par os estados correspondentes estão em energia mais baixa que os com $I-j$ ímpar; é a chamada inversão na signature.

No modelo de partícula(s) + rotor o acoplamento do momento angular entre as partículas de valência e o rotor é feito corretamente mas,

- os cruzamentos de bandas e o alinhamento não são descritos adequadamente, pois estes efeitos envolvem partículas do caroço que, neste modelo não tem estrutura;

- configurações envolvendo muitas partículas podem ser descritas pelo modelo mas a complexidade dos cálculos aumenta tremendamente com o número de partículas;

- o modelo tem vários parâmetros, as deformações (β e γ), os *gaps* de emparelhamento e o momento de inércia [13]. Se esses parâmetros forem ajustados aos dados, o poder preditivo torna-se muito baixo; melhora porém, se forem extraídos da sistemática.

O modelo partícula(s) + rotor é, entretanto, muito útil: nossa intuição é ainda marcadamente clássica e o modelo tem nas suas bases constructos para as quais temos modelos mentais.

[13] Eventualmente é incluido também um fator da ordem de dois (fator de atenuação de Coriolis), necessário para eliminar discrepância entre os elementos de matriz teóricos e os obtidos experimentalmente.

2.5. Movimento de partícula independente em um potencial em rotação

Retomemos agora a rota anteriormente traçada: encarando os efeitos da rotação (mais especificamente, seus efeitos não inerciais) como um tipo de interação residual, vamos incorporá-los a um novo campo médio. Transformando a hamiltoniana deformada de partícula independente (Nilsson ou Woods-Saxon, com ou sem a inclusão das correlações de emparelhamento) para o referencial fixo ao corpo obtém-se

$$H^{\omega} = H_{sp} - \hbar\omega j_r. \tag{2.14}$$

Na hamiltoniana acima (hamiltoniana de *cranking*), o segundo termo à direita pode a alterar as funções de onda dos orbitais dos núcleons e descreve as contribuições não-inerciais, i.e. centrífuga e de Coriolis (o índice r indica o eixo de rotação).

Os autovalores de (2.14) são freqüentemente chamados de routhianos (em analogia com a função de Routh em mecânica clássica). Eles podem ser escritos como,

$$\varepsilon_{\nu}^{\omega} = \langle\varphi_{\nu}^{\omega}|\, H^{\omega}\, |\varphi_{\nu}^{\omega}\rangle = \langle\varphi_{\nu}^{\omega}|\, H_{sp}\, |\varphi_{\nu}^{\omega}\rangle - \omega\, \langle\varphi_{\nu}^{\omega}|\, j_x\, |\varphi_{\nu}^{\omega}\rangle\,, \tag{2.15}$$

implicando que $\dfrac{d\varepsilon_{\nu}^{\omega}}{d_{\omega}} = -\langle\varphi_{\nu}^{\omega}|\, j_x\, |\varphi_{\nu}^{\omega}\rangle$; isto significa que o valor esperado do operador momento angular j_x na direção do eixo de rotação (momento angular alinhado) é igual à inclinação do routhiano de partícula independente, com o sinal trocado.

O momento angular total ao longo do eixo de rotação (que no limite de altos spins é aproximadamente o momento angular total) para um sistema composto de N núcleons é dado por

$$I_x = \sum_{\nu=1}^{N} \langle\varphi_{\nu}^{\omega}|\, j_x\, |\varphi_{\nu}^{\omega}\rangle \tag{2.16}$$

e a energia total no sistema de laboratório por

$$E = \sum_{\nu=1}^{N} \varepsilon_{\nu}^{\omega} + \omega I_x. \tag{2.17}$$

Se o eixo de rotação for o eixo de simetria do núcleo ($j_r = j_3 = j_z$; z é o eixo de simetria) a solução de (2.14) é particularmente simples,

$$\varepsilon_{\nu}^{\omega} = \varepsilon_{\nu} - \hbar\omega\Omega_z \tag{2.18}$$

e o momento angular é formado pela soma das contribuições ao longo de z; as autofunções de H_{sp} são também autofunções de j_z e portanto de H^ω. O papel do termo de rotação é apenas o de redefinir a superfície de Fermi: para aumentar o momento angular temos que alterar a ocupação no potencial deformado e promover partículas de estados com menor Ω_z para estados com maior Ω_z[14]. A rotação em torno de um eixo de simetria é não coletiva e não gera bandas rotacionais.

Mais rica é a situação quando o eixo de rotação é perpendicular ao eixo de simetria (por exemplo, $j_r = j_1 = j_x$). Como as autofunções da hamiltoniana de partícula independente não são autofunções de j_x, a rotação acarreta em uma mistura dos estados de partícula independente.

Devido à presença do termo $\hbar\omega j_x$, simetrias da hamiltoniana de partícula independente são perdidas; a hamiltoniana (2.14) não é mais invariante sob inversão temporal e nem sob $\mathcal{R}_y(\pi)$ ou $\mathcal{R}_z(\pi)$. Como as únicas simetrias remanescentes são a paridade e a invariância sob a ação do operador $\mathcal{R}_x(\pi)$, seus autovalores podem ser usados para rotular os estados de partícula independente no sistema em rotação. Chamando de r o autovalor de $\mathcal{R}_x(\pi)$ e introduzindo a notação $r = \exp(-i\pi\alpha)$ os estados nucleônicos podem ser classificados de acordo com o valor de α

$$\mathcal{R}_x(\pi)\varphi_\alpha = e^{-i\pi j_x}\varphi_\alpha = e^{-i\pi\alpha}\varphi_\alpha \tag{2.19}$$

onde φ_α denota a função de onda de partícula independente com *signature* r ($r = -i$ para $\alpha = 1/2$ ou $r = i$ para $\alpha = -1/2$); o próprio α é mais freqüentemente encontrado na literatura sob o nome de *signature* e tem a vantagem de ser uma quantidade aditiva. Assim, os routhianos são rotulados adequadamente pelos números quânticos ($\pi = \pm, \alpha = \pm 1/2$).

Em sistemas com um número par de núcleons temos

$$r = +1, \quad (\alpha = 0), \quad I = 0, 2, 4, ... \tag{2.20}$$

$$r = -1, \quad (\alpha = 1), \quad I = 1, 3, 5, ..., \tag{2.21}$$

ao passo que, quando o número de núcleons for ímpar

$$r = -i, \quad (\alpha = +1/2), \quad I = 1/2, 5/2, 9/2, ... \tag{2.22}$$

$$r = +i, \quad (\alpha = -1/2), \quad I = 3/2, 7/2, 11/2... \,. \tag{2.23}$$

Em $\omega = 0$ os estados nucleônicos com valores de $\alpha = \pm 1/2$ são degenerados; à medida que a rotação aumenta, essa degenerescência é quebrada e a interação de Coriolis age separando as componentes de diferentes *signatures*. O valor dessa

[14] O espectro *yrast* do ^{146}Gd na referência [13] foi construido dessa forma; o campo médio utilizado foi, porém, o de Woods-Saxon e o emparelhamento foi levado em conta.

separação em energia é *signature splitting* à qual nos referimos na seção anterior e a componente de menor energia é dita favorecida.

É quase desnecessário repetir que a correlação de emparelhamento desempenha um papel essencial na física de altos spins e portanto os routhianos construidos devem levá-la em conta se pretendem ter condições mínimas de representar a realidade. Dessa forma, a hamiltoniana de partícula independente deve incluir essas correlações (mais apropriadamente, deveríamos te-la chamado de H_{qp}).

Na abordagem acima descrita, a freqüência angular desempenhou um papel central ao invés da quantidade diretamente medida que é o momento angular; em termos das energias experimentais, ela pode ser escrita como

$$\hbar\omega = \frac{dE(I)}{dI} \approx \frac{1}{2}\left[E(I+1) - E(I-1)\right] \tag{2.24}$$

A freqüência angular pode ser entendida como um mutiplicador de Lagrange que fixa a quantidade de momento angular alinhado[15].

A comparação entre os resultados experimentais e os cálculos teóricos tem, no caso deste modelo, uma peculiaridade: os resultados da experiência têm que ser traduzidos para o referencial em rotação através de uma prescrição que parametriza o momento de inércia nuclear em termos de ω[16].

A figura 5 da referência [9] (em anexo) apresenta os routhianos como função da freqüência rotacional ω para o núcleo duplamente ímpar ^{108}Ag; é marcante a mudança da curvatura (que é um sinal do cruzamento de bandas) das curvas AB (nêutrons) em torno de $\hbar\omega = 0,35$ MeV e ab (prótons) em $\hbar\omega = 0,48$ Mev (a informação trazida pelas curvas oriundas da região de energias negativas, pode ser ignorada pois é redundante). Em ambos os casos, um par (situado no $h_{11/2}$, no caso dos quase-nêutrons, e no $g_{9/2}$, no caso dos quase-prótons) é quebrado pela ação das forças não inerciais e se alinha com o eixo de rotação. A *signature splitting* entre os quase-prótons em a e b é pequena, refletindo o fato de que eles estão fracamente acoplados ao eixo de rotação.

Alguns comentários são adequados antes de encerrarmos esta discussão:

- Uma das grandes limitações dessa abordagem é que ela foi concebida para descrever configurações alinhadas, i.e. configurações nas quais o momento angular das partículas é paralelo a uma dada direção; o modelo não tem a riqueza necessária para descrever bandas caracterizadas por j grande e pequeno K.

[15] Em completa analogia com o que ocorre na restauração do número de partículas no caso do BCS.

[16] Na verdade, usa-se o *cranking* de Harris [19].

- Estados com I pequeno também apresentam dificuldades; por exemplo, $I \lesssim j$ em núcleos ímpares.

- O modelo revelou ter um enorme poder de predição: afinal de contas, as bandas super-deformadas foram previstas teoricamente antes da sua descoberta experimental.

- Há um bom controle dos parâmetros do modelo; os potenciais de Nilsson e Woods-Saxon são já bastante estabelecidos na literatura; deformações e os *gaps* de emparelhamento podem ser determinados auto-consistentemente.

- Uma extensão do modelo, chamada TRS (Total Routhian Surface), permite que sejam efetuados cálculos em grande escala incluindo muitos nucleos e muitas configurações.[17].

- Finalmente, é bom lembrar que o momento angular total neste modelo é dado apenas pela componente na direção alinhada o que não deixa de ser uma aproximação forte (pelo menos para momentos angulares não muito grandes).

2.6. Modelo com projeção em momento angular e a transição de forma prolato-oblato

Os modelos apresentados anteriormente, em que pese seu sucesso, tem uma base semi-clássica muito marcante; não contém os ingredientes que se espera de uma teoria moderna: a) inteiramente quanto-mecânica, baseada em uma hamiltoniana microscópica, ainda que usando interações esquemáticas, b) quantidades físicas relevantes, como por exemplo o momento angular, devem ser bons números quânticos.

Sem dúvida, o modelo de camadas tradicional tem essas características, mas,

1. a construção de funções de onda de muitos corpos com bom momento angular é um procedimento complexo;

2. a base onde o problema é diagonalizado é imensa; para núcleos pesados e intermediários, mesmo supercomputadores são insuficientes;

3. devido ao tamanho da base, é difícil a interpretação das informações contidas nos autoestados.

[17] As deformações de equilíbrio na ref. [9] foram obtidas através desse procedimento.

Várias abordagens foram desenvolvidas tentando contornar essas dificuldades; dentre elas a do grupo da Universidade de Tübingen [20] e a desenvolvida por K. Hara e colaboradores [21] na Universidade Técnica de Munique, ambas na Alemanha. A abordagem desenvolvida em Munique e que foi utilizada na análise de núcleos duplamente ímpares na região de massa $A \approx 130$ [8] aqui em São Paulo, tem as seguintes características:

1. usa um campo médio deformado (Nilsson);
2. seleciona uma base que contém apenas os estados essenciais à física que se pretende descrever; desse modo, o espaço de configuração onde a hamiltoniana será diagonalizada diminui consideravelmente, se comparado com o do modelo de camadas usual;
3. a base do modelo é construida projetando-a em estados de bom momento angular.

A hamiltoniana do modelo pode ser escrita como

$$H = H_{esf} - \frac{\chi}{2} Q \cdot Q - G P_0^\dagger P_0 - G_2 P_2^\dagger \cdot P_2, \tag{2.25}$$

onde, H_{esf} é a hamiltoniana do modelo de camadas esférico e os demais termos constituem a interação residual e são, respectivamente, a interação quadrupolo-quadrupolo (cuja diagonalização na base de H_{esf} produz os estados de Nilsson), o emparelhamento usual (monopolar) e o emparelhamento quadrupolar[18].

A base usada na diagonalização dessa hamiltoniana é dada por $P^I_{MK} |\phi_\kappa\rangle$, onde

$$P^I_{MK} = \frac{2I+1}{8\pi^2} \int d\Omega \mathcal{R}(\Omega) \mathcal{D}^I_{MK}(\Omega), \tag{2.26}$$

é o operador de projeção usual e $|\phi_K\rangle$, no caso de núcleos duplamente ímpares é dado por

$$|\phi_\kappa\rangle = \alpha^\dagger_\nu \alpha^\dagger_\pi |0\rangle, \tag{2.27}$$

onde $\alpha^\dagger_\nu$ ($\alpha^\dagger_\pi$) é o operador e criação de um quase-nêutron (quase-próton) construido na base de Nilsson+BCS. $|0\rangle$ é o vácuo dessas quase-partículas.

Um conceito interessante neste modelo, e que é essencial na determinação dos estados relevantes na base, é o de diagrama de bandas. Cada estado projetado pode ser considerado como representante de uma banda rotacional; a energia rotacional da banda κ pode ser definida como

$$E_\kappa(I) = \frac{\langle \phi_\kappa | H P^I_{KK} | \phi_\kappa \rangle}{\langle \phi_\kappa | P^I_{KK} | \phi_\kappa \rangle}. \tag{2.28}$$

[18] A constante da interação de emparelhamento quadrupolar é assumida proporcional a G (nos núcleos na região $A \approx 130$ foi utilizado $G_2 = 0.20G$).

Um diagrama no qual as energias rotacionais de diversas bandas κ são representadas como função de I é denominado de diagrama de bandas (note-se que essas energias $E_\kappa(I)$ são calculadas antes da diagonalização final); ele nos permite, por exemplo, observar os diversos cruzamentos de bandas e identificar as configurações mais importantes para descrever o comportamento dos estados que estamos estudando. Exemplos de diagramas de banda podem ser encontrados na referência [8] em anexo.

Um resultado bastante interessante obtido, usando-se o modelo de camadas projetado, é a previsão de uma transição prolato→oblato passando por formas triaxiais na região de massa $A \approx 130$ (ver figura 10 da referência [8]); esta previsão não é, entretanto, quantitativa pois o modelo só é aplicável a sistemas com simetria axial.

Alguns comentários finais devem ser feitos acerca desta abordagem:

- é completamente quântica;
- tem bom momento angular;
- os estados relevantes são escolhidos de forma física;
- não é porém auto-consistente e
- não tem o número de partículas como uma quantidade conservada (embora não seja tecnicamente difícil implementá-lo).

2.7. Sumário

Fizemos nas páginas anteriores um breve vôo panorâmico sobre alguns aspectos da física dos estados de grande momento angular (sendo mais preciso, momentos angulares moderadamente grandes). Não pretendi reapresentar a discussão contida nos trabalhos em anexo, mas antes esboçar o quadro teórico onde esses trabalhos se inserem.

BIBLIOGRAFIA

[1] A. Bohr and B.R. Mottelson, *Nuclear Structure,* Vol. 2 (Benjamin, New York, 1975).

[2] L. Wu, H. Ding, Z. Yan and G. Liu, Phys. Rev. Lett. **76** (1996) 4132.

[3] G. Zeng, W. Liu and E. Zhao, Phys. Rev. **C52** (1995) 1864.

[4] R. Barbier, J. Meyer and M. Kibler, Int. J. Mod. Phys. **E4** (1995) 385.

[5] D. Bonatsos, et al, Phys. Lett. **B251** (1990) 477.

[6] J.R.B. Oliveira, L.G.R. Emediato, E.W. Cybulska, R.V. Ribas, W.A. Seale, M.N. Rao, N.H. Medina, M.A. Rizzutto, S. Botelho, and C.L. Lima, Phys. Rev. **C45** (1992) 2740.

[7] M.A. Rizzutto, E.W. Cybulska, V.R. Vanin, J.R.B. Oliveira, L.G.R. Emediato, R.V. Ribas, W.A. Seale, M.N. Rao, N.H. Medina, S. Botelho, J.C. Acquadro, and C.L. Lima, Z. Phys. **A344** (1992) 221.

[8] M.A. Rizzutto, E.W. Cybulska, L.G.R. Emediato, N.H. Medina, R.V. Ribas, K. Hara, and C.L. Lima, Nucl. Phys. **A569** (1994) 547. (Em anexo)

[9] F.R. Espinoza-Quiñones, E.W. Cybulska, L.G.R. Emediato, C.L. Lima, N.H. Medina, J.R.B. Oliviera, M.N. Rao, R.V. Ribas, M.A. Rizzutto, W.A. Seale, and C. Tenreiro, Phys. Rev. **C52** (1995) 104. (Em anexo)

[10] Ver por exemplo: J. Blomqvist, Proc. on high Spin Phenomena in Nuclei (1979), ANL-PHY-79-4.

[11] A. Bohr, Rev. Mod. Phys. **48** (1976) 305.

[12] K. Fujikawa and H. Ui, Prog. Theor. Phys. **75** (1986) 997.

[13] J. Dudek, T. Werner, Z. Szymansky, A. Faessler and C. Lima, Phys. Rev. **C26** (1982) 1712.

[14] A. Bohr and B.R. Mottelson, Mat. Fys. Medd. Dan. Vid. Selsk. **27**, no. 16; para uma discussão completa deste problema, nunca é demais citar a Ref. [1]

[15] A. Bohr and B.R. Mottelson, Phys. Scr. **24** (1981) 71.

[16] Celso L. Lima, tese de doutoramento, Universität Tübingen (1982) (em alemão); I. Morrisson, A. Faessler, and C. Lima, Nucl. Phys. **A372** (1981) 13 e referências lá citadas.

[17] A. Bohr, B.R. Mottelson, and D. Pines, Phys. Rev. **110** (1958) 1936.

[18] J. Bardeen, L.N. Cooper, and J.R. Schrieffer, Phys. Rev. **108** (1957) 1175.

[19] Ver por exemplo: M.J.A. de Voigt, J. Dudek, and Z. Szymańsky, Rev. Mod. Phys. **55** (1983) 949.

[20] K.W. Schmid and F. Gruemmer, Rep. Prog. Phys. **50** (1987) 731.

[21] K. Hara and Y. Sun, Nucl. Phys. **A529** (1991) 445; K. Hara and Y. Sun, Nucl. Phys. **A531** (1991) 221; K. Hara and Y. Sun, Nucl. Phys. **A537** (1992) 77

3. BCS e núcleos exóticos

3.1. Introdução

A pesquisa experimental com feixes radioativos abriu novas fronteiras para a física nuclear; eles permitiram a criação e o estudo de sistemas nucleares exóticos, i.e. ricos em prótons ou nêutrons, localizados em regiões fora do vale de estabilidade, forçando a uma reavaliação de modelos que haviam sido construidos para descrever núcleos nas proximidades desse vale.

Sob esse ponto de vista, mesmo o modelo de camadas, tão caro e presente na vida dos físicos nucleares, foi abalado; nesse novo terreno ainda sendo desbravado, descobriu-se que a interação spin órbita já não mais atua, que o ordenamento dos níveis de partícula encontrado nos livros texto não vige mais e que, no caso de núcleos exóticos leves, talvez nem mesmo o conceito de campo médio tenha sentido. A interação nêutron-próton, antes uma componente residual, desempenha agora um papel importante, mormente na descrição das propriedades de sistemas mais pesados com $N \approx Z \sim 100$.

Está portanto na ordem do dia a rediscussão das bases dos modelos nucleares tradicionais e ao mesmo tempo a investigação da sua aplicabilidade a esses novos domínios.

O que será reportado neste capítulo é o resultado de uma teimosa tentativa de ainda aplicar modelos nucleares tradicionais a núcleos exóticos leves. Uma vez que o fio condutor desta revisão é a idéia de deformação, farei uma breve discussão dos movimentos coletivos de emparelhamento, logo após a (re)apresentação da hamiltoniana de emparelhamento. Na seção 3.5 será discutida a aplicação da teoria de campo médio de BCS ao ^{11}Li. Um breve sumário na seção 3.6 encerra o capítulo.

Duas publicações [1, 2] e a dissertação de mestrado do sr. Ettore Baldini Neto originaram-se destes estudos acerca da aplicação da teoria de campo médo de BCS ao núcleo exótico ^{11}Li. A colaboração com Mauro Kyotoku, Nilton Teruya e Ettore Baldini Neto foi essencial para a obtenção dos resultados sumarizados.

3.2. Motivação Científica

As aproximações de campo médio desempenham um papel extremamente importante na física nuclear; o tradicional modelo de camadas, o tratamento BCS da interação de emparelhamento ou, como vimos no capítulo anterior, a inclusão dos efeitos não inerciais em orbitais de partícula independente, são exemplos claros do uso disseminado da idéia de partículas movendo-se independentemente em um campo médio gerado pelas correlações entre todos os constituintes do sistema.

O ^{11}Li, provavelmente o núcleo exótico leve mais intensamente estudado, apresenta características surpreendentes; sendo constituido por apenas onze partículas, é quase do tamanho do ^{208}Pb, apresentando um halo, isto é dois nêutrons fracamente ligados ocupando orbitais difusos, extensos e espacialmente simétricos em torno de um caroço deformado de ^{9}Li. Um novo modo coletivo foi também descoberto em núcleos desse tipo, no qual os nêutrons de valência vibram dipolarmente em relação ao caroço. Em adição a isso, o fato do ^{11}Li ser ligado o que não ocorre com o ^{10}Li, é um problema básico que merece ser entendido.

Pares de nêutrons constituem-se num *resort* privilegiado para a aplicação do emparelhamento nuclear [4]; é dessa forma tentador utilizar nesses novos sistemas velhas tecnologias, desenvolvidas ao longo de muitos anos, mesmo sabendo das dificuldades inerentes ao fato de estarmos lidando com sistemas diluídos e fracamente ligados.

Foi verificado experimentalmente [5] que o ^{10}Li apresenta duas ressonâncias com energias $0,10$ MeV e $0,50$ MeV, correspondendo aos estados $2s_{1/2}$ e $1p_{1/2}$, respectivamente. Isso indica que o estado fundamental e os estados excitados conhecidos do ^{11}Li são estruturalmente compostos por esses estados de partícula independente; é acrescentado então ao ^{11}Li um charme adicional, pois tem-se assim a manifestação na natureza de um antigo brinquedo dos físicos nucleares teóricos: o modelo de dois níveis.

3.3. Emparelhamento e BCS

Desde fins dos anos 50, o modelo de emparelhamento desempenha um papel importante na compreensão do comportamento nuclear [6]; sua solução utilizando a aproximação de campo médio de BCS [7], desenvolvida pelos físicos de estado sólido para descrever fenômenos de supercondutividade, é central na descrição de inúmeras propriedades nucleares. Sendo uma teoria de campo médio, o BCS viola necessariamente simetrias do sistema, neste caso a que está associada à conservação número de partículas; um grande esforço foi investido pelos físicos nucleares no desenvolvimento de técnicas que restauram essa simetria[1].

[1] É reconfortante verificar que as técnicas desenvolvidas no passado pelos físicos nucleares

Um sistema de N partículas movendo-se num campo médio esférico e interagindo através da interação de emparelhamento é descrito pela hamiltoniana

$$H = \sum_{jm} \varepsilon_j c^\dagger_{jm} c_{jm} - \frac{G}{4} \sum_{jm,j'm'} (-)^{j-m}(-)^{j'-m'} c^\dagger_{j'm'} c^\dagger_{j'-m'} c_{j-m} c_{jm}, \tag{3.1}$$

onde $c^\dagger_{jm}(c_{jm})$ é o operador de criação (destruição) de partículas no estado de partícula independente que tem energia ε_j (e degenerescência $2\Omega_j = 2j+1$); G é a intensidade da interação.

As técnicas para obter as soluções dessa hamiltoniana são conhecidas e não me deterei muito nelas. Vale lembrar que a transformação de Bogoliubov-Valatin, que leva partículas em quase-partículas,

$$\begin{aligned} c^\dagger_{jm} &= u_j \alpha^\dagger_{jm} + (-1)^{j-m} v_j \alpha_{j-m} \\ c_{jm} &= u_j \alpha_{jm} + (-1)^{j-m} v_j \alpha^\dagger_{j-m}, \end{aligned} \tag{3.2}$$

onde $u_j^2 + v_j^2 = 1$, permite que se escreva (3.1) como um campo médio nas quase-partículas, mais uma série de termos contendo interações residuais entre elas. Inerente à aproximação de campo médio, a violação da conservação do número de partículas exige providências para que, pelo menos em média, o número de constituintes do núcleo seja mantido; um termo $-\lambda \hat{N}$ ($\hat{N}$ indica o operador número de partículas) deve portanto ser previamente agregado a (3.1), onde o parâmetro λ é determinado de modo que a condição de conservação acima seja satisfeita, isto é tal que $N = \sum_j 2\Omega_j v_j^2$.

A hamitoniana (3.1) transforma-se então em $H = \mathcal{E}_0 + \sum_{jm} E_j \alpha^\dagger_{jm} \alpha_{jm} + H^{(qp)}_{res}$, onde

$$\begin{aligned} \mathcal{E}_0 &= \langle BCS | H - \lambda \hat{N} | BCS \rangle \\ &= 2 \sum_j \left(\varepsilon_j - \lambda - \frac{G}{2} v_j^2 \right) \Omega_j v_j^2 - G \sum_{ij} \Omega_i \Omega_j u_i v_i u_j v_j. \end{aligned} \tag{3.3}$$

Os u's e v's são escolhidos de tal forma que as quase-partículas movam-se independentemente com energia $E_j = \sqrt{(\varepsilon_\nu - \lambda)^2 + \Delta^2}$, onde $\Delta = G \sum_j \Omega_j u_j v_j$ é o

para dar conta dos problemas causados pelo número finito de núcleons no núcleo, estão sendo utilizadas pelos físicos de estado sólido, agora que têm que lidar com grãos supercondutores com $N \sim 10^2$ constituintes, ao invés de sistemas com $N \sim 10^{23}$ partículas [8].

Técnicas de projeção, mesmo tendo sido um assunto exaustivamente pesquisado pela comunidade nuclear, ainda apresentam algumas pontas soltas; recentemente [9] mostramos, usando teoria de grupos e resultados da teoria de números, como obter projetores exatos em espaços dimensionais finitos; aplicamos nosso método à restauração do número em BCS e mostramos a relação com técnicas de discretização utilizadas amplamente na literatura da área.

gap de emparelhamento; utilizando a definição de Δ, o último termo que aparece em (3.3) pode ser escrito como $-\frac{\Delta^2}{G}$.

A energia do estado fundamental é obtida transformando-se (3.3) para o referencial não deformado

$$U_0 = \mathcal{E}_0 + \lambda \sum_j 2\Omega_j v_j^2 = 2\sum_j \left(\varepsilon_j - \frac{G}{2}v_j^2\right)\Omega_j v_j^2 - G\sum_{ij}\Omega_i\Omega_j u_i v_i u_j v_j \qquad (3.4)$$

A interação residual entre as quase-partículas, $H_{res}^{(qp)}$, é desprezada em primeira ordem, consistentemente com a aproximação de campo médio desejada[2]. A contribuição de $-\frac{G}{2}v_j^2$, denominado termo de auto-energia, que aparece em (3.3) é também freqüentemente desprezada, sob a alegação de que ela corresponde a uma renormalização nos níveis de partícula independente que, em geral, são extraidos da fenomenologia.

3.4. Movimento coletivo de emparelhamento

O objetivo desta seção é apresentar o conceito de movimento coletivo de emparelhamento para, de alguma forma enviesada, mostrar a conexão entre a nossa abordagem ao problema do ^{11}Li e as deformações no espaço de gauge; com isso, vejo-me remetido, após longos anos, ao tema geral da minha dissertação de mestrado; não imaginava que esta "revisão crítica da minha contribuição" fosse levar-me tão longe no tempo. Talvez seja melhor não reagir fortemente e citar-me:

> "Uma reação que transferisse para um núcleo duas partículas em um estado com $\lambda = 0, S = 0$ e $T = 1$, onde λ é o momento angular, S o spin e T o isospin, seria uma boa ferramenta para testar as correlações de emparelhamento [4]. As reações diretas (t,p) e (p,t) satisfazem essas exigências e o acúmulo de dados na região dos núcleos médios e pesados trouxe à luz uma variedade de fenômenos: rotação e vibração de emparelhamento, transição de fase de emparelhamento, etc.
> Especificamente, na região próxima a uma camada N_0 duplamente fechada, as reações de transferência de dois nêutrons, tanto *pick-up* quanto *stripping*, apresentam secções de choque para alguns estados com $J^\pi = 0^+$ sensivelmente maiores que as previsões do modelo de camadas puro, indicando que o processo é de natureza coletiva. Além do mais, o espectro de energia dos

[2] $H_{res}^{(qp)} = H_{21} + H_{31} + H_{13} + H_{40} + H_{04}$, onde H_{mn} é escrito em termos de $\left(\alpha^\dagger\right)^m (\alpha)^n$. Fossem todos estes termos levados em conta, recuperaríamos o número de partículas como quantidade conservada (neste caso não teríamos mais a aproximação de campo médio).

estados 0^+, fundamental ou excitados, populados nessas reações assemelha-se (como função do número de massa A) a um espectro vibracional. Isso sugere uma espécie de vibração de emparelhamento em núcleos próximos à camada duplamente fechada (núcleos normais); se dirigirmos nossa atenção para regiões muito afastadas de uma camada fechada (núcleos supercondutores), vemos que a energia do estado fundamental de núcleos vizinhos, como função de A, toma a forma de uma banda rotacional e, novamente, a transição entre elementos de uma banda (adição ou remoção de pares) apresenta-se bastante incrementada em relação às previsões de configuração pura $(j_1 j_2)_{J=0}$, indicando a natureza coletiva dessa transição. Podemos então pensar em rotação de emparelhamento. [....]
O potencial de emparelhamento viola a conservação do número de partículas da mesma forma que os potenciais deformados violam a conservação do momento angular.
Se uma lei de conservação é violada, então podemos distinguir entre as diferentes orientações do sistema físico em algum espaço abstrato (por exemplo, na violação da conservação do momento angular total, no caso dos núcleos com deformação de quadrupolo, é o espaço tridimensional usual). Nesse caso, é possível falar em um sistema intrínseco e num conjunto de ângulos (ângulos de Euler, na deformação de quadrupolo - ângulo de gauge, na deformação de emparelhamento), que define a posição do sistema em relação a um sistema fixo de coordenadas.
A deformação de emparelhamento no sistema intrínseco Δ (o *gap* de emparelhamento) e o ângulo de gauge, podem ser utilizados para parametrizar a distorção de emparelhamento [...]
Em núcleos mágicos, a competição entre os aspectos superfluidos e normais é vencida pelos últimos; as correlações de emparelhamento não são suficientemente fortes para que o próximo nível de partícula independente possa ser atingido; o Δ oscila em torno do valor de equilíbrio zero e as excitações têm caráter vibracional. Entretanto, quando muitos quanta estão presentes, o sistema atinge um estado de deformação permanente (superfluido)..."

Seria perfeito se o nosso objeto de interesse não tivesse apenas dois nêutrons de valência podendo ocupar os orbitais $1p_{1/2}$ e $2s_{1/2}$. De um lado, é satisfeita a condição de rotação de emparelhamento, pois esses nêutrons correspondem à metade da ocupação dos estados disponíveis (semelhante ao que ocorre com os Sn pares com $A \sim 114$, exemplo típico desse fenômeno); por outro lado porém, há poucos pares ativos após a "camada fechada", como no caso dos isótopos pares em torno do ^{208}Pb, que se caracterizam por apresentar vibração de emparelhamento.

Tentando não perder o mote, eu diria que a própria utilização do BCS nesses sistemas difusos, justifica que se fale em deformação, pois se trata de uma teoria

de campo médio, que acarreta na violação de uma simetria do problema, o que implica numa deformação; no caso, deformação no espaço de gauge[3].

3.5. ^{11}Li e BCS

A importância do emparelhamento em sistemas fracamente ligados [4] foi ressaltada por A. Migdal quando o sonho de feixes radioativos era apenas uma miragem [11]. Mais tarde, assumindo que o par de nêutrons formava um *cluster* [12] foi obtido um valor grande para o raio quadrático médio do ^{11}Li.

O modelo que propusemos para o ^{11}Li é o de um caroço de ^{9}Li mais dois nêutrons de valência ocupando os níveis de partícula independente $1p_{1/2}$ e $2s_{1/2}$; a interação residual entre essas partículas de valência é o emparelhamento. O fato do ^{9}Li ser ligado e o ^{10}Li não, significa que os estados de partícula independente a serem ocupados pelo nêutron adicional do ^{10}Li estão no contínuo; isso nos impede de utilizar as energias fenomenológicas na descrição do ^{11}Li. Por outro lado, a contribuição do termo de auto-energia $(-\frac{G}{2}v_j^2)$ é subtrativa, significando que ela torna os níveis de partícula independente mais ligados, podendo trazer para a região discreta estados que, sem sua inclusão, permaneceriam no contínuo. Esse termo, que aparece em qualquer tratamento do problema de muitos corpos interagindo através de forças de um e de dois corpos, é oriundo da própria interação residual, neste caso o emparelhamento; daí ele ser efetivo apenas no ^{11}Li e não no ^{10}Li.

O tratamento desse termo de auto-energia foi feito de modo muito singelo, dando origem a uma variante da equação (3.4)[5]:

$$\tilde{U}_0 = \tilde{\mathcal{E}}_0 + \lambda \sum_j 2\Omega_j \tilde{v}_j^2 = 2\sum_j \left(\varepsilon_j - \frac{G}{2}\right)\Omega_j \tilde{v}_j^2 - G\sum_{ij}\Omega_j(\Omega_i - \delta_{ij})\tilde{u}_i\tilde{v}_i\tilde{u}_j\tilde{v}_j. \quad (3.5)$$

A contribuição do termo de auto-energia dividiu-se agora em duas partes: os níveis de partícula independente foram renormalizados, tornando-se mais ligados, enquanto o novo *gap* de emparelhamento, $\widetilde{\Delta}_j$, não é mais constante mas torna-se

[3] Como estou pretendendo justificar apenas utilização da deformação como linha condutora do texto e não a aplicação da abordagem de BCS ao ^{11}Li, isto talvez seja suficiente. Na verdade, mostramos em [3] que não temos solução supercondutora se $G \geq G_c = \frac{\epsilon}{2\Omega}\left(\frac{1}{1-\frac{1}{2\Omega}}\right)$ (o fator entre parênteses não aparece no tratamento usual. mas apenas no BCS "modificado" que será discutido na próxima seção): com os valores de G que utilizamos nas referências [1, 2], a solução supercondutora existe.

[4] Ou para ser mais exato, a importância da interação residual entre partículas de valência como um mecanismo para tornar ligados estados de partícula situados nas imediações do contínuo.

[5] Um til será usado para indicar que as quantidades são calculadas no BCS "modificado".

dependente de j

$$\widetilde{\Delta}_j = G\sum_i(\Omega_i - \delta_{ij})\tilde{u}_i\tilde{v}_i. \tag{3.6}$$

No primeiro dos trabalhos que publicados nesse assunto [1] exploramos a aplicabilidade das idéias expostas acima; utilizando inicialmente apenas o estado $1p_{1/2}$ verificamos a possibilidade de, utilizando valores realistas de G para essa região diluida, obter a energia de ligação do ^{11}Li; incluindo posteriormente também o $2s_{1/2}$, comparamos esse BCS "modificado" com o cálculo exato, com o cálculo com projeção em número de partículas e, é claro, com o BCS "usual". Mostramos que o estado fundamental do ^{11}Li tem um caráter predominantemente $2s_{1/2}$ ($\tilde{v}^2_{2s_{1/2}} = 0,81$) e estudamos também o comportamento da dispersão $\Delta N/N$.

Num trabalho posterior [2] ocupamo-nos adicionalmente da descrição do primeiro estado excitado desse núcleo que havia sido recentemente observado a uma energia de $E = 1.25$ MeV [10] e estudamos também o efeito da restauração da simetria quebrada devido à aproximação de campo médio[6]. Na sua dissertação de Mestrado, o sr. Baldini Neto estendeu esse BCS "modificado" para muitos níveis e efetou cálculos, ainda para o caso do ^{11}Li; como resultado do seu trabalho, constatamos que, para valores realistas de G, o estado fundamental desse núcleo é ainda predominantemente composto pelo $2s_{1/2}$.

3.6. Sumário

Reportei neste capítulo uma interpretação alternativa para o estado fundamental e para o primeiro estado excitado do ^{11}Li baseada em uma versão modificada do BCS usual. Acredito ter sido mostrado que a interação de emparelhamento usual desempenha um papel importante em núcleos exóticos leves. Na referência [2] é sugerido que uma impressão digital dessa importância seria a detecção do trítio na reação de *pick-up* $^{11}Li\,(p,t)^9\,Li$. Há, sem dúvida, vários aspectos dessa abordagem que estão merecendo alguma atenção da nossa parte; um deles é a aplicação desse esquema a núcleos emissores de prótons e, em particular, calcular fatores espectroscópicos; outro é obter o comportamento da cauda da função de onda do par de nêutrons de valência[7].

[6] Isso foi feito levando em conta a interação residual entre as quase-partículas, H_{qp}; a restauração da simetria foi parcial pois consideramos os pares de quase-partículas como bósons e tratamos a interação residual entre as quase-partículas na aproximação RPA.

[7] M. Kyotoku, C.L. Lima, E. Baldini Neto e N. Teruya, a ser submetido a publicação..

BIBLIOGRAFIA

[1] M. Kyotoku, N. Teruya, and C.L. Lima, Phys. Lett. **B377** (1996) 1. (Em anexo)

[2] M. Kyotoku, C.L. Lima, E. Baldini Neto, and N. Teruya, Mod. Phys. Lett. A **12** (1997) 2883. (Em anexo)

[3] M. Kyotoku, C.L. Lima, E. Baldini Neto, and N. Teruya, em preparação; a ser submetido para publicação no Int. J. Mod. Phys.

[4] R.A. Broglia, O. Hansen, and C. Riedel, Adv. Nucl. Phys. **6** (1973) 287.

[5] B. M. Young, et al.,Phys.Rev. C **49**, (1994) 279.

[6] A. Bohr, B.R. Mottelson, and D. Pines, Phys. Rev. **110** (1958) 1936.

[7] J. Bardeen, L.N. Cooper, and J.R. Schrieffer, Phys. Rev. **108** (1957) 1175.

[8] C.T. Black, D.C. Ralph, and M. Tinkham, Phys. Rev. Lett. **76** (1996) 688; A. Mastellone, G. Falci, and R. Fazio, Phys. Rev. Lett. **80** (1998) 4542; F. Braun and J. von Delft, Phys. Rev. Lett. **81** (1998) 4712.

[9] D. Galetti, B.M. Pimentel, C.L. Lima, and M. Kyotoku, Physica A **262** (1999) 428.

[10] A. A. Korsheninnikov et al.,Phys Rev. C **53**, (1996) R537.

[11] A. B. Migdal, Sov. J. Nucl. Phys. **16**, (1973) 238.

[12] P. G. Hansen and B. Jonson, Europhys. Lett. **4**, (1987) 408.

4. Álgebras e deformações

4.1. Introdução

As álgebras deformadas (q-álgebras ou álgebras q-deformadas, no jargão da área) têm se revelado nos últimos anos uma fértil área de pesquisa; uma grande quantidade de trabalhos foi publicada nesse assunto, tanto em matemática quanto em física. As álgebras deformadas apareceram no cenário da física em torno do início da década passada originalmente em conexão com problemas de modelos solúveis em mecânica estatística e espalhamento quântico inverso. Atualmente, encontram-se aplicações também em redes de spin anisotrópicas, física atômica e molecular, física de partículas, etc. Elas constituem-se numa estrutura matemática elegante, poderosa e em grande parcela ainda inexplorada.

A palavra deformação, tão comum no vocabulário dos físicos nucleares, tem nesta *terra incognita* significados peculiares e distintos daqueles a que estamos acostumados. Aqui, ela pode ser entendida como modificações nas relações de comutação entre os geradores do grupo de simetria do problema, de acordo com prescrições definidas, mas não únicas. A questão é a meu ver mais profunda do que simplesmente estabelecer uma correspondência entre possíveis significados da palavra deformação; o que deve de fato ser perguntado é se as álgebras deformadas permitem a descrição adequada de fenômenos físicos ou se são apenas belas e ricas estruturas matemáticas; colocando o problema de modo um tanto enfático, procura-se saber se elas tem aplicação no mundo físico ou se não passarão do estágio de "uma teoria em busca de uma realidade".

Nosso percurso na tentativa de entender essas novas estruturas começou, *noblesse oblige*, com a aplicação das álgebras deformadas a fenômenos de rotação nuclear; afinal de contas, o espectro dos núcleos rotacionais é, no caso de sistemas rígidos, proporcional ao autovalor do operador de Casimir do grupo $SU(2)$; para nossa decepção, logo nos demos conta de que muito do que estávamos começando a pensar em fazer já havia sido publicado [1, 2]; passamos em seguida ao estudo do emparelhamento nuclear pois, no caso de um único nível fora de uma camada fechada, a hamiltoniana tem uma estrutura de quase-spin; trabalhamos bastante nesse problema, mas fomos atropelados [3]. Concentramo-nos a seguir no estudo de problemas ligados à transição de fase em modelos solúveis.

Não creio que consiga produzir um resumo contendo as idéias básicas de álgebras deformadas muito diferente do que apresentei no *Theoretical Physics Symposium* alguns anos atrás [4]; vou portanto ser bastante sintético em alguns aspectos da discussão, remetendo o leitor para a referência mencionada linhas acima. Acrescentarei porém comentários sobre alguns novos desenvolvimentos ocorridos desde então, especificamente a aplicação de q-álgebras aos modelos BCS e de Nambu-Jona-Lasinio.

Colaborei no tema deste capítulo essencialmente com os profs. D. Galetti e B.M. Pimentel do IFT/UNESP e com meus estudantes srs. V.S. Timóteo e L. Tripodi; sem eles, as publicações em anexo [4, 5, 6, 7, 8] provavelmente não teriam vindo a prelo; vale também citar que o sr. V. S. Timóteo prepara seu doutoramento sobre a aplicação de álgebras deformadas ao modelo de Nambu-Jona-Lasinio[1].

4.2. Motivação científica

Álgebras q-deformadas parecem ser uma ferramenta interessante para a descrição de perturbações a uma simetria de um sistema físico.

Sistemas de muitos corpos são uma arena adequada para a exploração dos (eventuais) significados físicos das álgebras deformadas; não apenas porque os efeitos dessa deformação talvez se manifestem mais claramente em sistemas com múltiplas correlações entre seus constituintes, mas também por ter sido desenvolvido ao longo dos anos pelos cultores desse ramo da física teórica, todo um arsenal de modelos solúveis, artefatos adequadas para testes de modelos e aproximações; isso confere aos sistemas de muitos corpos não só a possibilidade da amplificação dos efeitos da deformação da algebra, mas também o instrumental adequado para a avaliação desses efeitos.

A questão básica que nos formulamos era qual o sentido físico que poderia ser atribuido à q-deformação de uma álgebra e, além disso, como seriam modificadas as propriedades de um sistema sob o efeito dessa q-deformação. Dado o seu caráter universal, escolhemos focar nosso estudo no comportamento de sistemas físicos em torno da transição de fase.

4.3. Álgebras deformadas: algumas aplicações

Talvez a maneira mais eficiente de nos familiarizarmos com a maneira como essas novas estruturas operam seja analisarmos o caso da álgebra do grupo $SU(2)$.

[1] Não posso deixar de também mencionar o sr. J.T. Lunardi; sua dissertação de Mestrado (IFT/UNESP, 1995), orientada pelo prof. B.M. Pimentel, deu origem à referência [6] cujos resultados serão aqui comentados.

A álgebra quântica $su_q(2)$ é uma deformação da álgebra do grupo $SU(2)$; deformação num sentido distinto daquele que estamos acostumados ao falarmos em um núcleo ou molécula não esféricos; trata-se de fato da deformação nas regras de comutação entre os geradores da álgebra conforme alguma prescrição (não unívoca). O quadro abaixo exemplifica uma realização possível da álgebra quântica $su_q(2)$:

$\mathbf{su(2)}$		$\mathbf{su_q(2)}$
$[J_0, J_\pm] = \pm J_\pm$	$\rightarrow$	$[J_0, J_\pm] = \pm J_\pm$
$[J_+, J_-] = 2J_0$	$\rightarrow$	$[J_+, J_-] = [2J_0]_q$

A quantidade entre colchetes $[x]_q$ é definida como

$$[x]_q = \frac{q^x - q^{-x}}{q - q^{-1}} = \frac{\sinh \gamma x}{\sinh \gamma}, \tag{4.1}$$

onde $q = \exp(\gamma)$ pode inclusive ser um número complexo (é claro que quando $q \rightarrow 1$ (ou $\gamma \rightarrow 0$) obtém-se a definição usual).

Correspondentemente, operador quadrático de Casimir é transformado em

$$\mathcal{C}_q = J_\pm J_- + [J_0]_q[J_0 - 1]_q = J_- J_+ + [J_0]_q[J_0 + 1]_q. \tag{4.2}$$

Na sub-seção seguinte será discutida a aplicação dos resultados acima a dois sistemas cuja álgebra é do tipo $SU(2)$.

4.3.1. Física nuclear e molecular

Aplicações singelas de álgebras deformadas ao espectro rotacional de núcleos e moléculas podem ser encontradas nas referências [1, 2, 9] bem como em [4], onde são feitos alguns comentários comparativos acerca dos diferentes esquemas de deformação empregados. É interessante notar que a modificação causada pela q-algebra nos operadores de Casimir produz um efeito equivalente ao da expansão da energia da banda rotacional em potências de $I(I+1)$.

Uma aplicação ao caso do emparelhamento nuclear foi feita em [3]. No caso de um único nível j de valência, a hamiltoniana de emparelhamento pode ser escrita em termos de operadores de quase-spin; reescrevendo-a agora com as relações de comutação da álgebra deformada, e aplicando ao caso dos isótopos pares do ^{40}Ca obtém-se um ajuste bastante razoável para as energias do estado fundamental desses núcleos; sem dúvida, temos um parâmetro a mais, porém parece ser algo mais do que apenas isso: através da q-deformação termos de ordem superior são incorporados de uma forma efetiva na interação residual.

4.3.2. Transições de fase: Lipkin, BCS e Nambu-Jona-Lasinio

Sistemas de partículas que interagem podem passar, sob certas circunstâncias bem definidas, de uma fase "normal" para outra "condensada" com propriedades radicalmente diferentes, como por exemplo na transição gás→líquido, quando a temperatura cai abaixo de um certo limiar, ou então na transição de um material paramagnético→ferromagnético. Neste último caso, acima de uma certa temperatura crítica há apenas ordem local e os spins dos elétrons do material separados por distâncias macroscópicas não se alinham; o sistema está numa fase normal (paramagnética). Abaixo dessa temperatura crítica, correlações de longo alcance ficam efetivas e todos os spins começam a se alinhar e o material sofre uma transição para fase ferromagnética. Nesse exemplo fica explícito também a quebra de simetria: na fase paramagnética todos os spins estão orientados aleatoriamente ao passo que na fase ferromagnética, há uma direção preferencial. Sumarizando, o parâmetro de ordem é a magnetização e a simetria quebrada é a invariância rotacional.

A universalidade dos conceitos de quebra de simetria e transição de fase pode ser ilustrada notando a profunda analogia que existe entre a situação descrita acima e as transições de fase presentes no modelo de Nambu e Jona-Lasinio (NJL) [10]. Neste modelo, férmions sem massa interagem através de uma interação de contato; ele foi proposto em analogia ao que ocorre em supercondutores. A idéia é que da mesma forma que o *gap* de energia em um supercondutor é criado pela interação de emparelhamento, a massa de uma partícula é também devida a algum tipo de interação entre férmions sem massa. No modelo NJL o parâmetro de ordem é o condensado $< \overline{\psi}\psi >$ e no exemplo apresentado no parágrafo anterior é a magnetização. O papel lá representado pela temperatura é aqui desempenhado pelo inverso do acoplamento. Da mesma forma que só há magnetização espontânea para temperaturas menores que a temperatura crítica T_c, os condensados só aparecem quando o acoplamento entre os férmions excede um valor cítico G_c. A quebra explícita da simetria envolvida também tem o mesmo efeito nos dois casos: suprimir a transição de fase. No exemplo acima, quem quebra explicitamente a simetria de rotação é um campo externo H. No modelo NJL quem quebra explicitamente a simetria quiral é uma massa de corrente para os férmions.

A quebra dinâmica de simetria que ocorre no modelo NJL também ocorre no Modelo de Lipkin e no Modelo BCS, embora as simetrias quebradas e os sistemas físicos descritos sejam diferentes. Y. Nambu foi o primeiro a perceber este caráter universal da quebra dinâmica de simetria [10].

Nas duas subseções seguintes apresentarei aplicações de álgebras deformadas aos modelos de Lipkin, BCS e Nambu-jona-Lasinio.

Sistemas fermiônicos: transições de fase em modelos solúveis

Após as aplicações mencionadas na seção 4.3.1, em que o caráter de quase-spin dos operadores foi explorado, era natural que se desse um passo adiante, passando ao estudo da influência da q-deformação quando o caráter fermiônico dos sistemas físicos fosse explicitado.

Galetti e Pimentel [11] haviam estudado anteriormente a influência da q-deformação no modelo de Lipkin[2] [12], deformando apenas os operadores de quase-spin, sem levar em conta a estrutura fermiônica subjacente. A situação complica-se muito quando se tenta tratar explicitamente os graus de liberdade fermiônicos (ou bosônicos) em sistema de muitos corpos. Neste caso, as estranhas características da *terra incognita* mencionada parágrafos atrás manifestam-se em toda sua plenitude. Um dos problemas é que, mesmo no caso sem interação, a hamiltoniana q-deformada (no caso bosônico [13] ou fermiônico [5]) deixa de ser apenas a soma dos termos de partícula independente, mas torna-se uma soma de co-produtos, sendo essa construção essencial para a preservação da simetria da álgebra quando ela for deformada.

Para apreciarmos o que ocorre, o caso bosônico é mais adequado pela sua maior simplicidade. O quadro abaixo compara ambas as situações, deformada e não deformada, no caso de apenas dois osciladores:

usual		**$q-$deformada**
$a^\dagger \lvert n\rangle = \sqrt{n+1}\,\lvert n+1\rangle$	$\rightarrow$	$a^\dagger \lvert n\rangle = \sqrt{[n+1]_q}\,\lvert n+1\rangle$
$a \lvert n\rangle = \sqrt{n}\,\lvert n-1\rangle$	$\rightarrow$	$a \lvert n\rangle = \sqrt{[n]_q}\,\lvert n+1\rangle$
$N \lvert n\rangle = \lvert n\rangle$	$\rightarrow$	$N \lvert n\rangle = n \lvert n\rangle$
$[a_i, a_i^\dagger] = 1$	$\rightarrow$	$a_i a_i^\dagger - q a_i^\dagger a_i = q^{-N_i}$
$H = h_1 + h_2$	$\rightarrow$	$H = H_1 + H_2$
		$\hookrightarrow H = \dfrac{\sinh\left(\frac{1}{2}\gamma\,(h_1+h_2)\right)}{2\sinh\left(\gamma/2\right)}$

onde, $N_i = a_i^\dagger a_i$, $h_i = N_i + \frac{1}{2}$ e $H_i = \frac{1}{2}([h_i + \frac{1}{2}]_q + [h_i - \frac{1}{2}]_q)$; $i = 1, 2$. Passando ao largo da obtenção da hamiltoniana de Lipkin q-deformada no nível fermônico, por ser muito técnica, abaixo são comparadas as situações não deformada e deformada no caso do modelo de Lipkin [5]

[2] Que pertence à classe dos modelos solúveis a que me referi na seção 4.2; sua hamiltoniana pode ser escrita em termos de operadores de quase-spin e uma de suas características mais interessantes é a de apresentar uma transição de fase de segunda ordem.

usual	q-deformada
$H = \epsilon S_0 + \frac{V}{2}(S_+^2 + S_-^2)$	$\rightarrow \quad H = \frac{\epsilon}{4\sinh\frac{\gamma}{2}} \sinh(2\gamma S_0^q) + \frac{V}{2}\left[(S_+^q)^2 + (S_-^q)^2\right]$

onde S_0, S_+, S_- (S_0^q, S_+^q, S_-^q) são os operadores de quase-spin usuais (q-deformados). Vê-se que os efeitos da q-deformação manifestam-se também no próprio campo médio; este comportamento não aparece quando se deforma o modelo de Lipkin apenas no nível dos operadores de quase-spin [11].

Usando a hamiltoniana de Lipkin q-deformada, o comportamento da transição de fase foi estudado; como um resultado marcante, verificamos que o valor crítico da constante de acoplamento depende de q; ou seja, ela não tem mais um caráter universal, deixando de ser uma característica da transição de fase, independente do sistema [5]. Os efeitos da inter-relação entre a deformação da álgebra e a temperatura foram posteriormente analisados [6]; a temperatura crítica mostrou apresentar uma forte dependência com a deformação da álgebra, indicando uma vez mais que conclusões acerca do comportamento da transição de fase têm que ser tomadas com cuidado, se o conceito de álgebras deformadas tem algum sentido físico.

Álgebras deformadas em física de hádrons

A referência [11] contém um resultado interessante: a supressão da transição de fase de segunda ordem com o aumento da q-deformação. Isso apresenta alguma semelhança com o que ocorre no modelo de Nambu-Jona-Lasinio (NJL) [10] quando é atribuida uma massa diferente de zero ao quark de corrente [14].

Essa similaridade chamou-me a atenção, mas não me senti com forças para atacar imediatamente o caso NJL; pareceu-me adequado proceder a um estudo preliminar em uma situação aparentemente mais controlável. Dessa forma resolvi abordar antes, e mais uma vez, o modelo BCS [7]

A deformação da hamiltoniana de emparelhamento para a obtenção da versão q-deformada do BCS[3] foi feita no nível fermiônico usando o esquema proposto

[3] Vou continuar usando o mesmo jargão que vinha empregando até agora; porém, na referência [7] usou-se, de fato, um procedimento covariante com relação a transformações de grupo especificadas, ao invés de uma generalização - i.e. deformação - das relações de comutação que definem a álgebra. O que obtivemos foi uma versão q-covariante do BCS e não uma versão q-deformada. Sob esse ponto de vista, o esquema adotado em [7] e que foi usado posteriormente em [8] é mas geral.

por Ubriaco [15]. Há aqui uma inconsistência em relação aos trabalhos sumarizados anteriormente, pois esse esquema de deformação é distinto do utilizado no modelo de Lipkin[4]. Sem dúvida, parte da responsabiblidade pela inconsistência pode ser creditada ao autor, uma vez que ele pressurosamente usou o esquema de deformação que lhe pareceu mais conveniente, mas, sob uma perspectiva mais geral, isto está mais ligado à não univocidade de procedimentos para efetuar a q-deformação e que foi aludida brevemente no início desta seção.

Utilizando então o esquema de Ubriaco, que estudou as propriedades termodinâmicas de um sistema fermionico deformado com dois apenas sabores, pudemos obter as seguintes correspondências:

BCS usual		**BCS q-deformado**
$\|BCS\rangle = \prod_{jm>0} [u_j + v_j c^\dagger_{jm} c^\dagger_{j-m}] \|0\rangle$	$\rightarrow$	$\|BCS\rangle_q = \prod_{jm>0} [u^q_j + v^q_j C^\dagger_{jm} C^\dagger_{j-m}] \|0\rangle_q$
c_{jm}	$\rightarrow$	$C_{jm} = c_{jm} \prod_{i=m+1}^{j} (1 + (q^{-1} - 1) c^\dagger_{ji} c_{ji})$
$c^\dagger_{jm}$	$\rightarrow$	$C^\dagger_{jm} c^\dagger_{jm} \prod_{i=m+1}^{j} (1 + (q^{-1} - 1) c^\dagger_{ji} c_{ji})$

O vácuo $|0\rangle_q$ é, a menos de uma constante, idêntico ao vácuo usual. Os resultados obtidos na referência [7] mostram que o *gap* deformado (de fato, *gap* quântico, como o denominamos) depende explicitamente do parâmetro de deformação, diminuindo à medida que a deformação cresce e que o sistema colapsa no seu estado fundamental quando q vai a zero (i.e. o *gap* vai a infinito, impossibilitando excitações do sistema).

Um esquema semelhante foi utilizado no modelo de Nambu-Jona-Lasinio. Neste modelo, fermions sem massa são descritos por uma lagrangiana invariante por simetria quiral. O modelo NJL é muito útil para estudar a quebra da simetria quiral e a geração de uma massa dinâmica para os quarks com o aparecimento dos condensados. Formalizando um pouco o que foi mencionado sobre esse modelo, sua lagrangiana é dada por

$$\mathcal{L}_{NJL} = \overline{\psi} i \gamma^\mu \partial_\mu \psi + \mathcal{L}_{int} + \boxed{\mathcal{L}_{mass}}, \tag{4.3}$$

onde

$$\mathcal{L}_{int} = G \left[\left(\overline{\psi} \psi \right)^2 + \left(\overline{\psi} i \gamma_5 \tau \psi \right)^2 \right]. \tag{4.4}$$

[4] Não creio que seja possível reduzir um no outro.

$\mathcal{L}_{NJL}$ é invariante por simetria quiral, desde que o termo adicional $\mathcal{L}_{mass} = -m_q \langle \overline{\psi}\psi \rangle$, que aparece dentro da moldura, seja zero. Assumindo $m_q = 0$, i.e. férmions com massa de corrente nula, temos soluções não triviais para a equação de *gap*

$$m = \frac{2Gm}{\pi^2} \int_0^\Lambda dp \frac{\mathbf{p}^2}{\sqrt{\mathbf{p}^2 + m^2}} = -2G < \overline{\psi}\psi >, \tag{4.5}$$

quando $G > G_{crítico}$. A inclusão de $m_q \neq 0$, que corresponde à quebra explícita da simetria quiral, alisa a transição de fase.

Estendendo os procedimentos descritos em [7] a este sistema, obteve-se

$$m = \frac{2Gm}{\pi^2} \left[\left(1 - \frac{Q}{2}\right) \int_0^\Lambda dp \frac{\mathbf{p}^2}{\sqrt{\mathbf{p}^2 + m^2}} + \frac{Q}{2} \int_0^\Lambda dp \frac{p^3}{\mathbf{p}^2 + m^2} \right] \tag{4.6}$$

que é a equação de *gap* deformada; $Q = q^{-1} - 1$.

Tentando sumarizar os resultados obtidos, estudamos a deformação da álgebra do modelo de NJL no caso de apenas dois sabores e investigamos a geração de massa dinâmica. O efeito principal da deformação é o de aumentar de modo efetivo a constante de acoplamento da interação de quatro férmions do modelo de NJL.Contrariamente às nossas expectativas iniciais, a transição de fase ainda era aguda na região em torno do ponto crítico.

4.4. Sumário

Vou fazer um breve sumário deste capítulo; como em [4] as conclusões serão divididas em gerais e específicas.

Quanto às conclusões gerais, creio que a q-deformação pode trazer à luz algum tipo de física diferente; em particular, os resultados que estão sendo obtidos com o modelo NJL[5] sugerem que as álgebras deformadas são candidatas em potencial para gerar um esquema que englobe tanto a quebra espontânea quanto a quebra explícita de simetria, gerando tanto massa dinâmica quanto massa de corrente. Em alguns sistemas simples é possível atribuir um significado físico para o parâmetro de deformação, como por exemplo no caso da descrição da rotação de núcleos ou moléculas; entretanto, parece ser impossível atribuir um sentido único a esse parâmetro q. A riqueza estrutural dessas álgebras, por outro lado, permite que se busque aquela adequada às peculiaridades de um dado sistema físico. Adicionalmente, a q-deformação permite incorporar efetiva e elegantemente a interação residual entre os constituentes do sistema.

[5] Estamos concluindo um trabalho onde, ao invés de deformar o condensado, como fizemos em [8], a deformação é feita diretamente na Hamiltoniana.

Apresentando agora as conclusões particulares, sistemas de muitos corpos exigem que se efetue a deformação já no nível bosônico ou fermiônico, pois a q-deformação dá origem a um campo médio que depende de q. Nos fenômenos envolvendo transições de fase, há que agir com cuidado, pois o valor crítico da constante de acoplamento não tem mais um caráter universal como um indicador, independente do sistema, da ocorrência da transição de fase; a inclusão da temperatura não altera este comportamento geral. Nossa abordagem ao modelo de NJL q-deformado mostrou mais uma vez que os efeitos da deformação incrementam as correlações no sistema levando, neste caso, a um aumento do valor do condensado.

BIBLIOGRAFIA

[1] S. Iwao, Prog. Theor. Phys. **83**, 363 (1990).

[2] D. Bonatsos, E.N. Argyres, S.B. Drenska, P.P. Raychev, R.P. Roussev, and Yu.F. Smirnov, Phys. Lett. **B251** (1990) 477.

[3] S. S. Sharma, Phys. Rev. **C46** (1992) 904.

[4] D. Galetti, J.T. Lunardi, B.M. Pimentel, and C.L. Lima, "Q-deformed algebras in many-body physics" publicado nos Anais do "Theoretical Physics Simposium" realizado em comemoração aos 70 anos do Prof. Paulo Leal Ferreira, Eds. V.C. Aguilera-Navarro, D. Galetti, B.M. Pimentel e L. Tomio, (IFT, São Paulo, Brasil, 1995). (Em anexo)

[5] S.S. Avancini, A. Eiras, D. Galetti, B.M. Pimentel, and C.L. Lima, J. Phys. **A28** (1995) 4915. (Em anexo)

[6] D. Galetti, J.T. Lunardi, B.M. Pimentel, and C.L. Lima, Physica A **242** (1997) 501. (Em anexo)

[7] L. Tripodi and C.L. Lima, Phys. Lett **B412** (1997) 7. (Em anexo)

[8] V.S. Timóteo and C.L. Lima, Phys. Lett. **B448** (1999) 1. (Em anexo)

[9] R.H. Capps, Prog. Theor. Phys. **91**, (1994) 835.

[10] Y. Nambu and G. Jona-Lasinio, Phys. Rev. **122** (1961) 345.

[11] D. Galetti and B.M. Pimentel, Ann. Acad. Bras. Cien. **64** (1994) 1.

[12] H.J. Lipkin, N. Meshkov, and A.J. Glick, Nucl. Phys. **62** (1965) 132.

[13] E.G. Floratos, J. Phys. A **24** 4739 (1990).

[14] U. Vogl and W. Weise, Prog. Part. Nucl. Phys. **27** (1991) 195.

[15] M. R. Ubriaco, Phys. Lett. **A219** (1996) 205.

5. Comentários finais

Algumas palavras, fruto de uma análise retrospectiva do texto, talvez caiam bem. Esta revisão ficou longa, maior do que eu havia planejado, mesmo tendo eu tentado apresentar pouquissimos detalhes técnicos e concentrado a discussão nos aspectos mais gerais.

Ela resultou também não uniforme. O capítulo 2 ficou maior e com um estilo distinto dos demais; nele, a ênfase foi colocada na descrição da física dos modelos que foram utilizados na interpretação dos resultados experimentais obtidos; nele, praticamente não estão expressas as perplexidades, os desvios e os problemas que, de quando em vez, afloram nos outros capítulos. Pensei em redigí-lo novamente mas logo constatei que talvez não fosse possível e, quiçá, nem mesmo correto. Ocorre que assim escrito ele espelha melhor a realidade; nos problemas de pesquisa relatados nos demais capítulos, os graus de liberdade que eu dispunha eram maiores; os problemas estavam em aberto e, de certa forma, eu podia arbitrar para onde eles iriam (embora temo que, às vezes, o problema tenha criado vida própria e decidido qual caminho tomar); meu controle era aparentemente maior. No caso do capítulo 2, centrado na minha colaboração com o Grupo γ do Laboratório Pelletron, os problemas já estavam prontos: os dados existentes eram os que haviam sido tomados, os núcleos estudados eram os possíveis e conseqüentemente a minha margem pessoal de manobra muito menor. Tivesse sido outra a minha atuação, qual seja, a de buscar desenvolver novos modelos para esse tipo de física, outra teria sido a situação; ocorre porém que o nível de sofisticação que os meus colegas experimentais dessa área têm, supera de muito os modelos rudimentares que, pelo menos num primeiro momento, eu talvez fosse capaz de propor. Há nessa área, na minha opinião, um descompassso entre a qualidade do que se pode medir e do que se consegue calcular (mantenho essa frase, mesmo sabendo da competência dos colegas teóricos que trabalham nesse assunto e da excepcional qualidade de alguns cálculos existentes no mercado).

Os demais capítulos relatam tentativas de fazer física com um grau menor de sofisticação técnica mas com alguma engenhosidade, tentando aplicar idéias simples em situações novas.

Olhando em retrospecto, trabalhei em assuntos bastante distintos nos últimos anos e talvez tivesse produzido mais (pelo menos em quantidade) se houvesse

me concentrado em um único assunto. Pessoalmente porém, creio o modo como procedi foi mais divertido e deu-me maior prazer. Entendo ser isso o que vale.

ANEXOS

Anexos ao Capítulo 2

Nuclear Physics A569 (1994) 547–561
North-Holland

NUCLEAR
PHYSICS A

Shape transition in odd–odd $A \approx 130$ nuclei

M.A. Rizzutto, E.W. Cybulska, L.G.R. Emediato, N.H. Medina, R.V. Ribas, K. Hara [1]

Laboratório Pelletron, Departamento de Física Nuclear, Instituto de Física, Universidade de São Paulo, São Paulo, Brazil

C.L. Lima

Nuclear Theory and Elementary Particle Phenomenology Group, Instituto de Física, Universidade de São Paulo, São Paulo, Brazil

Received 24 November 1992
(Revised 17 May 1993)

Abstract

A systematic analysis of rotational bands in doubly odd nuclei in the mass region $A = 130$–140 is carried out using a shell model configuration mixing approach. The shell model (many-body) basis is constructed by projecting out deformed quasiparticle (Nilsson + BCS) states onto good angular momenta. The hamiltonian is assumed to be a sum of (spherical) single-particle hamiltonian and a schematic two-body interaction, which consists of $Q \cdot Q$ + (monopole) pairing + quadrupole-pairing forces. The analysis indicates a shape transition from prolate ($N = 73$) to oblate ($N = 79$) shape as a function of neutron number. Agreement between theoretical results and experimental data is quite satisfactory except for γ-deformed nuclei ($N = 75$ and 77).

1. Introduction

In recent years there has been a veritable avalanche of publications about high spin states in doubly odd nuclei in the 130 mass region [1]. This surge of interest is mainly due to a rather special characteristic of these nuclei, namely, the Fermi levels for neutrons and protons lie at the top and bottom of the intruder subshell $h_{11/2}$, respectively, resulting in semidecoupled bands in these odd–odd nuclei, characterized by small staggering. Experimentally, strong bands with the above properties have been observed in this mass region and the $\pi h_{11/2} \otimes \nu h_{11/2}$ configuration was therefore attributed to them. Leander et al. [2] suggested that the effect of this configuration is to produce shape-driving forces on the nuclear core which, in the case of protons, tend to drive the nuclei toward prolate shapes with $\gamma = 0°$, while for the neutron they tend to drive the nuclei toward oblateness with $\gamma = -60°$ (in the Lund convention). In the odd–odd nuclei the driving forces, produced by the valence nucleons, compete between themselves, which may lead to triaxial shapes.

[1] Permanent address: Physics Department, Technische Universität München, W-8046 Garching, Germany.

SSDI 0375-9474(93)E0318-3

Most of the experimental data in this region was interpreted within the framework of the cranked shell model (CSM). Total routhian calculations show an overall result of prolate shapes with small triaxiality ($-10° \leqslant \gamma \leqslant 2°$).

In this paper we present calculations using a model based on a microscopic hamiltonian with schematic forces and projection onto a good angular momentum [3], applied to the 130 mass region, focussing on the experimental results obtained in the Pelletron Laboratory. These calculations show a definite shape transition, from prolate to oblate, as a function of increasing neutron number. This effect was not evidenced by the CSM analysis.

In sect. 2 we review a shell model theory based on the projected shell model (PSM), in sect. 3 the numerical results are presented and a comparison with the experimental data is discussed. Concluding remarks follow in sect. 4.

2. Summary of the theory

The hamiltonian employed in the present work is

$$\hat{H} = \hat{h} - \tfrac{1}{2}\chi \sum_{\mu} \hat{Q}^{+}_{\mu}\hat{Q}_{\mu} - G_M \hat{P}^{+}\hat{P} - G_Q \sum_{\mu} \hat{P}^{+}_{\mu}\hat{P}_{\mu}, \tag{1}$$

composed of the single-particle spherical shell model hamiltonian ($\hat{h}$), the $\hat{Q}\cdot\hat{Q}$, monopole- and quadrupole-pairing forces.

The strength of the $\hat{Q}\cdot\hat{Q}$ interaction (χ) is adjusted in such a way that the known quadrupole deformation parameter [4] can be obtained as a result of the Hartree–Fock–Bogolyubov self-consistent procedure. The pairing force constant G_M was adjusted to give the known energy gap and G_Q was taken to be proportional to G_M, with a proportionality constant 0.20 for all nuclei in this mass region ($A \approx 130$), which corresponds to the best fits. Smaller values of G_Q result in a much larger staggering than experimentally observed, and in a significant decrease in the absolute values of the energy levels. Similar effects have been seen in (i) odd rare-earth nuclei where it has been shown that the quadrupole pairing force attenuates the strength of the Coriolis force [5]; (ii) in even–even nuclei the same force is also responsible for reproducing the correct band crossing [6].

A characteristic feature of the theory is the shell model in a broader sense, which allows a choice of the many-body basis, according to the physical importance of the states. We select a basis that contains only those states which are essential to the physics we want to describe (e.g. low energies or moderate spins). Thus, the configuration space in which the hamiltonian is to be diagonalized is small in comparison to the standard shell model. This makes not only numerical calculations feasible but also facilitates the interpretation of the results even for heavy nuclei. We stress here that this approach is a fully quantum mechanical theory in which the eigenvalues and eigenstates of the hamiltonian are computed in a truncated basis. The main difference between this approach and the usual shell model is that the truncation is done in a physically motivated way.

Before constructing the shell model basis appropriate for the diagonalization, we must

establish the quasi-particle basis. This is done by using the BCS representation built upon a Nilsson single-particle basis fixed by the deformation parameter of the nucleus in question. The deformed quasi-particle basis is advantageous over the usual spherical basis because the main part of the correlations on the average is taken already into account.

The many-body states are classified by the number of quasi-particles (0, 2, 4, ... for even or 1, 3, 5, ... for odd systems), which will define a natural hierarchy of the configuration. However, some symmetries of the original system such as the rotational and gauge invariances are violated (the angular momentum and particle number, respectively, are no longer good quantum numbers). Fortunately, states with good angular momentum can be restored with the help of projection operators, while the particle number is restored on the average by a Lagrange multiplier, as is usually done in BCS theory.

The angular momentum projection operator is given explicitly by the expression

$$\hat{P}^I_{MK} = \frac{2I+1}{8\pi^2} \int \mathrm{d}\Omega \, \hat{R}(\Omega) \hat{D}^I_{MK}(\Omega) , \tag{2}$$

where $\hat{R}(\Omega)$ is the rotation operator, $\hat{D}^I_{MK}(\Omega)$ the D-function (irreducible representation of the rotation group) and Ω the Euler angle. It commutes with all scalar operators (e.g. hamiltonian) and has the following property:

$$\hat{P}^I_{KK'} = \hat{P}^I_{K'K} = \hat{P}^I_{KM} \hat{P}^I_{NK'} \delta_{IJ} \delta_{MN} . \tag{3}$$

Thus, for a quasi-particle state $|\phi_k\rangle$ we generate the corresponding state having a good angular momentum I by $\hat{P}^I_{MK}|\phi_k\rangle = |\Psi^{Ik}_{MK}\rangle$. In this way we construct the new shell model basis in which the hamiltonian is diagonalized.

It is therefore quite easy to select physically important configurations to be used as a basis of the shell model calculations. There are some advantages in this approach in comparison to the usual spherical shell model. In the first place the vector addition of angular momenta, an awkward procedure in the usual shell model, is done automatically by the projector irrespective of the number of quasi-particles involved. Secondly, projected states constructed by using few quasi-particles span already a reasonably large shell model basis because of the above mentioned hierarchy of the quasi-particle states while, in the usual shell model, all possible configurations that result from the active nucleon degrees of freedom (no hierarchy known for deformed systems) have to be taken into account.

The shell model basis taken in the present work is as follows:

$$\hat{P}^I_{MK}|\phi_k\rangle , \tag{4}$$

where $|\phi_k\rangle$ represents one of the following quasi-particle states:

$$a^+_\nu \, a^+_\pi |0\rangle . \tag{5}$$

Here, a^+_ν (a^+_π) is the neutron (proton) quasi-particle creation operator, constructed in the Nilsson + BCS representation, and $|0\rangle$ is the quasi-particle vacuum state. The neutron (proton) single-particle basis extends over three major shells $N = 3, 4, 5$.

TABLE 1
Parameters used in the PSM model calculations

Nuclei	G_Q	Δ_n (MeV)	Δ_p (MeV)	ϵ_2
^{130}La	0.20	1.01	0.93	+0.22
^{132}La	0.20	0.96	0.94	+0.20
^{134}La	0.20	0.96	0.96	+0.18
^{136}Pr	0.20	0.95	0.97	+0.18
		0.96	1.03	−0.18
^{138}Pr	0.20	0.86	1.01	+0.16
		0.70	1.06	−0.16

The space spanned by basis (4) contains too many unimportant states if we let the labels (ν's and π's) run over all active Nilsson states since most of them have very large excitation energies. So, we take only those which are close to the neutron and proton Fermi level.

An eigenstate of the hamiltonian in this basis is expanded as follows:

$$|\Psi_M^I\rangle = \sum_k f_k \hat{P}_{MK}^I |\phi_k\rangle . \tag{6}$$

The eigenvalue equation (for a given spin I) then takes the form

$$\sum_{k'} (H_{kk'} - E N_{kk'}) f_{k'} = 0 , \tag{7}$$

where

$$H_{kk'} = \langle \phi_k | \hat{H} \hat{P}_{KK'}^I | \phi_{k'} \rangle , \quad N_{kk'} = \langle \phi_k | \hat{P}_{KK'}^I | \phi_{k'} \rangle . \tag{8}$$

The rotational energy of a band k, before diagonalization, is defined by

$$E_k^I = \frac{\langle \varphi_k | \hat{H} \hat{P}_{KK}^I | \phi_k \rangle}{\langle \varphi_k | \hat{P}_{KK}^I | \phi_k \rangle} = \frac{H_{kk}}{N_{kk}} . \tag{9}$$

It represents the expectation value of the hamiltonian with respect to a projected quasi-particle state k. A diagram in which rotational energies of various bands are plotted as functions of spin I will be referred to as a band diagram.

3. Application to the $A \approx 130$ mass region

We have performed extensive calculations with the above mentioned model (PSM) for a number of doubly odd and odd mass nuclei in the mass region $A \simeq 130$, with an emphasis on the experimental results of ^{130,132,134}La [7,8,1] and ^{136,138}Pr [1,9] obtained at the Pelletron Laboratory, University of São Paulo.

The parameters used in these calculations (see Table 1) were adjusted to this light rare-earth mass region, and the single particle basis included three major shells $N = 3, 4$ and 5 for protons and neutrons. The best value for G_Q was found to be 0.20. The Fermi

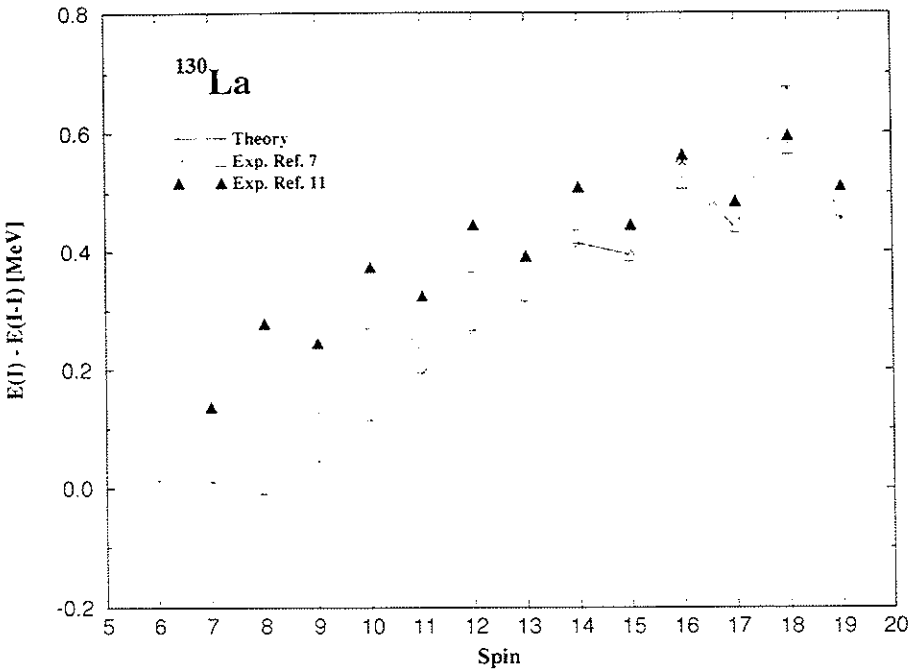

Fig. 1. Comparison of the theoretical calculations (asterisk) for the 55 band of ^{130}La with the experimental points from ref. [7] (open triangle) and ref. [11] (full triangle).

level was adjusted to the number of protons and neutrons in each nucleus and the value of the gap parameter was taken to be approximately 1.0 MeV. The best agreement with the experimental data for the quadrupole deformation parameter ϵ_2 was obtained with the values taken from the systematics of the region [1], while the hexadecapole deformation parameter was set equal to zero.

In the following discussion, the results of the calculations are subdivided into three groups according to the deformation of the nucleus.

3.1. $N \leqslant 75$

The nucleus ^{130}La was studied extensively [7,10,11] in several laboratories. The calculations for a band in which the odd particles occupy $N_n = 5$ and $N_p = 5$ shells (henceforth called 55 band) for ^{130}La ($\epsilon_2 = +0.22$) are presented in Fig. 1, together with the experimental data from refs. [7,11], where the $\pi h_{11/2} \otimes \nu h_{11/2}$ configuration was assigned to the yrast band. Very good agreement was obtained between the Pelletron data [7] and the theory, reproducing the observed staggering and confirming the attribution of spin 8^+ to the bandhead. It is to be emphasized that the Pelletron [7], Stony Brook [10] and Liverpool data [11] are essentially the same concerning transition energies of the two bands. The main difference between the Liverpool results and the other two appears in

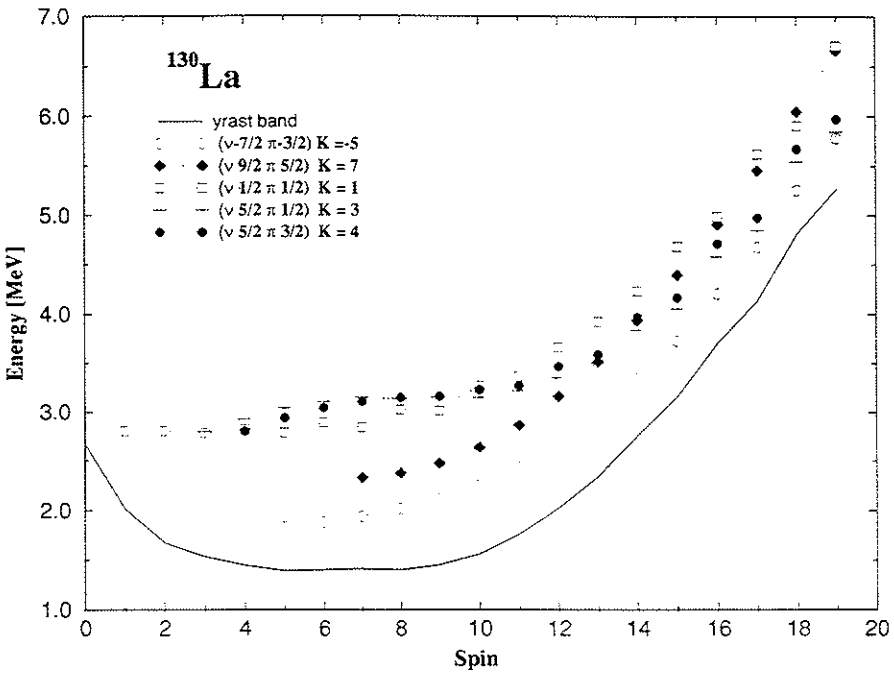

Fig. 2. Band diagram for the 55 configuration of ^{130}La. The yrast band is shown with full line in order to emphasize the staggering at higher spins. All the projection assignments and the corresponding K values belong to the $\nu h_{11/2} \otimes \pi h_{11/2}$ configuration, except for $K = 1$ which is $\nu f_{7/2} \otimes \pi h_{11/2}$.

the spin assignments.

An analysis of the corresponding band diagram for each nucleus is useful in order to investigate the configuration of the band. Rotational band energies versus spin, for the most relevant K values of the 55 band in ^{130}La are plotted in Fig. 2. The thick line represents the yrast energies after diagonalization, while the other curves represent some of the principal rotational bands before diagonalization for different K values ($K = K_\pi \pm K_\nu$). The lower lying curves (circles and diamonds) show a smooth behaviour and correspond to large K values, whereas if K is small and either or both K_ν and K_π, are $\frac{1}{2}$ or $\frac{3}{2}$, a zig-zag-like behaviour is observed, which is equivalent, in the Bohr model, to the decoupling effect and is responsible for the staggering in the yrast band.

The configuration of the above band is not a simple one. The lowest lying energy of the yrast band (Fig. 2) corresponds to the bandhead spin 8^+, with a mixed configuration of several states, the most important being $\nu h_{11/2}(\frac{7}{2}) \otimes \pi h_{11/2}(\frac{3}{2})$ and $\nu h_{11/2}(\frac{9}{2}) \otimes \pi h_{11/2}(\frac{5}{2})$, $K = -5$ and 7, respectively. At higher spins the bands $K = 3$ and 4 (configurations $\nu h_{11/2}(\frac{5}{2}) \otimes \pi h_{11/2}(\frac{1}{2})$ and $\nu h_{11/2}(\frac{5}{2}) \otimes \pi h_{11/2}(\frac{3}{2})$) cross the $K = 7$ band, becoming thus more important and responsible for the small staggering that appears in the yrast band. The $K = 1$, $\nu f_{7/2}(\frac{1}{2}) \otimes \pi h_{11/2}(\frac{1}{2})$ configuration, with a small zig-zag of an opposite phase, has no overall effect on the yrast curve. It should be remembered that the K assigned to

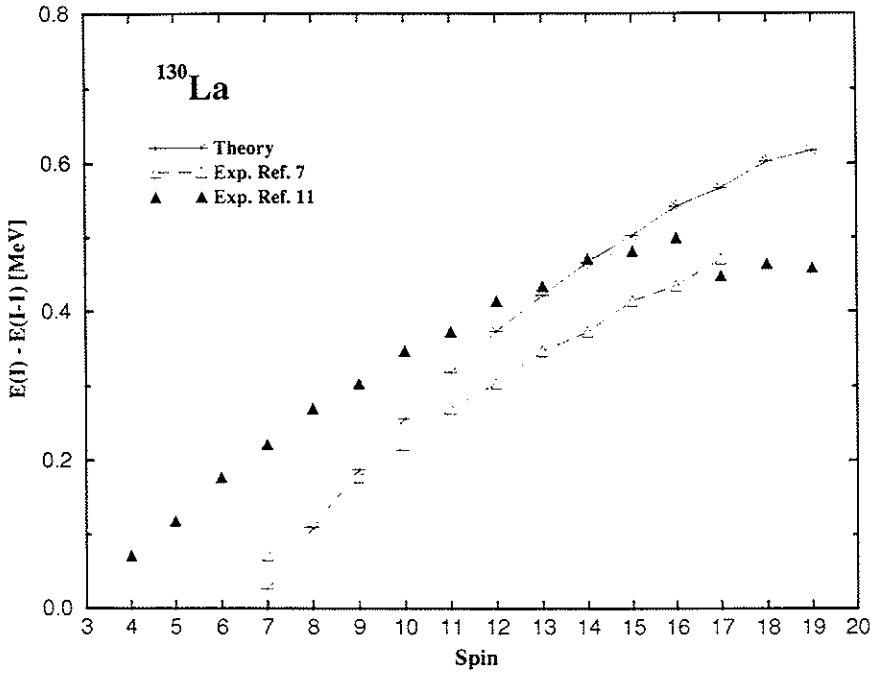

Fig. 3. Same as Fig. 1 for the 45 band.

each band is not a quantum number in the strict sense. In fact, after diagonalization, all K's are mixed. K is not even an asymptotic quantum number; it simply characterizes the intrinsic states.

In a similar way, the bands 54, 45 and 44 were calculated for the above nucleus. The results for the 45 band in ^{130}La are shown in Fig. 3. The general tendency of the experimental results is well reproduced, although in absolute terms the agreement is not as good as in the 55 band. Again, one can see that the spin assignment of the Pelletron data [7] agrees better than that of the Liverpool data [11]. In the above 45 band the experimental data reveal no significant staggering, indicating that small $K_{\nu,\pi}$ components do not contribute considerably to the final result, which is confirmed by the theoretical calculations. An examination of the corresponding band diagram shows that the structure of this band consists mainly of $\nu g_{7/2}(\frac{7}{2}) \otimes \pi h_{11/2}(\frac{3}{2})$ and $\nu g_{7/2}(\frac{7}{2}) \otimes \pi h_{11/2}(\frac{1}{2})$ configurations. The 54 and 44 bands have shown no similarity whatsoever to the experimental data and were therefore discarded as candidates for the configuration of the observed bands.

A similar agreement between theory and experiment is shown in Fig. 4 for ^{132}La [8] ($\epsilon_2 = +0.20$), although lack of experimental data for higher spins makes the comparison less significant. Similarly no theoretical fit was possible for the second band, due to an even smaller number of experimental points at higher spins.

The same calculations were also performed for other nuclei, namely for ^{128}La ($\epsilon_2 =$

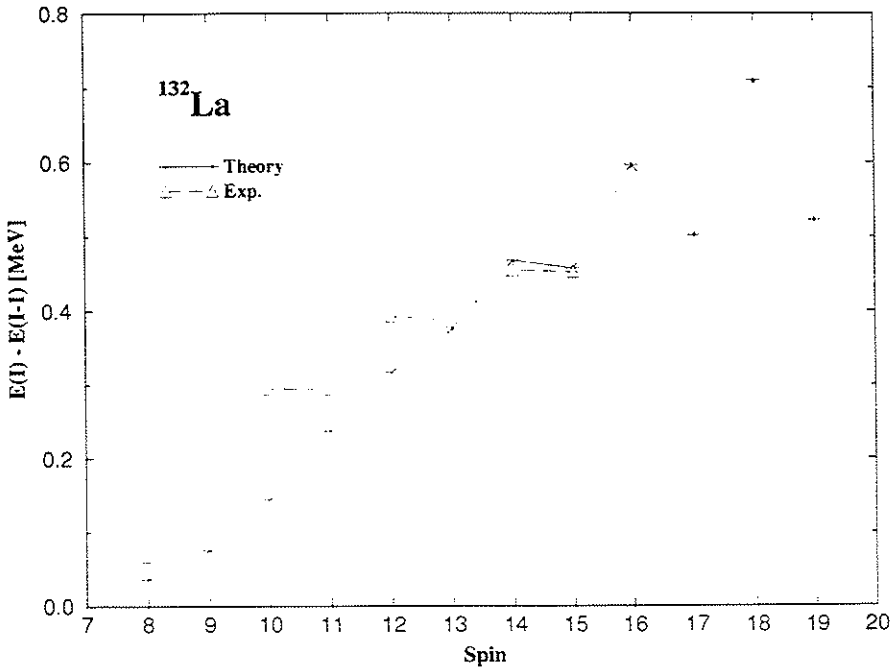

Fig. 4. Comparison of the theoretical calculations (asterisk) for the 55 band of ^{132}La with the experimental points from ref. [8] (open triangle).

+0.24) [11], ^{130,132}Pr ($\epsilon_2 = +0.24$ and 0.22 respectively) [12,13] and very similar results to ^{130}La were obtained for the 55 and 45 bands. In ^{134}Pr ($\epsilon_2 = +0.20$) [14] the 55 band shows an analogous agreement with the data, whereas no agreement was possible for the second band. This may be explained by the fact that the band under consideration was observed only above the backbend, with an attributed four quasi-particle configuration, while the basis used in the present calculations consists of two quasi-particles.

3.2. $N = 79$

The data of the most recently studied nucleus ^{138}Pr [9], consists essentially of three bands. The theoretical analysis of the yrast band (attributed configuration $\nu h_{11/2} \otimes \pi h_{11/2}$), showed equally good agreement for both positive and negative values of the deformation parameter ($\epsilon_2 = 0.16$), see Fig. 5. This can be understood in terms of the unique behaviour of the $h_{11/2}$ intruder Nilsson subshell and by the location of the Fermi levels for this nucleus. The $h_{11/2}$ levels are symmetric with respect to zero deformation, while the neutron and proton Fermi levels are situated at the very top and bottom of the above subshell. The oblate deformation was chosen for the 55 band (see the discussion below). The corresponding band diagram (Fig. 6) indicates that, at low spins, the significant configurations are $\nu h_{11/2}(\frac{1}{2}) \otimes \pi h_{11/2}(\frac{11}{2})$ and $\nu h_{11/2}(\frac{1}{2}) \otimes \pi h_{11/2}(\frac{9}{2})$ with the

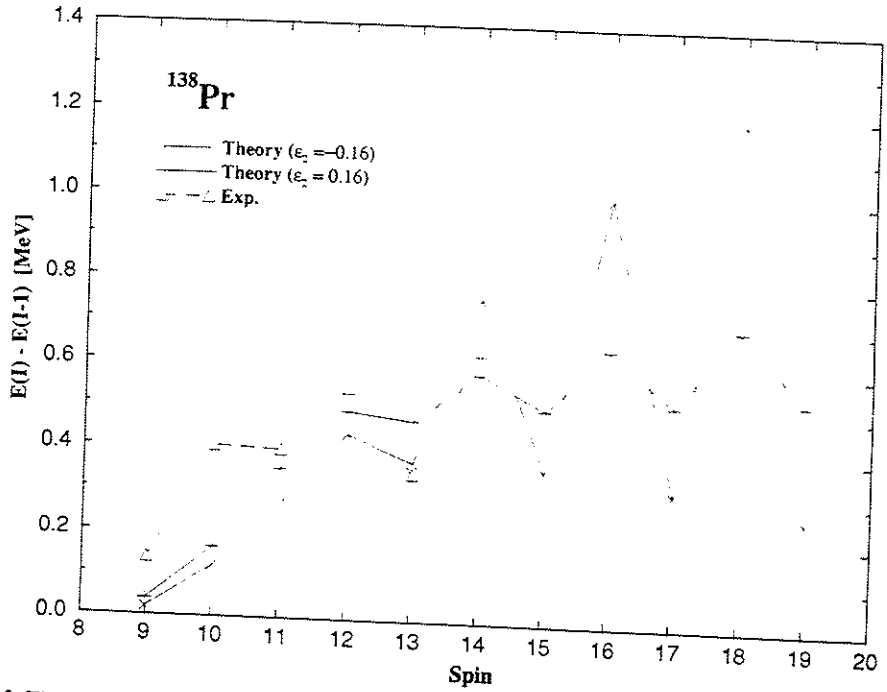

Fig. 5. Theoretical calculations for the 55 band of ^{138}Pr for oblate deformation $\epsilon_2 = -0.16$ (cross) and prolate deformation $\epsilon_2 = 0.16$ (plus) as compared to experimental points from ref. [9] (open triangle).

bandhead spin of 8^+, in agreement with ref. [9]. At higher spins the $\nu h_{11/2}(\frac{1}{2})\otimes\pi h_{11/2}(\frac{5}{2})$ configuration predominates, producing staggering in the yrast curve. Unfortunately the experimental data stops at spin 14 and just indicates the predicted staggering.

Based on the systematics of odd-A neighbouring nuclei [15–17] an oblate deformation was assumed for the second doubly decoupled band in ^{138}Pr [9], with a $\nu h_{11/2}\otimes\pi[411]\frac{1}{2}^+$ configuration. The best agreement between theory and experimental data was obtained with $\epsilon_2 = -0.16$ for the 54 band (Fig. 7). It means that both positive (55) and negative (54) parity bands can be described consistently by assuming an oblate shape. A few of the most characteristic rotational bands (54) are displayed in the band diagram of Fig. 8, emphasizing the zig-zag behaviour of the low K bands. No high K bands were obtained thus confirming the assignment of the above configuration. For the odd A isotones, the theory reproduces well the experimental data for oblate deformations; however, for the neighbouring isotope ^{137}Pr [18] the agreement was equally good for oblate and prolate deformations. Thus on the basis of the above analysis we are therefore confident that the ^{138}Pr nucleus is oblate.

It should be observed that for this doubly decoupled band, shown in Fig. 7, this model predicts completely degenerate levels for the favoured and unfavoured signatures. The knowledge of theoretical electromagnetic transition probabilities as compared with the

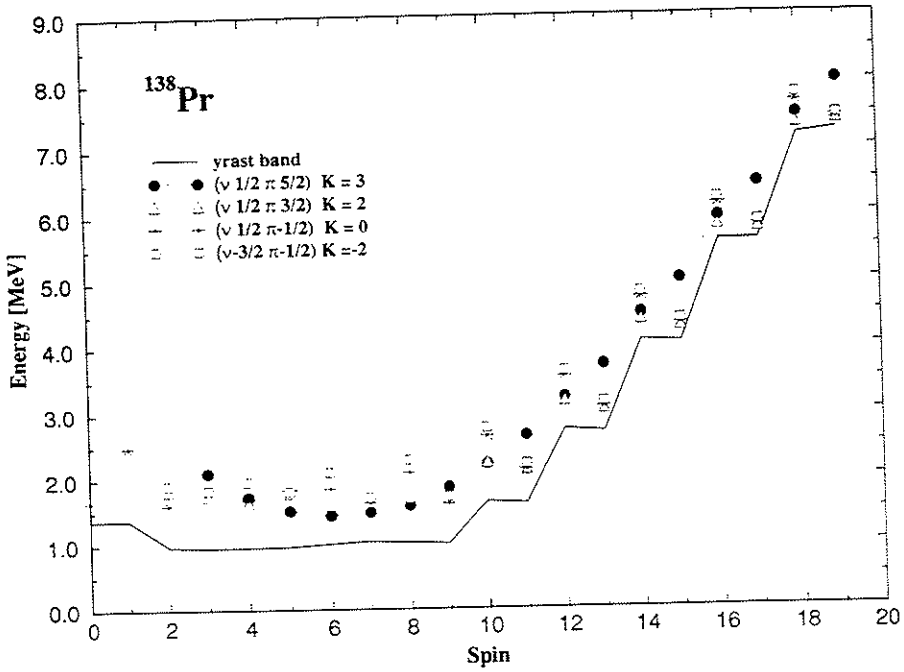

Fig. 8. Same as Fig. 6 for the 54 band. All the projection assignments and the corresponding K values belong to the $\nu h_{11/2} \otimes \pi g_{7/2}$ configuration.

way of interpreting quantum mechanical results using classical terminology is discussed in ref. [3].

The negative parity band (54) of ^{138}Pr is an interesting example of the application of the PSM to this mass region. Calculations with prolate shapes give spectra which have no similarity to the observed level scheme, while those with oblate shapes (the best one being $\epsilon_2 = -0.16$) predict that the pairs of states $(8^-, 9^-)$, $(10^-, 11^-)$, $(12^-, 13^-)$, etc. are nearly degenerate. Experimentally, there is a $\Delta I = 2$ sequence consisting of stretched E2 transitions. Although it has been assigned [9] the spins 9^-, 11^-, 13^-, it may very well be the other sequence $(8^-, 10^-, 12^-)$. We shall eventually attempt to identify experimentally which is the correct sequence. How to measure the missing (i.e. undetected) partner states poses an interesting technical question. On the other hand, the theory shows that the positive parity band (55) of ^{138}Pr can be well described by assuming either a prolate or oblate shape. This is due to a unique shell filling of the last neutron and proton in this particular nucleus in which neutron and proton states interchange their role (high Ω versus low Ω Nilsson levels) when the sign of the deformation parameter is changed. In view of the negative parity band (54), however, we may exclude the prolate deformation so that both positive and negative parity bands are described consistently using the same deformation parameter. Therefore, we suggest that this nucleus should

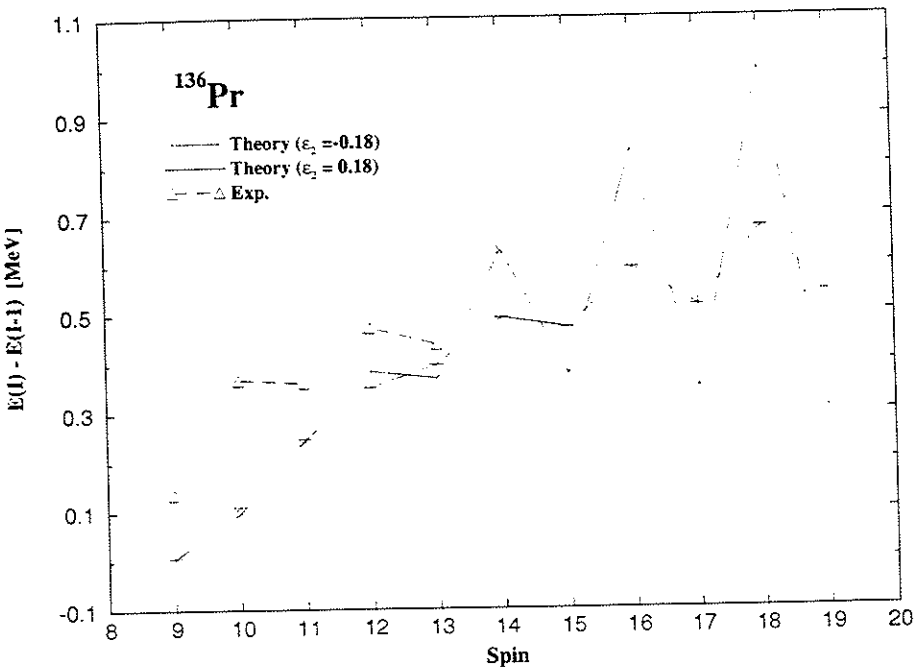

Fig. 9. Theoretical calculations for the 55 band of ^{136}Pr for oblate deformation $\epsilon_2 = -0.18$ (cross) and prolate deformation $\epsilon_2 = 0.18$ (plus) as compared to experimental points from ref. [1] (open triangle).

have an oblate shape.

The lighter nuclei in the mass region ($A \approx 130$) can be well described by assuming prolate shapes while the theory fails to describe the spectra of nuclei lying somewhere between prolate and oblate ones. We have attributed this to the occurrence of permanent γ-deformation, as seen in Fig. 10. Unfortunately, our present computer code assumes axial symmetry so that we cannot investigate these (presumably γ-deformed) nuclei quantitatively. We shall eventually remove this restriction and extend the program to include triaxiality in the near future.

The yrast band (for each parity) obtained by the theory shows a rather broad plateau (degeneracy) of states around the bandhead as one can see from the band diagrams. This is due to our schematic interaction which contains no neutron–proton (particle–particle-type) force. An attempt to discover whether or not this is indeed the case in nature will provide us with useful information about the interaction between the neutron and the proton. A careful experimental investigation around the bandhead is therefore very important in this connection. Generally speaking, there is no reason to believe that such a force is unimportant. In spite of the overall good agreement between experiment and theory, the experimental staggering at lower spins is not reproduced in these calculations. Another aspect to be mentioned is that the theoretical level spacings just above the band-

Z \ N	73	74	75	76	77	78	79
60	^{133}Nd ε_2=0.22 prolate		^{135}Nd ε_2=0.20 prolate		^{137}Nd ε_2=0.17 * Ref. (19)		^{139}Nd ε_2=-.16 oblate Ref. (16)
59	^{132}Pr ε_2=0.22 prolate Ref. (13)	^{133}Pr ε_2=0.21	^{134}Pr ε_2=0.20 prolate Ref. (14)	^{135}Pr ε_2=0.19 * Ref. (21)	^{136}Pr ε_2=0.18 * Ref. (1)	^{137}Pr ε_2=0.17 * Ref. (18)	^{138}Pr ε_2=-.16 oblate Ref. (9)
58	^{131}Ce ε_2=0.22 prolate		^{133}Ce ε_2=0.20 prolate		^{135}Ce ε_2=0.18 * Ref. (20)		^{137}Ce ε_2=-.16 oblate Ref. (15)
57	^{130}La ε_2=0.22 prolate Ref. (7)	^{131}La ε_2=0.21 Ref. (22)	^{132}La ε_2=0.20 prolate Ref. (8)	^{133}La ε_2=0.19 Ref. (23)	^{134}La ε_2=0.18 * Ref. (1)		

* probable triaxial shape

Fig. 10. Summary of the PSM model calculations emphasizing the shape transition as a function of the neutron number.

head are usually smaller than the observed ones. This may either indicate the presence of a neutron–proton interaction or reflect simply the effect of the non-conservation of particle number, inherent to the BCS approximation. In the latter case, we have to project out the shell model basis onto a good particle number in addition to the angular momentum. Our program was recently extended for this purpose and we are now in a position to investigate the above possibility. We will clarify this problem in a future publication.

This work was partially supported by the Fundação de Amparo a Pesquisa do Estado de São Paulo (FAPESP), Coordenadoria de Aperfeiçoamento de Pessoal de Ensino Superior (CAPES) and by the Comissão de Cooperação Internacional (CCInt).

References

[1] J.R.B. Oliveira, L.G.R. Emediato, E.W. Cybulska, R.V. Ribas, W.A. Seale, M.N. Rao, N.H. Medina, M.A. Rizzutto, S. Botelho and C.L. Lima, Phys. Rev. C45 (1992) 2740, and references therein

[2] G.A. Leander, S. Frauendorf and F.R. May, Proc. Conf. on high angular momentum properties of nuclei, Oak Ridge 1982, ed. N.R. Johnson (Harwood Academic, New York, 1983) p. 281

[3] K. Hara and Y. Sun, Nucl. Phys. A529 (1991) 445; A531 (1991) 221; A537 (1992) 77

[4] I.L. Lamm, Nucl. Phys. A125 (1969) 504

[5] I. Hamamoto, Nucl. Phys. A232 (1974) 445;
K. Hara and S. Kusuno, Nucl. Phys. A245 (1975) 147
[6] S. Iwasaki and K. Hara, Prog. Theor. Phys. 68 (1982) 1782
[7] M.A. Rizzutto, Thesis, Laboratório Pelletron, Departamento de Física Nuclear, Universidade de São Paulo, Brazil 1989, unpublished
[8] J.R.B. Oliveira, L.G.R. Emediato, M.A. Rizzutto, R.V. Ribas, W.A. Seale, M.N. Rao, N.H. Medina, S. Botelho and E.W. Cybulska, Phys. Rev. C39 (1989) 2250
[9] M.A. Rizzutto, E.W. Cybulska, V.R. Vanin, J.R.B. Oliveira, L.G.R. Emediato, R.V. Ribas, W.A. Seale, M.N. Rao, N.H. Medina, S. Botelho, J.C. Acquadro and C.L. Lima, Z. Phys. A344 (1992) 221
[10] E.S. Paul, C.W. Beausang, D.B. Fossan, R. Ma, W.F. Piel, Jr., N. Xu and L. Hildingsson, Phys. Rev. C36 (1987) 1853
[11] M.J. Godfrey, Y. He, I. Jenkins, A. Kirwan, P.J. Nolan, D.J. Thornley, S.M. Mullins and R. Wadsworth, J. Phys. G15 (1989) 487
[12] R. Ma, E.S. Paul, S. Shi, C.W. Beausang, W.F. Piel, Jr., N. Xu, D.B. Fossan, T. Chapuran, D.P. Balamuth and J.W. Arrison, Phys. Rev. C37 (1988) 1926
[13] S. Shi, C.W. Beausang, D.B. Fossan, R. Ma, E.S. Paul, N. Xu and A.J.Kreiner, Phys. Rev. C37 (1988) 1478
[14] C.W. Beausang, L. Hildingsson, E.S. Paul, W.F. Piel, Jr., N. Xu and D.B. Fossan, Phys. Rev. C36 (1987) 1810
[15] M. Kortelahti, T. Komppa, M. Piiparinen, A. Pakkanen and R. Komu, Phys. Scripta 27 (1983) 166
[16] M. Muller-Veggian, H. Beuscher, D.R. Haenni, R.M. Lieder, A. Neskakis and C. Mayer-Boricke, Nucl. Phys. A344 (1980) 89
[17] M.A. Cardona, G. de Angelis, D. Bazzacco, M. de Poli and S. Lunardi, Z. Phys. A340 (1991) 345
[18] N. Xu, C.W. Beausang, R. Ma, E.S. Paul, W.F. Piel, Jr., D.B. Fossan and L. Hildingsson, Phys. Rev. C39 (1989) 1799
[19] J. Gizon, A. Gizon, M.R. Maier, R.M. Diamond and F.S. Stephens, Nucl. Phys. A222 (1974) 557
[20] R. Ma, E.S. Paul, D.B. Fossan, Y. Liang, N. Xu, R. Wadsworth, I. Jenkins and P.J. Nolan, Phys. Rev. C41 (1990) 2624
[21] T.M. Semkov, D.G. Sarantites, K. Honkanen, V. Abenante, L.A. Adler, C. Baktash, N.R. Johnson, I.Y. Lee, M. Oshima, Y. Schutz, Y.S. Chen, J.X. Saladin, C.Y. Chen, O. Dietzsch, A.J. Larabee, L.L. Riedinger and H.C. Griffin, Phys. Rev. C34 (1986) 523
[22] E.S. Paul, C.W. Beausang, D.B. Fossan, R. Ma, W.F. Piel, Jr., N. Xu, L. Hildingsson and G.A. Leander, Phys. Rev. Lett. 58 (1987) 984
[23] J. Chiba, R.S. Hayano, M. Sekimoto, H. Nakayama and K. Nakai, J. Phys. Soc. Japan 43 (1977) 1109
[24] K. Hara, Y. Sun and R.V. Ribas, work in progress

Band structures in ^{108}Ag

F. R. Espinoza-Quiñones, E. W. Cybulska, L. G. R. Emediato, C. L. Lima,
N. H. Medina,* J. R. B. Oliveira, M. N. Rao, R. V. Ribas, M. A. Rizzutto, W. A. Seale, and C. Tenreiro†
Laboratório Pelletron, Depto. de Física Nuclear, Instituto de Física, Universidade de São Paulo, Caixa Postal 20516, 01452-990, São Paulo, Brazil
(Received 24 February 1995)

The ^{108}Ag nucleus has been studied by in-beam γ spectroscopy with the heavy-ion fusion-evaporation reaction ^{100}Mo(^{11}B,3$n\gamma$) at 39 MeV. Excitation functions, γ-γ-t coincidences, angular distributions, and DCOQ ratios were measured. A level scheme has been constructed and various bands have been identified with characteristics similar to those in other $A \approx 100$ nuclei. Total Routhian surface calculations predict prolate axially symmetric shapes with collective and noncollective character and satisfactorily account for most of the experimental results.

PACS number(s): 21.10.Re, 23.20.Lv, 27.60.+j

I. INTRODUCTION

In recent years, the influence of the high-j intruder orbits on the deformation of γ-soft nuclei has been studied in various mass regions such as $A \approx 100$, 130, 150, and 190. In each of these regions the Fermi levels for the protons and the neutrons are in different parts of an intruder subshell. In odd-odd nuclei, this leads in general to conflicting tendencies of the proton and neutron intruder quasiparticles, one of these being coupled mainly to the rotational axis and the other to the deformation axis. Several interesting phenomena have emerged in this context, such as triaxiality, shape transitions, shape coexistence, oblate bands, etc. The phenomenon of signature inversion, first observed in $A \approx 150$ odd nuclei at high spin, is also seen in odd-odd nuclei at relatively low spins and, despite several attempts, has not been fully understood [1]. In the $A \approx 100$ odd-odd nuclei, the active intruder orbits are near the top of the $\pi g_{9/2}$ and the bottom of the $\nu h_{11/2}$ subshells. The former orbits are oblate driving, while the latter are strongly prolate driving and favor increased elongations.

In this paper we present an investigation of ^{108}Ag [illegible]-ion induced reaction. Various bands were [illegible] which resemble previously observed structures in neighboring odd-odd Ag isotopes. In particular, the $\pi g_{9/2} \otimes \nu h_{11/2}$ band, which has been systematically seen in the ^{102,104,106}Ag [2–4] and the corresponding Rh isotones [5] and also in the present work in ^{108}Ag. In both ^{106}Ag and ^{108}Ag the ($I^\pi = 1^+$) ground state and the ($I^\pi = 6^+$) isomeric states have been assigned $\pi g_{9/2} \otimes \nu d_{5/2}$ configuration. Similar bandlike structures (based on this 6^+ state) were observed in both nuclei. Another band resembles the $\pi(p_{1/2}, f_{5/2})$ bands seen in odd-A Ag isotopes [6,7] and thus has been tentatively assigned the $\pi(p_{1/2}, f_{5/2}) \otimes \nu h_{11/2}$ configuration. Total Routhian surface (TRS) calculations of the Strutinsky type with a cranked Woods-Saxon potential with pairing were performed and indicate a stabilization of the quadrupole deformation around $\beta_2 = 0.16$, $\gamma = 0°$ (prolate collective) for all configurations containing at least one $h_{11/2}$ quasineutron excitation. For the $\pi g_{9/2} \otimes \nu d_{5/2}$ configuration an equilibrium deformation around $\beta_2 = 0.1$, $\gamma = -120°$ (prolate, noncollective) is predicted and can probably be associated with the 6^+ isomer bandhead. In addition a structure was observed with characteristics of high-K bands (probably $K = 8$).

II. EXPERIMENTAL PROCEDURE

High-spin states in ^{108}Ag were populated by the ^{100}Mo(^{11}B,3$n\gamma$) reaction. The beam was provided by the Pelletron Accelerator of the University of São Paulo. The target used was a ~ 20 mg/cm^2 metallic self-supporting foil of enriched ^{100}Mo.

The γ-ray measurements included excitation functions, angular distributions, and γ-γ coincidences and were obtained with HPGe detectors having $\sim 20\%$ efficiencies and energy resolutions of 2.1–2.4 keV at 1332 keV. The excitation functions were obtained by varying the beam energy in steps of 5 MeV from 35 to 50 MeV. The peak cross section of the desired (^{11}B,3n) reaction is near the Coulomb barrier (34 MeV) and substantial contribution from the 4n channel was observed, which is in reasonable agreement with the statistical model calculations (PACE). A beam energy of 39 MeV was chosen for the other measurements. This energy was the best compromise between the enhancement of population of high-spin states and the competition from the 4n channel. The 4n channel (^{107}Ag) has a well-established decay scheme [6,4], permitting the identification of its γ rays. Other very weak channels such as 2$n\alpha$ and 4np were also observed.

*Present address: Istituto Nazionale di Fisica Nucleare, Sezione di Padova, Padova, Italy.
†Present address: Facultad de Ciencias, Depto. de Física, Universidad de Chile, Santiago de Chile, Chile.

The coincidence data were obtained with two BGO Compton suppressed HPGe detectors placed at ±50° and two HPGe detectors at ±140° to the beam direction. At least one of a set of one 4 in. × 4 in. NaI(Tl) and seven 3 in. × 3 in. detectors placed, respectively, above and below the target, was required to trigger for an accepted γ-γ coincidence event. The angular distribution data were taken using a Compton suppressed HPGe detector positioned at four angles varying from 0° to +90° and a second HPGe detector at −90° was used as a monitor. Due to the complexity of the singles spectra, it was possible to obtain reliable angular distributions only for the strong M1 transitions of the yrast band.

The total number of γ-γ coincidence events was about 7×10^7 and the data were gain matched and sorted into two-dimensional arrays. A symmetrized $E_\gamma \times E_\gamma$ matrix was constructed and the analysis of the data was performed using PANORAMIX [8] and VAXPAK [9] codes.

TABLE I. Energies, spin assignments, relative intensities, and DCOQ ratios for the γ-ray transitions in the ^{100}Mo(^{11}B,3n)^{108}Ag reaction at 39 MeV. The γ-ray energies are accurate to ± 0.3 keV. E_i and E_f are the energies of the initial and final states corresponding to each transition.

E_γ [keV]	E_i [keV]	E_f [keV]	$I_i^\pi \rightarrow I_f^\pi$	I_γ	DCOQ ratio	E_γ [keV]	E_i [keV]	E_f [keV]	$I_i^\pi \rightarrow I_f^\pi$	I_γ	DCOQ ratio
35.3	533.8	498.5	$(8^-) \rightarrow (7^-)$	10.0(20)		506.7	1942.4	1435.7	$(12^-) \rightarrow (11^-)$	41.8 (9)	0.53 (8)
54.8	420.7	366.3		4.0(10)		532.6	4092.1	3559.5	$(16^-) \rightarrow (15^-)$	6.4 (9)	
58.5	498.5	440.1	$(7^-) \rightarrow (6^-)$	23.6(9)		537.4	2908.9	2371.1	$(13^+) \rightarrow (11^+)$	5.3 (9)	
75.5	366.3	290.8				550.9	2994.9	2444.0	$(14^-) \rightarrow (13^-)$	10.3 (9)	0.65 (9)
75.5	290.8	215.0				557.0	1091.0	533.8	$(10^-) \rightarrow (8^-)$	5.3 (8)	
75.0	810.1	735.3	$(8^+) \rightarrow (7^+)$	9.0(20)		570.8	1490.2	919.4	$(9^+) \rightarrow (8^+)$	7.2 (9)	
103.1	523.8	420.7		10.4 (5)	0.96 (10)	564.6	3559.5	2994.9	$(15^-) \rightarrow (14^-)$	7.0 (9)	0.59 (14)
117.8	919.4	802.0	$(8^+) \rightarrow (7^+)$	5.6 (4)	0.62 (14)	573.6	4179.7	3606.1	$(16^-) \rightarrow (15^-)$	4.7 (9)	
122.6	498.5	376.2	$(7^-) \rightarrow (7^+)$	1.7 (4)		585.4	3494.7	2908.9	$(15^+) \rightarrow (13^+)$	3.6 (9)	
148.2	523.9	376.1	$(6^+) \rightarrow (7^+)$	4.1 (5)	0.42 (12)	595.1	2536.9	1942.4	$(12^-) \rightarrow (12^-)$	6.0 (9)	
153.9	687.7	533.8	$(9^-) \rightarrow (8^-)$	81.5 (9)	0.64 (9)	623.7	734.6	110.9	$(7^+) \rightarrow (6^+)$	5.7 (9)	
157.6	533.8	376.2	$(8^-) \rightarrow (7^+)$	4.2 (7)		688.2	1490.2	802.0	$(9^+) \rightarrow (7^+)$	6.3 (9)	
157.9	523.8	366.3		1.9 (4)	0.69 (14)	692.0	2064.1	1372.3	$(10^+) \rightarrow (9^+)$	5.4 (9)	
183.5	1674.2	1490.2	$(10^+) \rightarrow (9^+)$	1.5 (4)		697.0	2371.1	1674.2	$(11^+) \rightarrow (10^+)$	3.2 (9)	
215.5	215.0	0.0	$3^+ \rightarrow 1^+$	7.3 (5)	1.00 (18)	699.2	810.1	110.9	$(8^+) \rightarrow 6^+$	5.3 (9)	
233.3	2908.9	2675.5	$(13^+) \rightarrow (12^+)$	13.1 (6)	0.71 (6)	700.1	3872.7	3172.3	$(16^+) \rightarrow (14^+)$	4.0 (9)	
234.0	2536.9	2302.9	$(12^-) \rightarrow (11^-)$	4.8 (6)		722.0	1098.2	376.2	$(8^+) \rightarrow (7^+)$	12.2 (13)	
240.4	2908.9	2668.6	$(13^+) \rightarrow (12^+)$	7.3 (5)	0.70 (10)	748.0	1435.6	687.4	$(11^-) \rightarrow (9^-)$	15.4 (11)	0.90 (12)
249.2	2675.5	2426.8	$(12^+) \rightarrow (11^+)$	4.0 (6)	0.59 (17)	754.8	1674.2	919.4	$(10^+) \rightarrow (8^+)$	37.7 (12)	1.08 (18)
255.4	366.3	110.9		10.7 (5)	0.61 (8)	818.0	4313.2	3494.7	$(17^+) \rightarrow (15^+)$	3.4 (8)	
261.8	2536.9	2275.1	$(12^-) \rightarrow (11^-)$	3.0 (5)		851.2	1942.3	1090.8	$(12^-) \rightarrow (10^-)$	9.5 (11)	0.82 (17)
263.4	3172.3	2908.9	$(14^+) \rightarrow (13^+)$	17.7 (6)	0.69 (6)	880.9	2371.1	1490.2	$(11^+) \rightarrow (9^+)$	5.0 (9)	
265.3	376.2	110.9	$(7^+) \rightarrow 6^+$	19.9 (7)	0.63 (11)	895.3	2536.9	1641.7	$(12^-) \rightarrow (10^-)$	5.2 (9)	
278.2	802.0	523.8	$(7^+) \rightarrow (6^+)$	4.9 (5)	0.46 (16)	934.6	1669.9	735.3	$(9^+) \rightarrow (7^+)$	4.4 (11)	
304.5	2675.5	2371.1	$(12^+) \rightarrow (11^+)$	4.2 (6)		936.6	2426.8	1490.2	$(11^+) \rightarrow (9^+)$	4.2 (9)	
310.7	2847.6	2536.9	$(13^-) \rightarrow (12^-)$	6.3 (6)	0.57 (15)	954.0	1641.5	687.4	$(10^-) \rightarrow (9^-)$	9.5 (9)	0.73 (13)
322.4	3494.7	3172.3	$(15^+) \rightarrow (14^+)$	14.5 (7)	0.75 (9)	965.9	2064.1	1098.2	$(10^+) \rightarrow (8^+)$	4.6 (9)	
329.2	440.1	110.9	$(6^-) \rightarrow 6^+$	100.0 (9)	0.84 (9)	977.2	1787.3	810.1	$(10^-) \rightarrow (8^-)$	6.7 (9)	
340.8	3188.4	2847.6	$(14^-) \rightarrow (13^-)$	6.2 (6)	0.83 (18)	987.0	1098.2	110.9	$(8^+) \rightarrow 6^+$	5.6 (12)	
344.7	1435.7	1091.0	$(11^-) \rightarrow (10^-)$	48.4 (9)	0.59 (9)	992.0	4179.7	3188.4	$(16^-) \rightarrow (14^-)$	1.7 (7)	
359.1	735.3	376.2	$(7^+) \rightarrow (7^+)$	5.9 (7)		994.4	2668.6	1674.2	$(12^+) \rightarrow (10^+)$	15.5 (12)	1.00 (19)
361.0	2302.9	1942.4	$(11^-) \rightarrow (12^-)$	2.2 (6)		996.1	1372.3	376.2	$(9^+) \rightarrow (7^+)$	5.7 (12)	
378.0	3872.7	3494.7	$(16^+) \rightarrow (15^+)$	10.9 (5)	0.86 (20)	999.3	2371.6	1372.3	$(11^+) \rightarrow (9^+)$	5.4 (10)	
387.5	498.5	110.9	$(7^-) \rightarrow (6^+)$	10.5 (7)	0.67 (10)	1001.3	2675.5	1674.2	$(12^+) \rightarrow (10^+)$	18.6 (11)	0.89 (16)
393.2	2536.9	2143.7	$(12^-) \rightarrow (11^-)$	8.3 (7)	0.62 (14)	1008.5	2444.1	1435.6	$(13^-) \rightarrow (11^-)$	11.0 (10)	0.93 (14)
395.6	919.4	523.8	$(8^+) \rightarrow (6^+)$	32.3 (9)	0.91 (14)	1041.0	2710.9	1669.9	$(11^+) \rightarrow (9^+)$	5.3 (12)	
403.3	1091.0	687.7	$(10^-) \rightarrow (9^-)$	72.7 (9)	0.70 (9)	1052.5	2995.0	1942.3	$(14^-) \rightarrow (12^-)$	7.0 (11)	
412.9	523.8	110.9	$(6^+) \rightarrow 6^+$	16.4 (8)	0.90 (12)	1052.8	2143.3	1090.8	$(11^-) \rightarrow (10^-)$	2.5 (5)	
417.7	3606.1	3188.4	$(15^-) \rightarrow (14^-)$	5.8 (6)		1096.8	4092.0	2995.0	$(16^-) \rightarrow (14^-)$	3.0 (9)	
425.8	802.0	376.2	$(7^+) \rightarrow (7^+)$	7.2 (7)	0.93 (27)	1101.8	2536.6	1435.6	$(12^-) \rightarrow (11^-)$	3.8 (9)	
434.3	810.1	376.2	$(8^+) \rightarrow (7^+)$	13.0 (9)		1108.0	1641.5	533.5	$(10^-) \rightarrow (8^-)$	3.0 (9)	
440.5	4313.2	3872.7	$(17^+) \rightarrow (16^+)$	5.5 (7)	0.68 (17)	1115.2	3559.5	2444.1	$(15^-) \rightarrow (13^-)$	4.7 (9)	
496.5	3172.3	2675.5	$(14^+) \rightarrow (12^+)$	5.6 (9)		1117.3	2904.6	1787.3	$(12^+) \rightarrow (10^+)$	4.3 (8)	
501.6	2444.0	1942.4	$(13^-) \rightarrow (12^-)$	15 (3)	0.62 (9)	1184.0	2275.1	1091.0	$(11^-) \rightarrow (10^-)$	4.8 (8)	
502.0	2143.7	1641.7	$(11^-) \rightarrow (10^-)$	6 (1)	0.58 (21)						

Background subtracted gate spectra were generated, and efficiency corrected relative intensities of the γ rays were extracted. Typical examples of coincidence spectra are shown in Fig. 1. The energy and efficiency calibration for the spectra were made using ^{152}Eu and ^{133}Ba lines. The intensities of γ rays in Table I were extracted from the γ-γ coincidence data and represent the sum of the efficiency corrected areas of the transitions (placed in the level scheme) in coincidence with each gate of energy E_γ.

The multipolarities for most of the γ rays were obtained applying the DCOQ method (directional correlation from oriented states referred to quadrupole transitions) [10]. An $E_\gamma(\pm 50°) \times E_\gamma(\pm 140°)$ matrix was constructed to extract multipolarity information from the two coincidence intensities $N_{12}(\gamma_1 \rightarrow \pm 50°, \gamma_2 \rightarrow \pm 140°)$ and $N_{21}(\gamma_2 \rightarrow \pm 50°, \gamma_1 \rightarrow \pm 140°)$. The DCOQ$(\gamma_1, \gamma_2)$ ratios (N_{21}/N_{12}) corrected for relative efficiencies of detectors at $\pm 140°$ and $\pm 50°$ are referred to quadrupole transition gate (γ_2) and reflect the multipolarity and mixing ratio of γ_1. The sum of gates on several quadrupole transitions was used in order to determine the DCOQ ratios of weak γ-ray transitions. The theoretical DCOQ ratio depends on the pair of fixed observation angles, multipole character of the transition γ_1, the ΔI involved, and on the orientation of the spin of the initial state of the cascade. For cascades of predominantly stretched transitions there is very little dependence on the particular state depopulated by transition γ_1 [11]. Therefore the DCOQ ratios for transitions with pure multipolarities (L) can be estimated from the values of L and ΔI. Table II shows the ratios calculated specifically for the present measurements. It should be pointed out that $\Delta I = 1$ transitions could give DCOQ ratios less than or greater than 0.85 for $\delta < 0$ or $\delta > 0$, respectively. Also, $\Delta I = 0$ transitions could give a DCOQ ratio between 0.81 and 1.03 for large mixing ratios.

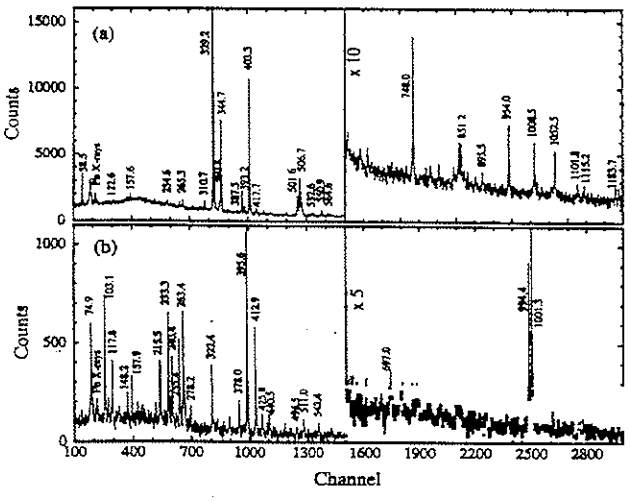

FIG. 1. Background-subtracted γ-γ coincidence spectra of the ^{100}Mo(^{11}B,3n)^{108}Ag reaction at 39 MeV gated by (a) the 153.9 keV line and (b) the 754.8 keV line.

TABLE II. Theoretical DCOQ ratios for mixing ratio δ=0. L is the multipolarity of the γ ray involved and ΔI is the spin change in the transition.

L	ΔI	DCOQ ratio
1	0	1.03
1	1	0.85
2	0	0.81
2	1	0.98
2	2	1.00

III. EXPERIMENTAL RESULTS

A. Level scheme

The level scheme of ^{108}Ag, shown in Fig. 2, was constructed on the basis of the γ-γ coincidence relations and intensity-energy balances. The relative intensities of the γ rays belonging to ^{108}Ag and the measured DCOQ ratios are listed in Table I, together with the level energies and their proposed spins and parities. Six structures with rotational band characteristics can be observed in the level scheme. Negative parity bands with strong $M1$ and weak $E2$ transitions and a small staggering (e.g., band 1) are typical of this mass region. On the other hand, bands 3, 4, and 5, show strong $E2$ with very weak $M1$'s transitions and a large staggering (200–400 keV).

In ^{108}Ag, the-spin and parity of the $I^\pi = 1^+$ ground

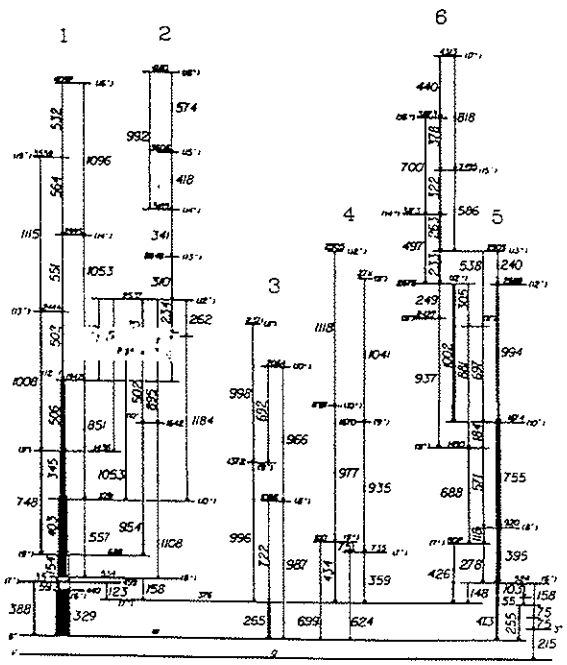

FIG. 2. The level scheme of ^{108}Ag obtained from the ^{100}Mo(^{11}B,3$n\gamma$) reaction at 39 MeV.

TABLE III. The assigned K values and configurations in ^{108}Ag. The signature splittings listed were taken at $\hbar\omega$=0.35 MeV.

Band	K	(π, α)	Configuration	$\Delta e'_{exp}$ (keV)
1	4	(-,0); (-,-1)	$aA; bA$	60
2	4	(-,0); (-, 1)	$aAEF; bAEF$	0
3	0	(+,0); (+, 1)	$aG; aH(aG; bG)$	250
4	0	(+,0); (+, 1)	$aE; aF(aE; bE)$	350
5	0	(+,0); (+, 1)	$gA; hA$	180
6	8	(+,0); (+, 1)	$gacA$	0

state and of the two isomeric states at 110.9 keV ($I^\pi = 6^+$) and at 215 keV ($I^\pi = 3^+$) are well known from atomic beam resonance [12], from the β decay properties to Pd and Cd isotopes [13] and from $(p, n\gamma)$ reactions [14]. The assignments of the other spins in the level scheme were made on the basis of the DCOQ ratios and the systematics for this mass region. The 533.8-keV level of the negative parity band 1 decays through two low energy γ rays of 35 and 59 keV. A similar decay has been also observed in other Ag and Rh isotopes [2,3,5]. Taking into account electron conversion coefficients, the intensity balance shows that the 35- and 59-keV transitions are necessarily of $M1$ nature. The DCOQ ratio indicates a dipole of $\Delta I = 1$ type for the 388-keV transition. Since this transition populates the 6^+ isomer at 110.9 keV we propose $I^\pi = 7^-$ for the 498.5 keV level, and $I^\pi = 6^-$ for the 440.1 keV level. This choice of spins is also consistent with the similar level scheme of ^{106}Ag [2]. The remaining attributions of the spins in band 1 were based on angular distributions, DCOQ ratios, and rotational band characteristics.

In the case of band 2, according to the DCOQ ratios, the transitions of 954, 502, and 393 keV are of type ΔI = 0 or 1. Therefore the maximum spin of the 2536.9 keV level is $I = 12$. The value of $I = 12$ was chosen in order to maintain band 2 nearest to the yrast line. The DCOQ ratio for the 265-keV γ ray which feeds the 6^+ isomer (the bandhead of band 3) indicates a change of no more than one unit of spin. Besides this, the proposed spins for the levels of band 3 were chosen in analogy to a similar structure in ^{106}Ag. The bandhead of band 5 (6^+) at 523.8 keV and the spins of the levels in band 4 were inferred from theoretical arguments (see discussion). The other spins in bands 5 and 6 were attributed relative to this 6^+

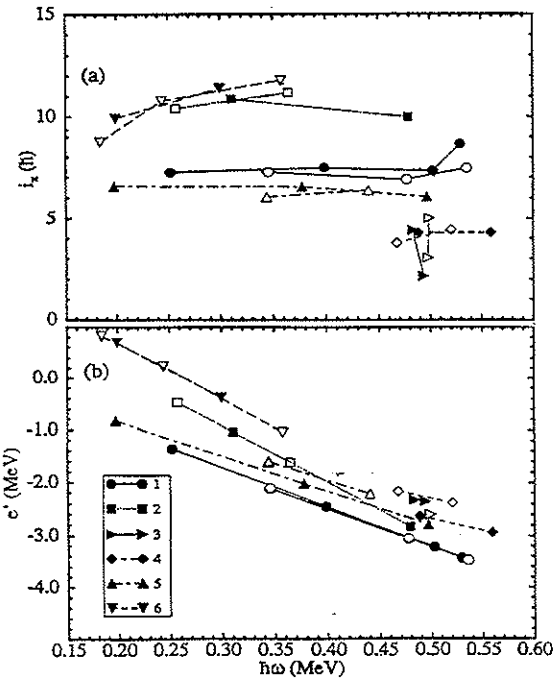

FIG. 3. Experimental quasiparticle (a) alignments and (b) Routhians for the six rotational bands of ^{108}Ag. The solid symbols correspond to α=0 and the open ones to α=1. The following symbols are used for the bands: circles band 1, squares band 2, diamonds band 4, triangles right, up and down bands 3, 5, and 6, respectively.

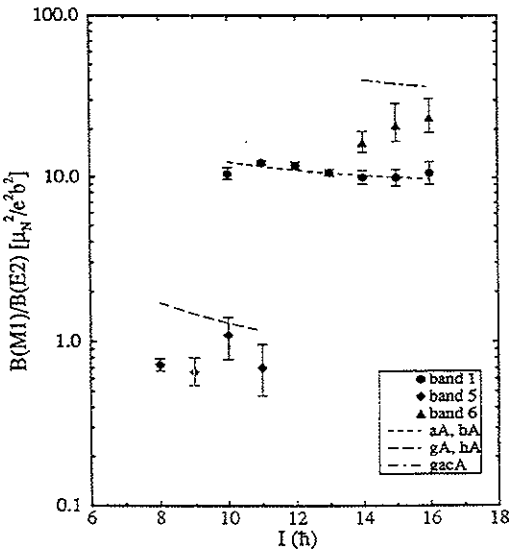

FIG. 4. Experimental and calculated $B(M1)/B(E2)$ ratios for bands 1, 5, and 6 in ^{108}Ag. The calculations were made using the deformation parameters $\beta_2 = 0.16$, $\beta_4 = 0$, $\gamma = 0°$ and $K = 4, 2$, and 8 for bands 1, 5, and 6, respectively. Circles band 1, diamonds band 5, and triangles up band 6.

bandhead and are consistent with the DCOQ results.

The experimental Routhians and alignments (Fig. 3) were calculated following the procedure described in [15,16] with the Harris parameters of $\mathcal{J}_0 = 3.6\ \hbar^2\text{MeV}^{-1}$ and $\mathcal{J}_1 = 29.8\ \hbar^4\text{MeV}^{-3}$, giving a nearly constant alignment for band 1. The K values used, experimental signature splittings, and proposed configurations are given in Table III.

The experimental in-band branching ratios $I_\gamma(\Delta I = 1)/I_\gamma(\Delta I = 2)$ from each level of spin I can provide valuable information regarding the intrinsic configuration of the band. The intensities I_γ were obtained from the spectra gated by the transitions populating the level of interest. Experimental reduced transition probability ratios can be obtained as

$$\frac{B(M1; I \to I-1)}{B(E2; I \to I-2)} = 0.693\ \frac{1}{1+\delta^2}\ \frac{[E_\gamma(I \to I-2)]^5}{[E_\gamma(I \to I-1)]^3}\ \frac{I_\gamma(I \to I-1)}{I_\gamma(I \to I-2)}.$$

The results obtained for bands 1, 5, and 6 ($\delta = 0$) can be seen in Fig. 4, together with theoretical estimates (described in the Discussion). No reliable results were obtained for the other bands due to the poor statistics.

IV. THEORETICAL CALCULATIONS AND RESULTS

A. Quasiparticle Routhians

Figure 5 shows the quasiparticle Routhians calculated from the cranked shell model based on a deformed Woods-Saxon potential including monopole pairing interaction [17]. The diagrams are specific for $Z = 47$ and $N = 61$. The states are classified by the two remaining symmetries, parity and signature (π, α). The signature splitting for each configuration can be read off the diagrams. The aligned angular momentum (i_x) can be obtained from the derivative of the Routhian with respect to the rotational frequency: $i_x = -de'/d\omega$. Table IV shows the correspondence between the letter code used to specify the various quasiparticle states, parity, signature, Nilsson labels, and spherical shell model states most closely related.

It can be seen that the first band crossing occurs around $\hbar\omega = 0.35$ MeV and corresponds to the alignment of the first two $h_{11/2}$ quasineutrons (A and B) with the axis of rotation. The next crossing corresponds to the breaking of the first $g_{9/2}$ quasiproton pair (ab), around $\hbar\omega = 0.48$ MeV. The signature splitting between the a and b quasiprotons is small, which reflects the fact that the quasiprotons are weakly coupled to the rotational axis.

The deformation parameters used ($\beta_2 = 0.16$, $\beta_4 = 0$, $\gamma = 0°$) were chosen in accordance with the TRS calculations (see next section), and are appropriate, in general, to the bands which present at least one $\nu h_{11/2}$ quasineutron excitation.

TABLE IV. The letter code used to denote the quasiparticle states.

j shell	$[Nn_z\Lambda]\Omega$	Parity	$\alpha = -\frac{1}{2}$	$\alpha = +\frac{1}{2}$
$\nu h_{11/2}$	$[550]\frac{1}{2}$	-	A	B
$\nu h_{11/2}$	$[541]\frac{1}{2}$	-	C	D
$\nu g_{7/2}$	$[413]\frac{5}{2}$	+	E	F
$\nu d_{5/2}$	$[402]\frac{5}{2}$	+	G	H
$\pi g_{9/2}$	$[413]\frac{9}{2}$	+	b	a
$\pi g_{9/2}$	$[404]\frac{9}{2}$	+	d	c
$\pi g_{9/2}$	$[422]\frac{9}{2}$	+	f	e
$\pi(p_{1/2}, f_{5/2})$	$[301]\frac{1}{2}$	-	h	g

B. Equilibrium deformations

Standard total Routhian surface calculations were performed for the least excited configurations of ^{108}Ag. The calculations employ a deformed Woods-Saxon potential and a monopole pairing residual interaction [17,18]. The results are summarized in Fig. 6 which show the contour plots for the total energy in the intrinsic frame (mini-

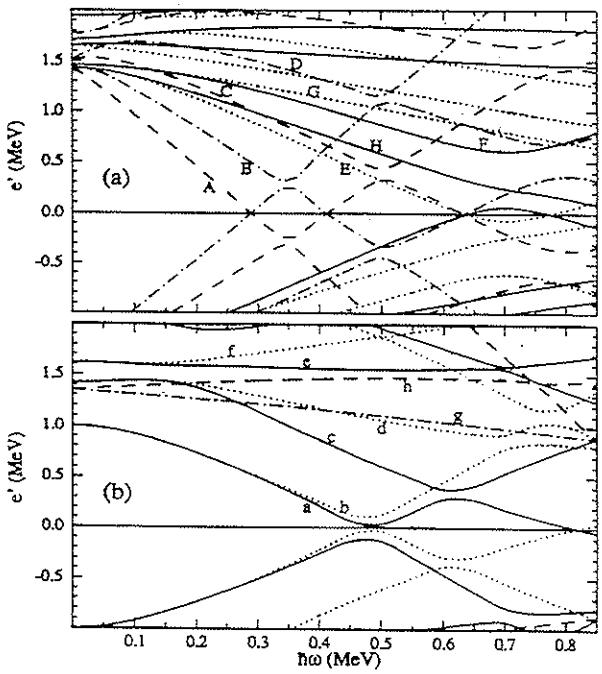

FIG. 5. Quasiparticle Routhians as a function of rotational frequency in ^{108}Ag for (a) neutrons and (b) protons ($\beta_2 = 0.16$, $\beta_4 = 0$, $\gamma = 0°$). The following convention is used for the levels: solid line ($\pi = +, \alpha = +\frac{1}{2}$), dotted line ($\pi = +, \alpha = -\frac{1}{2}$), dashed-dotted line ($\pi = -, \alpha = +\frac{1}{2}$), dashed line ($\pi = -, \alpha = -\frac{1}{2}$).

mized with respect to β_4) as a function of the deformation parameters β_2 and γ. The equilibrium deformation is indicated by the position of a thick dot.

Figures 6(a,b) show the results for the yrast configuration aA at two different rotational frequencies. The equilibrium is stable at a prolate-collective shape ($\gamma \approx 0°$) for a wide frequency range ($\hbar\omega = 0.2 - 0.5$ MeV) where the calculations were performed. The results are essentially the same for the theoretically unfavored signature $\alpha = 1$ (bA).

Figure 6(c) shows the result for the gA configuration (the positive parity configuration with the lowest excitation energy). The energy minimum is close to the one for the aA configuration but is very shallow with respect to γ. It fluctuates slightly around $\gamma = 0°$ as a function of frequency according to our calculations. The same is true for the unfavored signature configuration hA.

Figures 6(d,e,f) show the results for the aG configuration at three different frequencies. Below $\hbar\omega = 0.4$ MeV the energy minimum remains close to $\beta_2 = 0.1$, $\gamma = -120°$, representing a noncollective prolate state with about $6\hbar$ of angular momentum aligned with the symmetry axis. Above $\hbar\omega = 0.4$ MeV the configuration changes adiabatically into the $aABG$ configuration which contains the first aligned pair of $h_{11/2}$ quasineutrons (AB). As a consequence of the strong driving forces of the AB pair, the equilibrium deformation becomes prolate collective ($\beta_2 = 0.16$, $\gamma = 0°$). As a result of the collective rotation and the combined alignment of the four quasiparticles, the total spin for this configuration is at least $16\hbar$. A band based on this configuration is unlikely to be populated by the reaction used in this paper due to the limitation in the input angular momentum. This calculation is representative of other configurations containing one positive parity quasineutron and a $g_{9/2}$ quasiproton, viz., aE, aF, aH. This is rather surprising since the $g_{9/2}$ quasiproton has also a rather strong shape driving force. Oblate- or triaxial-collective deformations were previously expected for these positive parity configurations [7]. On the other hand it is possible to conclude from these calculations that the strong β_2 and γ driving properties of the $\nu h_{11/2}$ intruder orbit apparently tend to stabilize the equilibrium deformation around $\beta_2 = 0.16$, $\gamma = 0°$, rather independently of the other quasiparticles present.

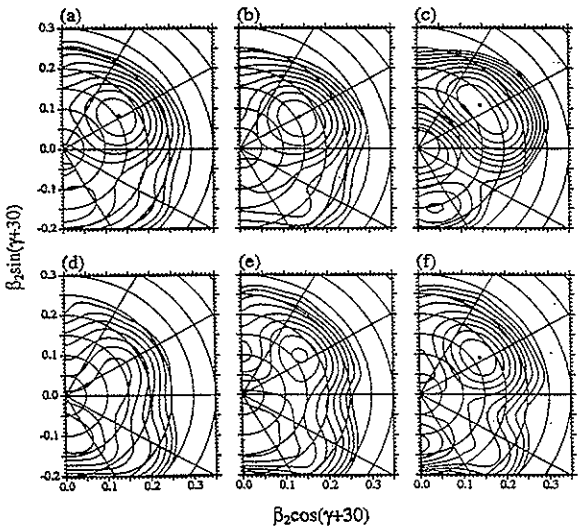

FIG. 6. Total Routhian surfaces for ^{108}Ag. (a) aA configuration, $\hbar\omega$=0.251 MeV (β_2=0.156, β_4=0.001, $\gamma = 2.2°$). (b) aA configuration, $\hbar\omega$=0.377 MeV (β_2=0.158, β_4=0.002, $\gamma = 0.0°$). (c) gA configuration, $\hbar\omega$=0.377 MeV (β_2=0.180, β_4=0.013, $\gamma = 6.5°$). (d) aG configuration, $\hbar\omega$=0.314 MeV (β_2=0.092, β_4=0.006, $\gamma = -120.0°$). (e) aG configuration, $\hbar\omega$=0.377 MeV (β_2=0.114, β_4=0.009, $\gamma = -120.0°$). (f) aG configuration, $\hbar\omega$=0.440 MeV (β_2=0.166, β_4=0.000, $\gamma = 3.2°$). The thick dots indicate the position of the equilibrium deformation.

C. Estimated branching ratios $B(M1)/B(E2)$

The theoretical branching ratios $B(M1)/B(E2)$ between in-band $\Delta I = 1$ and $\Delta I = 2$ transitions from each band state can be estimated from the geometrical model proposed by Dönau and Frauendorf [16]. In this semiclassical model the $M1$ transitions are assumed to originate from the precession of the magnetic moment vector around the total angular momentum vector. The intensity of the radiation is therefore proportional to the component of the magnetic moment vector perpendicular to the spin axis. Effective g factors are used to relate the angular momentum of each quasiparticle configuration to its magnetic moment vector. The estimates are then made from assumptions with respect to the orientation of the angular momentum of each quasiparticle, parametrized by the alignment and the projection onto the symmetry axis (K). The effective g factors are obtained from the Schmidt estimates, with an attenuation factor of 0.7 for the spin g-factors g_s [19].

The calculated branching ratios for the relevant configurations of ^{108}Ag can be compared to the experimental results in Fig. 4 (see also Sec. V). The deformation parameters used were $\beta_2 = 0.16$, $\beta_4 = 0$, $\gamma = 0°$, and the alignments of each quasiparticle were obtained from Fig. 5. For the aA and bA configurations, a $K = 4$ projection was assumed, arising essentially from the $g_{9/2}$ quasiproton (a, b). The $h_{11/2}$ quasineutron A is almost fully aligned ($i_x = 5.2\hbar$). In this situation the perpendicular components of the magnetic moments of the two quasiparticles tend to add, since the neutron g factor is negative and the proton positive, leading to rather high $M1$ transitions. The estimates shown for the gA, hA configurations are actually upper limits, calculated assuming the g factor of a pure $f_{5/2}$ ($g = 0.548$) component for the g, h quasiparticles and $K = 2$. For a fully rotation-aligned $\pi p_{1/2} \otimes \nu h_{11/2}$ configuration no $M1$ transitions are expected. The actual states g, h are of mixed $p_{1/2}, f_{5/2}$ parentage. For the $K = 8$ band ($gacA$), with a pair of $g_{9/2}$ quasiprotons (ac) coupled to the deformation

axis, very large $B(M1)/B(E2)$ ratios are calculated. A value of $K = 7$ would reduce the $B(M1)/B(E2)$ values by roughly 50%.

V. DISCUSSION

A. Bands 1 and 2

Band 1 is the yrast band and presents strong $M1$ transitions and weak $E2$ crossovers. The signature splitting is ≈ 60 keV at $\hbar\omega = 0.35$ MeV, decreasing as the frequency increases. This type of semidecoupled band is characteristic of a "conflicting" coupling between two intruder-orbit quasiparticles in odd-odd nuclei. We assign the $\pi g_{9/2} \otimes \nu h_{11/2}$ (aA and bA) configurations for this band, which corresponds to the lowest two quasiparticle excitations available. Bands with this configuration have been observed in other odd-odd Ag isotopes [2–4]. TRS calculations [see Fig. 6(a)] predict nearly axially symmetric prolate equilibrium deformations and a signature splitting of ≈ 35 keV (around $\hbar\omega = 0.35$ MeV), essentially the splitting between the a and b quasiproton orbits of opposite signatures [see Fig. 5(b)]. However, the theoretically favored signature is $\alpha = 0$ while experimentally it is $\alpha = -1$ (the same is true for the other odd-odd Ag and Rh isotopes cited in Sec. I). The quasiproton Routhians show signature inversion (with very small splitting) for γ between 10° and 20°. Indeed the TRS minima show a weak tendency toward positive γ values insufficient, though, to produce signature inversion.

For $\gamma \approx 0°$ the angular momenta of the two quasiparticles are nearly perpendicular to each other. This results, according to the geometrical model, in rather large $B(M1)/B(E2)$ ratios as shown in Fig. 4. The alignment expected for this configuration comes mostly from the quasineutron, which contributes with $5.2\hbar$, while the deformation aligned quasiproton contributes with about $2.7\hbar$, in reasonable agreement with the experimental result of $7.3\hbar$ [Fig. 3(a)]. The first neutron and proton crossings, AB and ab, respectively, are blocked for this configuration. The next two crossings expected are the BC (at $\hbar\omega = 0.51$ MeV) and the EF (around $\hbar\omega = 0.7$ MeV). We believe that the BC crossing is responsible for the upbend observed around $\hbar\omega = 0.53$ MeV [Fig. 3(a)]. Band 2 has negligible signature splitting and presents a gain in alignment of about $3.8\hbar$ relative to band 1. This is close to the expected alignment ($i_x = 4.2\hbar$) from the EF quasiparticles. On the other hand, the BC quasiparticles would contribute with an alignment of about $6.9\hbar$, therefore we tentatively assign the $aAEF$ and $bAEF$ configurations for band 2. The calculated splitting between the above configurations is ≈ 20 keV, around $\hbar\omega = 0.35$ MeV. The extrapolated crossing frequency between band 2 and band 1 lies above the upbend in band 1, which is qualitatively consistent with the present assignment. A band with similar characteristics to band 2 has been observed in ^{106}Ag by Popli *et al.* [2] and Jerrestam *et al.* [4]. The latter authors seem to suggest a $\pi g_{9/2} \otimes \nu(h_{11/2})^2(g_{7/2}, d_{5/2})$ configuration for this band. However, our calculations predict too large an alignment ($i_x = 6.8\ \hbar$) relative to band 1 for this configuration.

B. Bands 3 and 4

Both bands 3 and 4 present large signature splitting (250 keV and 350 keV, respectively), strong $E2$ transitions, and weak or absent $M1$ transitions. The 6^+ isomer has been interpreted as $[\pi(g_{9/2})^{-3} \otimes \nu d_{5/2}]_{6^+}$ coupled to the ^{110}Sn core [14]. This would correspond to the aG, $\alpha = 0$ configuration (and aH for the favored signature $\alpha = 1$). We believe that this state is the bandhead of band 3. A similar band has also been observed above the 6^+ isomer of ^{106}Ag. The equilibrium deformation for this configuration is calculated to be around $\beta_2 = 0.1$, $\gamma = -120°$, i.e., slightly prolate, noncollective (Fig. 6) for frequencies below 0.4 MeV which might be interpreted as the $I = 6$ bandhead. Above 0.4 MeV the miminum is shifted to $\beta_2 = 0.16$, $\gamma = 0°$ (prolate, collective) as a result of the alignment of the prolate-driving AB quasineutrons. For the latter deformation a small signature splitting, an alignment of $13\hbar$, and strong $M1$ transitions as in the case of band 1, are expected, in evident contradiction with the experiment. Experimentally, band 3 is observed at $\hbar\omega \approx 0.47$ MeV. TRS calculations show that, as the frequency approaches 0.4 MeV, the total energy minimum becomes shallow, extending toward oblate-collective deformations. Oblate or triaxial deformations could account for an increase in signature splitting between the $g_{9/2}$ quasiprotons and for the absence of strong $M1$ transitions. The AB crossing is also shifted to larger frequencies and therefore no contribution to the alignment is expected from the AB quasiparticles. However, no clear explanation is available for the steady increase in alignment of band 3, which might be an indication of either deformation changes or quasiparticle alignment. More detailed calculations as well as experimental results are necessary to resolve these difficulties.

Similar TRS results are obtained for the aH (the unfavored signature of band 3), bG, bH, aE, aF, bE, and bF configurations, since the natural parity (+) quasineutron orbits present a rather weak dependence on β_2 and γ. We tentatively assign the aE and aF (aE, bE would also be possible) configurations to the favored and unfavored signatures of band 4. The spin of the levels in band 4 were chosen to be consistent with this assignment.

C. Bands 5 and 6

Band 5 shows a rather constant alignment of 6–$6.5\hbar$ in the frequency range from 0.2 to 0.5 MeV and a large signature splitting (200 keV). The absence of the neutron AB crossing (predicted to be at $\hbar\omega \approx 0.35$ MeV) and the large alignment is a clear indication of the presence of a $h_{11/2}$ quasineutron (A) in the configuration of this band. The signature splitting of 200 keV is close

to those calculated for both the $(p_{1/2}, f_{5/2})$ (g,h) and the second $g_{9/2}$ (c,d) quasiproton excitations. The calculated signature splitting of the latter configuration is strongly dependent on frequency, while the experimental one is constant. In addition, at low spins the experimental $B(M1)/B(E2)$ ratios are rather small (around 0.6 $\mu_N{}^2/e^2b^2$). For a fully aligned (doubly decoupled) pure $\pi p_{1/2} \otimes \nu h_{11/2}$ configuration no $M1$ transitions are expected at all $[B(M1)/B(E2) = 0]$. However, admixtures from $p_{1/2}$, $f_{5/2}$, and $p_{3/2}$ are present in the first two negative parity quasiproton excitations (g,h), increasing the effective g factor and the quasiparticle angular momentum projection along the symmetry axis (K). Figure 4 shows the theoretical estimates for the limit of pure $\pi f_{5/2} \otimes \nu h_{11/2}$ $(K = 2)$ configuration (dashed line). On the other hand, the presence of the $g_{9/2}$ quasiproton would lead to $M1$ transitions an order of magnitude stronger. In view of the above arguments we propose gA, hA for the 1 and 0 signatures of band 5, respectively. Also in the odd isotopes (^{105}Ag, ^{107}Ag) [7,6], admixed $\pi p_{1/2}$ bands have been observed with similar characteristics. We estimate $I = 6\hbar$ for the bandhead assuming $I = I_x = i_{x\pi} + i_{x\nu} \approx 0.5 + 5.5 = 6\hbar$ for this rotation aligned band.

Band 6 decays to band 5 around $I = 12\hbar$. The experimental signature splitting is negligible and the experimental $B(M1)/B(E2)$ ratios surprisingly show an increase of more than an order of magnitude relative to band 5, which points toward a major configuration change. The above-mentioned characteristics of band 6 indicate a large K value. A $(\pi g_{9/2})^2$ configuration is known to produce $K^\pi = 8^+$ isomers in neighboring even-even Cd isotopes [20,21], and related high-K bands in odd Cd isotopes [22]. The possibility of the coupling of $[\pi g_{9/2}{}^2]_{K=8}$ to the configuration of band 6 was considered, and provides a possible explanation for the negligible signature splitting and in particular, the large $B(M1)/B(E2)$ ratios observed (this configuration is labeled $gacA$ in Fig. 4). However, it is puzzling that such a presumably large change in K value from band 6 to band 5 does not result in an observable delay in the interband transitions. The experimental setup of this paper is sensitive to lifetimes above 20 ns.

VI. CONCLUSION

A level scheme for the states populated in a heavy ion reaction has been proposed for ^{108}Ag. Six bandlike structures are observed. Tentative configuration assignments were proposed for each band by combining low-lying quasiproton excitations of $g_{9/2}$, $(p_{1/2}, f_{5/2})$ parentage, with quasineutron excitations of $h_{11/2}$, $g_{7/2}$, $d_{5/2}$. Similar structures have been observed by previous experiments in other nearby odd-odd or odd-A Ag isotopes. Most of the band structures observed can be understood within the cranked shell model. A weakly deformed prolate shape is predicted by TRS calculations for the configurations containing at least one $h_{11/2}$ quasineutron excitation. This prediction seems to be consistent with the data presently available. The band developed above the 6^+ isomer appears to have characteristics of triaxial or oblate shapes and cannot be fully understood with the present TRS calculations which predict only prolate axially symmetric shapes at moderate rotational frequencies. More detailed calculations with parameters optimized specifically for the ^{108}Ag region might clarify these matters.

ACKNOWLEDGMENTS

This work was partially supported by the Conselho Nacional de Desenvolvimento Científico e Tecnológico (CNPq), Coordenação de Aperfeiçoamento de Pessoal de Nível Superior (CAPES), and Fundação de Amparo à Pesquisa do Estado de São Paulo (FAPESP).

[1] T. Komatsubara, K. Furuno, T. Hosoda, J. Mukai, T. Hayakawa, T. Morikawa, Y. Iwata, N. Kato, J. Espino, J. Gascon, N. Gjørup, G.B. Hagemann, H.J. Jensen, D. Jerrestam, J. Nyberg, G. Sletten, B. Cederwall, and P.O. Tjøm, Nucl. Phys. **A557**, 419c (1993), and references therein.

[2] R. Popli, F.A. Rickey, L.E. Samuelson, and P.C. Simms, Phys. Rev. C **23**, 1085 (1981).

[3] J. Tréherne, J. Genevey, S. André, R. Béraud, A. Charvet, R. Duffait, A. Emsallem, M. Meyer, C. Bourgeois, P. Kilcher, J. Sauvage, F.A. Beck, and T. Byrski, Phys. Rev. C **27**, 166 (1983).

[4] D. Jerrestam, W. Klamra, J. Gizon, F. Lidén, L. Hildingsson, J. Kownacki, Th. Lindblad, and J. Nyberg, Nucl. Phys. **A577**, 786 (1994).

[5] R. Duffait, A. Charvet, K. Deneffe, R. Beraud, A. Emsallem, M. Meyer, T. Ollivier, J. Tréherne, A. Gizon, F. Beck, and T. Byrski, Nucl. Phys. **A454**, 143 (1986).

[6] R. Popli, J.A. Grau, S.I. Popik, L.E. Samuelson, F.A. Rickey, and P.C. Simms, Phys. Rev. C **20**, 1350 (1979).

[7] H.J. Keller, S. Frauendorf, U. Hagemann, L. Käubler, H. Prade, and F. Stary, Nucl. Phys. **A444**, 261 (1985).

[8] V.R. Vanin and M. Aïche, Nucl. Instrum. Methods Phys. Res. Sect. A **284**, 452 (1989).

[9] W.T. Milner, VAXPAK programs, Oak Ridge National Laboratory (1986).

[10] K.S. Krane, R.M. Steffen, and R.M. Wheeler, Nucl. Data Tables **11**, 351 (1973).

[11] J.E. Draper, Nucl. Instrum. Methods Phys. Res. Sect. A **247**, 481 (1986).

[12] G.K. Rochester and K.F. Smith, Phys. Lett. **8**, 266 (1964).

[13] O.C. Kistener and A.W. Sunyar, Phys. Rev. **143**, 918 (1966).

[14] T. Hattori, M. Adachi, and H. Taketani, J. Phys. Soc. Jpn. **41**, 1830 (1976).

[15] R. Bengtsson and S. Frauendorf, Nucl. Phys. **A237**, 139 (1979).
[16] F. Dönau and S. Frauendorf, in *Proceedings International Conference on High Spin Properties of Nuclei*, Oak Ridge, 1982, edited by N.R. Johnson (Harwood, New York, 1983) Nucl. Sci. Res. Ser., Vol **4**, p. 143.
[17] R. Wyss, J. Nyberg, A. Johnson, R. Bengtsson, and W. Nazarewicz, Phys. Lett. B **215**, 211 (1988).
[18] W. Nazarewicz, J. Dudek, R. Bengtsson, T. Bengtsson, and I. Ragnorsson, Nucl. Phys. **A435**, 397 (1985).
[19] S. Frauendorf, Phys. Lett. **100B**, 219 (1981).
[20] I. Thorslund, C. Fahlander, J. Nyberg, S. Juutinen, R. Julin, M. Piiparinen, R. Wyss, A. Lampinen, T. Lönnroth, D. Müller, S. Törmänen, and A. Virtanen, Nucl. Phys. **A564**, 285 (1993).
[21] S. Juutinen, R. Julin, M. Piiparinen, P. Ahonen, B. Cederwall, C. Fahlander, A. Lampinen, T. Lönnroth, A. Maj, S. Mitarai, D. Müller, J. Nyberg, P. Šimeček, M. Sugawara, I. Thorslund, S. Törmänen, A. Virtanen, and R. Wyss, Nucl. Phys. **A573**, 306 (1994).
[22] S. Juutinen, P. Šimeček, C. Fahlander, R. Julin, J. Kumpulainen, A. Lampinen, T. Lönnroth, A. Maj, S. Mitarai, D. Müller, J. Nyberg, M. Piiparinen, M. Sugawara, I. Thorslund, S. Törmänen, and A. Virtanen, Nucl. Phys. **A577**, 727 (1994).

Anexos ao Capítulo 3

ELSEVIER

6 June 1996

PHYSICS LETTERS B

Physics Letters B 377 (1996) 1–4

BCS self-energy term and the ^{11}Li

M. Kyotoku [a], N. Teruya [a], C.L. Lima [b]

[a] *Departamento de Física, Universidade Federal da Paraíba, 58051-970 João Pessoa, Pb, Brazil*

[b] *Nuclear Theory and Elementary Particle Phenomenology Group, Instituto de Física, Universidade de São Paulo, C.P. 66318, 05389-970 São Paulo, SP, Brazil*

Received 18 September 1995; revised manuscript received 13 February 1996
Editor: G.F. Bertsch

Abstract

A careful treatment of the self-energy term in the BCS approach to the nuclear pairing problem is performed. A slightly modified gap equation is proposed and applied to light exotic nuclei. Our results are in agreement with the experimental binding energies for ^{11}Li.

PACS: 21.60.-n; 27.20.+n; 21.10.Dr

The recent interest on nuclei around the drip-line brought new structures and dynamics very different from those previously studied [1,2]. These new systems have presented challenges to nuclear models, which were developed to describe nuclei near the valley of stability. Fundamental questions, for instance the one related to the binding energy of drip line nuclei, are still on debate. The probably most studied exotic nuclei, ^{11}Li, may be viewed as a inert ^{9}Li core plus two valence neutrons and a basic problem is to understand the reasons why ^{11}Li is bound whereas ^{10}Li is not.

In this new field one of the puzzling questions for a nuclear theorist is whether the pairing phenomena plays any role in the understanding of the properties of this exotic nuclei region [3]. The fermionic pairing has been one of the building blocks to explain complicated nuclear phenomena [4], and the Bardeen-Cooper-Schrieffer (BCS) approximation is one of the cornerstones to treat it. This approximation however, breaks the number symmetry [5]. Since the nucleus has a fixed number of particles, the BCS wave functions have to be number projected leading to the Projected BCS (PBCS) but, in order to proceed in a consistent way, it is also necessary to project first and then to perform the variational calculation. This scheme is known as Fixed BCS (FBCS) and recently [6] the variation after projection equation was rederived by performing analytically all the integrals induced by the number projection. Furthermore, taking the gaussian limit of some binomial factors appearing in the integration procedure, the well known BCS gap equation was reobtained in a slightly modified form. However, in the limit of small number of available states to the valence particles, as in the low A exotic nuclei, this method cannot be applied. In this case a suitable gap equation can be obtained in the framework of the standard BCS. To achieve this goal the traditional BCS approach will be revisited, with a particular care on the treatment of the self-energy contribution, which may be important in the light exotic nucleus. As a result, a simple Pauli-blocking effect appears in the new gap

PII S0370-2693(96)00324-3

equation, which corresponds to the above mentioned one in the limit of large number of particles.

To begin with, let us write down the usual variational principle,

$$\delta\langle \mathrm{BCS}|\hat{H}-\lambda\hat{N}|\mathrm{BCS}\rangle \equiv \delta\langle \mathrm{BCS}|\hat{H}'|\mathrm{BCS}\rangle = 0 \tag{1}$$

or equivalently,

$$\left(\frac{\partial}{\partial v_j}-\frac{v_j}{u_j}\frac{\partial}{\partial u_j}\right) < \mathrm{BCS}|H'|\mathrm{BCS} >= 0. \tag{2}$$

In the above equations $\hat{N}$ is the number operator and λ is a Lagrange multiplier necessary to fix the mean particle number. u_j and v_j are the well known Bogoliubov Valatin coefficients [7]. Additionally, if it is considered that the fermions are occupying single particle levels of angular momentum j ($\Omega_j = j+\frac{1}{2}$) in a mean field (ε_j) interacting through a pure pairing force of state independent strength G, the mean value in Eq. (1) is given by,

$$h \equiv < \mathrm{BCS}|H'|\mathrm{BCS} > = 2\sum_j\left(\varepsilon_j-\lambda-\frac{G}{2}v_j^2\right)\Omega_j v_j^2 - G\sum_{ij}\Omega_i\Omega_j u_i v_i u_j v_j. \tag{3}$$

Inserting (3) into (2) and performing the algebra one obtains,

$$(u_j^2-v_j^2)\Delta + 2\left(\varepsilon_j-\lambda-Gv_j^2\right)u_j v_j = 0, \tag{4}$$

where,

$$\Delta \equiv G\sum_j \Omega_j u_j v_j. \tag{5}$$

From the above equation for the pairing gap Δ, the well known BCS gap equation can be obtained. The so called self-energy term, $\frac{G}{2}v_j^2$, is a contribution to the self-consistent field from the interacting valence particles. It is in general neglected with the argument that its only effect is to renormalize the single particle energies, which are normally extracted from, or fitted to experimental data in neighbor nuclei. It is also worth to note, that the self-energy depends on the variational parameter v_j which makes the single particle energy renormalization state dependent.

In the present paper a straightforward way to treat the self-energy term is suggested by using the normalization condition, $u_j^2+v_j^2=1$, of the Bogoliubov-Valatin transformation in Eq. (3) to get,

$$h = 2\sum_j\left(\varepsilon_j-\lambda-\frac{G}{2}\right)\Omega_j v_j^2 - G\sum_{ij}\Omega_j(\Omega_i-\delta_{ij})u_i v_i u_j v_j. \tag{6}$$

Following the same procedure used to derive Eq. (2) we obtain,

$$(u_j^2-v_j^2)\tilde{\Delta}_j + 2\left(\varepsilon_j-\lambda-\frac{G}{2}\right)u_j v_j = 0 \tag{7}$$

where,

$$\tilde{\Delta}_j = G\sum_i(\Omega_i-\delta_{ij})u_i v_i. \tag{8}$$

(In the remaining of this paper a tilde will be used to indicate the modified BCS quantities.)

The above modified gap equation is in agreement with previous results [6]. Eq. (8) can be obtained from Eq. (5) by simply replacing $\Omega_i \rightarrow \Omega_i-\delta_{ij}$. One may notice that the coefficient $\Omega_i-\delta_{ij}$ is similar to a Pauli-blocking, discussed around thirty years ago in the deformed nuclei [8] and recently [9] in the spherical odd nuclei. However, in the present case the interpretation is different, since it prevents a given pair to be rescattered to the same state it was occupying. For example, if a $j=1/2$ level is fully occupied, no particle pair can be rescattered to it because the factor δ_{ij} hinder this situation.

Since the gap parameter reflects the two-body interaction, giving rise to a smearing of the Fermi surface, the appearance of the additional δ_{ij} term in Eq. (8) was counterbalanced by the corresponding contribution to the self-energy term. This is very convenient, particularly in weakly bound systems where the continuum lies at low energy, being near to the bound states. The term $G/2$ in Eq. (7) is a real renormalization, shifting the mean field at once and it is not necessary anymore to treat it explicitly in a self-consistent calculation.

We proceed now to apply this technique to the light exotic nuclei region, where we believe that our results will be more sensible. To begin with, let's consider the most simple description of ^{11}Li namely, a ^{9}Li inert core plus a neutron pair occupying the $1p_{1/2}$ single

particle level. In this case Eq. (6) reduces to the first term at the rhs, since all the available states are occupied. The single particle energy is taken from the experimental data for ^{10}Li ($\varepsilon_{1p_{1/2}} = +0.50$ MeV). It should be emphasized that the self-energy term is not included in the single particle energy of the state $1p_{1/2}$, since ^{10}Li is unbound. Using for the pairing strength, $G \sim 15/A$, a not unrealistic value since we are dealing with a single j shell, the $1p_{1/2}$ state is now bound with a shifted energy $\bar{\varepsilon}_{1p_{1/2}} = -0.18$ MeV, resulting in a ^{11}Li bound state with energy -0.36 MeV. The adopted pairing strength gives raise to a pairing energy in good agreement with the experimental dineutron binding energy and moreover, seems to agree with the expected behavior of pairing in light nuclei [3]. The most conspicuous manifestation of pairing interaction, the pairing gap, is now zero. (In fact, the modified gap $\tilde{\Delta}$ is zero.) The pairing interaction is, however, still there since its effects are fully embodied in the renormalized mean field. The obtained $\bar{\varepsilon}_{1p_{1/2}}$ energy is similar to the one adopted by Bertsch and Foxwell (~ -0.19 MeV) [10] in their RPA calculation of the dipole strength function in ^{11}Li. Their rather unrealistic value for the single particle energy seems to be simulating the pairing interaction [2]. Although the previous application may be seen as a trivial one, since the same results could be obtained by treating exactly one pair in a single j-shell, it has the merit of showing the importance of a careful treatment of the self-energy contribution in dealing with exotic light nuclei.

We can now go one step further by including the additional contribution of the broad resonant state $2s_{1/2}$ lying at $\varepsilon_{2s_{1/2}} \sim 0.1$ MeV discussed in some recent papers [11,12]. (In fact, Ref. [12] considers this state as a virtual one, and hence with negative energy. This would imply, however, only in slight changes in the obtained pairing constant G, remaining the main conclusions of this paper unchanged.) Strictly speaking we have to deal with two levels of the same j ($\Omega \equiv \Omega_j$) separated by an energy $\epsilon = 0.4$ MeV. This is the standard two-level model of BCS theory. Using our method, the modified BCS ground state energy is given by,

$$E_{\widetilde{\mathrm{BCS}}} = h + \lambda \hat{N}. \tag{9}$$

Some simple algebra reduces Eq. (9) to,

Table 1
Comparison between the present results ($\widetilde{\mathrm{BCS}}$), the usual BCS (no self-energy term included) and PBCS approximations with the exact solution in the symmetric two level model. Column 2 presents the expressions for the ground state energies divided by Ω (in the present case equal to 1), in terms of a dimensionless parameter $\kappa = \epsilon/G$, whereas the third one shows the numerical values. $\varepsilon_{12} = \varepsilon_{2s_{1/2}} + \varepsilon_{1p_{1/2}}$. See text for details

Method	Ground state energy	Numerical value
BCS	$\varepsilon_{12} - \frac{1}{2}\kappa\epsilon - G$	-0.10
$\widetilde{\mathrm{BCS}}$	$\varepsilon_{12} - \frac{1}{2}\kappa\epsilon - \frac{3}{2}G$	-0.48
PBCS	$\varepsilon_{12} - 2G$	-0.67
Exact	$\varepsilon_{12} - G\left(1 + \sqrt{1+\kappa^2}\right)$	-0.79

$$\frac{E_{\widetilde{\mathrm{BCS}}}}{\Omega} = (\varepsilon_{2s_{1/2}} + \varepsilon_{1p_{1/2}}) - \frac{1}{2}\frac{\epsilon^2}{G(2\Omega - 1)} - \frac{G}{2}(2\Omega + 1). \tag{10}$$

In order to put in perspective our results, they will be compared with the usual BCS, PBCS and the exact solutions in the framework of a soluble model . In the symmetric two level model with $j = 1/2$, both exact solution using the quasi-spin scheme [13] and the projected BCS solution [6] can be performed analytically and the final ground state energy are shown in Table 1 in terms of a dimensionless parameter $\kappa = \epsilon/G$.

As usual, the state independent pairing strength G has to be lowered, in the multi-level case, regarding the value adopted for the single j-shell. From a technical point of view, it would not be a serious difficulty to use a state dependent one, viz. $G_{ij} = \langle i\bar{i}|V|j\bar{j}\rangle$. However, to keep the discussion as simple as possible, a state independent pairing strength was adopted. $G \sim 7/A$ (which corresponds to $\tilde{\Delta}_1 = \tilde{\Delta}_2 = 0.25\ MeV$) gives good agreement with the experimental data. This can be understood by comparing the results shown in the second column of Table 1 with the exact ones in the single j-shell limit (in this particular case of $\Omega = 1$, $E_{exact} = E_{\mathrm{BCS}} = E_{\widetilde{\mathrm{BCS}}} = 2\varepsilon_{1p_{1/2}} - G$): in the multi-level case, in order to get similar binding energies, one can see that G has to be decreased. Alternatively, we could think that the increase on the number of states available to the valence particles leads to a *correspondent* increase on the effectiveness of the pairing interaction.

With the above values, the BCS ground state energy is given by $E_{\widetilde{\mathrm{BCS}}} = -0.48$ MeV. Table 1 shows

Table 2
The second column shows the occupancies for the $2s_1/2$ state according to usual BCS, modified ($\widetilde{\text{BCS}}$) and exact solutions, in terms of a dimensionless parameter $\kappa = \epsilon/G$. The numerical values for the present calculation are shown in parentheses. The third column presents the number dispersion values for the same models

Method	Occupancy ($v^2_{2s_{1/2}}$)	$\Delta N/N$
BCS	$\frac{1}{2}\left[1+\frac{\kappa}{2}\right]$ (0.65)	0.67
$\widetilde{\text{BCS}}$	$\frac{1}{2}\lvert 1+\kappa\rvert$ (0.81)	0.55
Exact	$\frac{1}{2}\left(1-\frac{1}{\sqrt{1+\kappa^2}-\kappa}\right)$ (0.77)	–

additionally, on its third column, the numerical values for the exact, usual BCS and PBCS solutions. The improvement of the modified BCS calculation regarding the usual one is clear. It is worth to call again the readers attention to the importance of the adequate treatment of the self-energy term in order to obtain better results for the binding energies of nearly unbound systems within a technically simple approach.

Table 2 on its second column presents the expressions for the ground state occupancy of the $v_{2s_{1/2}}$ state for BCS, $\widetilde{\text{BCS}}$, and exact calculations. The numerical values for the $\widetilde{\text{BCS}}$ ground state occupancies are, respectively, $v^2_{2s_{1/2}} = 0.81$ and $v^2_{1p_{1/2}} = 0.19$ indicating, therefore, a $2s_{1/2}$ predominant character for the ground state. Table 2 shows also the numerical values for the particle number dispersion, $\Delta N/N = \sqrt{\left(\langle \hat{N}^2\rangle - N^2\right)}/N$, for the above mentioned models. We are then faced with a common disease of BCS-like approaches namely, the large dispersion on the particle number in the small particle number limit, indicating that the wave function contains significant amounts of $N \pm 2$, $N \pm 4$, ... particles. Regarding to this it is worth to note that: a) the present approach goes one step in the right direction, since both the occupancies and the particle number dispersion are closer to the exact ones, as can be seen in Table 2 and b) in recent papers Dobaczewski et al. [14] have discussed drip-line nuclei in the mass region $100 \leq A \leq 176$ using mean-field models taking into account the continuum. There it is discussed the break down of the simple HF+BCS model near the drip-line, due to difficulties in taken into account correctly the pairing coupling to the continuum states. In our case, however, the situation is different since the continuum states are sufficiently low in energy in order to allow the diving of one of its states to the discrete states region due to the self-energy term. Additionally it is also difficult to extrapolate the results of Ref. [14] to very low-A mass region.

To summarize the results of the present paper, a modified gap equation, suitable to low mass systems, was derived. It was discussed the reliability of a BCS pairing treatment in light exotic nuclei and also the importance of a careful treatment of the self-energy term in this mass region.

This work was supported in part by Conselho Nacional de Desenvolvimento Científico e Tecnológico (CNPq), Brasil.

References

[1] I. Tanihata et al., Phys. Lett. B 160 (1985) 380;
I. Tanihata et al., Phys. Rev. Lett. 55 (1985) 2676;
T. Kobayashi et al., Phys. Lett. B 232 (1989) 51.
[2] For a recent review see: C.A. Bertulani, L.F. Canto and M.S. Hussein, Phys. Rep. 226 (1993) 281.
[3] P.G. Hansen and B. Jonson, Europhys. Lett. 4 (1987) 408.
[4] A. Bohr, B.R. Mottelson and D. Pines, Phys. Rev. 110 (1958) 936.
[5] B.F. Bayman, Nucl. Phys. 15 (1960) 33.
[6] M. Kyotoku, K.W. Schmid, F. Grümmer and A. Faessler, Phys. Rev. C 41 (1990) 284.
[7] P. Ring and P. Schuck, The Nuclear Many-Body Problem, (Springer Verlag, New York, 1980).
[8] S. Wahlborn, Nucl. Phys. 37 (1962) 554.
[9] N. Sandulescu and R.J. Liotta, J. Phys. G: Nucl. Part. Phys. 20 (1994) 2001.
[10] G.F. Bertsch and J. Foxwell, Phys. Rev. C 41 (1989) 1300.
[11] B.M. Young et al., Phys. Rev. C 49 (1994) 279.
[12] I.J. Thompson and M.V. Zhukov, Phys. Rev. C 49 (1994) 1904.
[13] M. Rho and J.O. Rasmussen, Phys. Rev. 135 (1964) B 1295.
[14] J. Dobaczewski, I. Hamamoto, W. Nazarewicz and J.A. Sheikh, Phys. Rev. Lett. 72 (1994) 981;
J. Dobaczewski, H. Flocard and J. Treiner, Nucl. Phys. A 422 (1984) 103.

Modern Physics Letters A, Vol. 12, No. 37 (1997) 2883–2888

A BCS-LIKE APPROACH TO THE EXCITED STATE IN ^{11}Li

M. KYOTOKU*,†, C. L. LIMA‡, E. BALDINI NETO and N. TERUYA*
Nuclear Theory and Elementary Particle Phenomenology Group, Instituto de Física, Universidade de São Paulo, C.P. 66318, 05389-970 São Paulo, SP, Brazil

Received 28 August 1997
Revised 13 October 1997

A modified BCS approach is used to interpret the first excited state of ^{11}Li halo nuclei. In this scheme, a simple two-level model calculation is performed leading to results in good agreement with the experimental results for ^{11}Li for both ground and first excited states. A comparison with exact and QRPA calculations is also presented.

Nuclear theorists need to know more about the neutron-rich nuclei[1] ^{11}Li. One of the most important of them is to test, in the region of the drip line, the validity of nuclear models built primarily to describe nuclei in the valley of stability. Recently, an experimental study of ^{11}Li$+p$ collisions performed by a Riken/Kurchatov group[2] confirmed some spectroscopic data taken previously.[3,4] In this new experiment four excited states were observed in this nucleus, with energies $E^* = 1.25 \pm 0.15$, 3.0 ± 0.2, 4.9 ± 0.25 and 6.4 ± 0.25 MeV. The state at $E^* = 1.25$ MeV was measured for the first time through the charge exchange reaction[3] ^{11}B$(\pi^-, \pi^+)^{11}$Li and it was interpreted as a good candidate for the soft Giant Dipole Resonance[4] meanwhile the Riken/Kurchatov group reinterpreted it as an excitation of halo neutrons. The next state at $E = 3.0$ MeV is supposed to be an excitation of ^{9}Li core, the third is the sum of the two previously mentioned states and the last one is an excitation of $^7\text{Li} + 4n$ type.

The confirmation of the existence of these states, the suggestion that the first state can be a halo excitation and the lack of convincing structure calculations on these nuclei up to now, allow us to attempt a description of both the binding energy of the ^{11}Li and one of the above excited states using a schematic pairing Hamiltonian as a first-order approximation. We have shown[5] that the ^{11}Li ground state is bound with the small binding energy due to the pairing correlations. Our interpretation, based on the well-known fact that the pairing degree of freedom

PACS Nos.: 21.60.-n, 27.20.+n, 21.10.Dr
*On leave from Departamento de Física, Universidade Federal da Paraíba, 58051-970 João Pessoa, Pb, Brazil.
†E-mail: mkyotoku@fisica.ufpb.br
‡E-mail: cllima@if.usp.br

has an important role in the explanation of the nuclear structure of nuclei around the valley of stability, understands the ^{11}Li as an inert ^{9}Li core plus two valence neutrons occupying the single-particle states $2s_{1/2}$ and $1p_{1/2}$ seen experimentally a couple of years ago.[6] Aside from the inherent simplicity of the pairing model, the nature of these two single-particle states imply in a further simplification, since we are faced with the situation where the symmetric two-level toy model, laid many years ago,[7] become realistic. In this case most of the calculations can be performed analytically. The main goal of this letter is to extend our previous calculation,[5] aiming at an interpretation of the halo neutrons contribution to the first excited state of ^{11}Li as a 0^{-} one.

Thus, let us consider that our system has nucleons in a spherical mean field, ε_j, interacting through a residual pairing force with strength G, represented by the well-known pairing Hamiltonian. In spite of dealing with only two paired particles out of a core, it is always worthwhile to push the limits of the broken symmetry mean field concept. Recently, using the standard variational procedure and treating carefully the self-energy term, the standard BCS scheme was slightly modified and we could reproduce the experimental value of ^{11}Li two neutron separation energy.[5] In order to calculate the seniority zero excited state in this modified BCS framework, it is necessary to perform the Bogoliubov–Valatin canonical transformation[a] $c_{jm} = \tilde{u}_j a_{jm} + (-)^{j-m}\tilde{v}_j a^{\dagger}_{j-m}$ over the pairing Hamiltonian, written in terms of $c^{\dagger}_{jm}$ and c_{jm} which are, respectively, the particle creation and annihilation operators in the shell model basis. With such a transformation, the pairing Hamiltonian becomes

$$H = H_{00} + H_{11} + H_{20} + H_{02} + H_{22} + H_{31} + H_{13} + H_{40} + H_{04}\,,$$

where H_{mn} is written in terms of $(a^{\dagger})^n(a)^m$ or $(a)^n(a^{\dagger})^m$ as in Ref. 8. To obtain a quasi-particle mean field approximation we need, in the first place, to neglect the so-called residual terms $H_{22} + H_{31} + H_{13} + H_{40} + H_{04}$ and further to impose the condition $H_{20} + H_{02} = 0$. In Ref. 5, the following modified BCS equation was obtained

$$(\tilde{v}_j^2 - \tilde{u}_j^2)\tilde{\Delta}_j + 2\left(\varepsilon_j - \lambda - \frac{G}{2}\right)\tilde{u}_j\tilde{v}_j = 0\,.$$

Here $\tilde{u}_j$ and $\tilde{v}_j$ are the coefficients of the Bogoliubov transformation and

$$\tilde{\Delta}_j = G\sum_i(\Omega_i - \delta_{ij})\tilde{u}_i\tilde{v}_i\,,$$

is the modified gap equation ($\Omega_j = (2j+1)/2$ is the pair degeneracy). The simplicity of the BCS scheme is partially lost as we have to solve $M+1$ coupled nonlinear equations, where M is the number of single-particle levels. However, the coefficients

[a]In order to ease the comparison with the usual BCS quantities we use a tilde over the modified BCS ones. We call the reader's attention to the fact that in Ref. 5 only the modified gap was written using such a notation.

$\tilde{u}_j$ and $\tilde{v}_j$ of the Bogoliubov transformation are as simple as before and are given by

$$\begin{pmatrix} \tilde{u}_j^2 \\ \tilde{v}_j^2 \end{pmatrix} = \frac{1}{2}\left\{1 \pm \frac{\varepsilon_j - \lambda - G/2}{\tilde{E}_j}\right\},$$

where

$$\tilde{E}_j = \sqrt{\left(\varepsilon_j - \lambda - \frac{G}{2}\right)^2 + \tilde{\Delta}_j^2}.$$

With the above equations U_0, the ground state energy is determined,

$$U_0 = H_{00} + \lambda \sum_j 2\Omega_j \tilde{v}_j^2 = 2\sum_j \left(\varepsilon_j - \frac{G}{2}\right)\Omega_j \tilde{v}_j^2 - G\sum_{ij}(\Omega_i - \delta_{ij})\Omega_j \tilde{u}_i \tilde{v}_i \tilde{u}_j \tilde{v}_j\,.$$

The next term, which originates the quasi-particle mean field, already rewritten in terms of the bare self-energy is

$$H_{11} = \sum_{jm}\left[\left(\varepsilon_j - \lambda - \frac{G}{2}\right)\left(\tilde{u}_j^2 - \tilde{v}_j^2\right) + 2G\bar{\Delta}_j \tilde{u}_j \tilde{v}_j + \frac{G}{2}\right] a_{jm}^\dagger a_{jm}\,.$$

Replacing the above obtained $\tilde{u}_j$ and $\tilde{v}_j$, we get the following single quasi-particle Hamiltonian

$$H \approx U_0 + \sum_{jm} \mathcal{E}_j a_{jm}^\dagger a_{jm}\,,$$

where

$$\mathcal{E}_j = \tilde{E}_j + \frac{G}{2}\,.$$

Here, we should note that the self-energy term acts differently on the single quasi-particle energies as compared with its influence on the single-particle ones. On the latter it deepens the potential well whereas on the former it adds a factor to the "usual" single quasi-particle energy. This factor appears to compensate the deepening of the single-particle potential in such a way as to keep the excitation energy constant. This is shown in Table 1 where the same excited state energy is obtained in both approaches in a two-level model calculation. Another consequence of the renormalization of the single-particle energies is that the slope in the pair occupation ($\tilde{v}_j^2$) is sharper, or in other words, if the particles are more tightly bound ($\varepsilon_j \to \varepsilon_j - G/2$), less mass ($\bar{\Delta}$) would be created when the number symmetry is broken. This effect is presented in the second column of Table 1.

Table 2 compares the experimental result for the first excited state of the ^{11}Li with the theoretical predictions. The adopted values for the single-particle energies (after the subtraction of the factor $G/2$) are $\varepsilon_{2s_{1/2}} = -0.23$, $\varepsilon_{1p_{1/2}} = 0.17$

Table 1. The energy of first excited state calculated in the two-level model is displayed for the BCS, modified BCS, modified QRPA and exact solution as a function of G and the two-level model energy difference $\delta\varepsilon = \varepsilon_2 - \varepsilon_1$. The second column displays the gap parameter.

	Excited State	Δ^2
BCS	$2G$	$G^2 - \left(\frac{1}{2}\delta\varepsilon\right)^2$
$\widetilde{\text{BCS}}$	$2G$	$\frac{1}{4}G^2 - \left(\frac{1}{2}\delta\varepsilon\right)^2$
$\widetilde{\text{QRPA}}$	$2G\left[1+\frac{1}{2}\left(\frac{\delta\varepsilon}{G}\right)^2\right]$	—
Exact	$2\sqrt{G^2+(\delta\varepsilon)^2}$	—

Table 2. Comparison between modified BCS, QRPA and exact calculations for two values of the pairing strength constant G/A (in MeV) with the experimental results. The adopted value of the single-particle energy difference was $\delta\varepsilon = 0.4$ MeV. See text for details.

G/A	$\widetilde{\text{BCS}}$	$\widetilde{\text{QRPA}}$	Exact	Exp.
5/11	0.91	1.26	1.21	1.25
7/11	1.27	1.52	1.50	1.25

for $G = 5/11$ and $\varepsilon_{2s_{1/2}} = -0.32$, $\varepsilon_{1p_{1/2}} = 0.08$ for $G = 7/11$ (all energies in MeV). The corresponding single quasi-particle energies are $\mathcal{E}_{2s_{1/2}} = \mathcal{E}_{1p_{1/2}} = G$. Although the agreement is quite nice for a G value of 7/11 MeV, the same was used in the ground state energy calculation of Ref. 5, it is worthwhile to see the influence of the restoration, at least partially, of the broken symmetry. This can be done by reincorporating some of the neglected residual quasi-particle interaction terms, leading to the following quadratic Hamiltonian

$$H_{\text{bosons}} = \sum_j 2\mathcal{E}_j \mathcal{A}_j^\dagger \mathcal{A}_j - \frac{G}{4}\left[\sum_j \sqrt{\Omega_j}(\tilde{u}_j^2 - \tilde{v}_j^2)(\mathcal{A}_j^\dagger + \mathcal{A}_j)\right]^2 ,$$

where the two quasi-particle operator is defined as

$$\mathcal{A}_j^\dagger = \frac{1}{\sqrt{\Omega_j}} \sum_{m>0} a_{jm}^\dagger a_{j\bar{m}}^\dagger$$

and is approximated by a boson creation operator. The above Hamiltonian can be diagonalized exactly with the help of the following Bogoliubov transformation for bosons

$$\mathcal{B}_{nj}^\dagger = \sum_j \{a_{nj}\mathcal{A}_j^\dagger + b_{nj}\mathcal{A}_j\}$$

in such a way that,

$$[H_{\text{bosons}}, \mathcal{B}^{\dagger}_{nj}] = W_n \mathcal{B}^{\dagger}_{nj} .$$

Performing the algebra, the following $\widetilde{\text{QRPA}}$ equation is obtained

$$\begin{pmatrix} A & B \\ -B & -A \end{pmatrix} \begin{pmatrix} X \\ Y \end{pmatrix} = W_n \begin{pmatrix} X \\ Y \end{pmatrix} ,$$

where

$$A_{\alpha\beta} = 2\mathcal{E}_j \delta_{\alpha\beta} - \frac{G}{2}\sqrt{\Omega_\alpha \Omega_\beta}(\bar{u}^2_\alpha - \bar{v}^2_\alpha)(\bar{u}^2_\beta - \bar{v}^2_\beta) ,$$

$$B_{\alpha\beta} = 0 .$$

For the two-level model the above matrix is 4×4. Since the anti-diagonal term does not exist, it can be simplified further giving rise to

$$\begin{pmatrix} 2\left(G + \dfrac{(\varepsilon_2 - \varepsilon_1)^2}{4G}\right) & -\dfrac{(\varepsilon_2 - \varepsilon_1)^2}{2G} \\ -\dfrac{(\varepsilon_2 - \varepsilon_1)^2}{2G} & 2\left(G + \dfrac{(\varepsilon_2 - \varepsilon_1)^2}{4G}\right) \end{pmatrix} \begin{pmatrix} x_{n1} \\ x_{n2} \end{pmatrix} = W \begin{pmatrix} x_{n1} \\ x_{n2} \end{pmatrix} .$$

Table 1 presents the first excited state obtained with this framework whereas Table 2 shows its numerical value in the ^{11}Li case.

Since our system has only two particles outside the core, an exact solution can be obtained. In this case, rewriting the Hamiltonian in terms of quasi-spin operators we have

$$H = \varepsilon_1(\Omega_1 + 2S^0_1) + \varepsilon_2(\Omega_2 + 2S^0_2) - G(S^+_1 S^-_1 + S^+_2 S^-_1 + S^+_1 S^-_2 + S^+_2 S^-_2) ,$$

where

$$S^+_j = (S^-_j)^- = \frac{1}{2}\sum_m (-)^{j-m} c^{\dagger}_{jm} c^{\dagger}_{j-m}$$

and

$$S^0_j = \frac{1}{2}\left(\sum_m c^{\dagger}_{jm} c_{jm} - \Omega_j\right) .$$

The Schrödinger equation reduces to the following 2×2 analytically solvable eigenvalue equation

$$\begin{pmatrix} 2\varepsilon_1 - G & -G \\ -G & 2\varepsilon_2 - G \end{pmatrix} \begin{pmatrix} A \\ B \end{pmatrix} = E \begin{pmatrix} A \\ B \end{pmatrix}$$

furnishing the eigenvalues

$$E_{\pm} = (\varepsilon_1 + \varepsilon_2) - G \pm \sqrt{G^2 + (\varepsilon_2 - \varepsilon_1)^2}\,.$$

The minus sign corresponds to the ground state whereas $E_+ - E_-$ is the excitation energy displayed in Table 1. We should note that the $\widetilde{\text{QRPA}}$ is just the first-order Taylor expansion of the exact solution. Therefore, taking into account the usual QRPA with the self-energy term furnishes almost the exact result. Table 2 provides the numerical value of the energy of the first excited state measured recently by the Riken/Kurchatov group and compares the several approximations, beginning with the usual BCS, in a symmetric two-level model.

To summarize, we present an alternative interpretation of the first excited state in ^{11}Li, based on a modified version of the standard pairing model, which was applied previously to the ground state.[5] We claim that the pairing interaction do play a role even in this light exotic nuclei. Since the ^{11}Li is produced in the fragmentation process of heavier nuclei, the two halo neutrons could occupy any of the above discussed pair states. A fingerprint of this could be the detection of triton nuclei in a pick-up reaction of the type $^{11}\text{Li}(p,t)^9\text{Li}$. The entrance channel of this reaction is the same examined by the Riken/Kurchatov group, it would be interesting to look for the presence of triton on the final reaction products.

Acknowledgments

This work was supported in part by Conselho Nacional de Desenvolvimento Científico e Tecnológico (CNPq), Brazil and Fundação de Amparo à Pesquisa do Estado de São Paulo (FAPESP), Brazil.

References

1. I. Tanihata *et al.*, *Phys. Lett.* **B160**, 380 (1985); I. Tanihata *et al.*, *Phys. Rev. Lett.* **55**, 2676 (1985); T. Kobayashi *et al.*, *Phys. Lett.* **B232**, 51 (1989).
2. A. A. Korsheninnikov *et al.*, *Phys. Rev.* **C53**, R537 (1996).
3. H. G. Bohlen *et al.*, *Z. Phys.* **A351**, 7 (1995).
4. T. Kobayashi, *Nucl. Phys.* **A538**, 343c (1992).
5. M. Kyotoku, N. Teruya and C. L. Lima, *Phys. Lett.* **B377**, 1 (1996).
6. B. M. Young *et al.*, *Phys. Rev.* **C49**, 279 (1994).
7. J. Högaasen-Feldman, *Nucl. Phys.* **28**, 258 (1961).
8. M. Kyotoku, K. W. Schmid, F. Grümmer and A. Faessler, *Phys. Rev.* **C41**, 284 (1990).

Anexos ao Capítulo 4

J. Phys. A: Math. Gen. **28** (1995) 4915–4923. Printed in the UK

Phase transition in a q-deformed Lipkin model

S S Avancini†§, A Eiras†, D Galetti†, B M Pimentel† and C L Lima‡

† Instituto de Física Teórica, Universidade Estadual Paulista, Rua Pamplona 145, 01405-900, São Paulo, SP, Brazil

‡ Nuclear Theory and Elementary Particle Phenomenology Group, Instituto de Física, Universidade de São Paulo, CP 66318, 05389-970, São Paulo, SP, Brazil

Received 29 November 1994, in final form 15 June 1995

Abstract. Assuming q-deformed commutation relations for the fermions, an extension of the standard Lipkin Hamiltonian is presented. The usual quasi-spin representation of the standard Lipkin model is also obtained in this q-deformed framework. A variationally obtained energy functional is used to analyse the phase transition associated with the spherical symmetry breaking. The only phase transitions in this q-deformed model are of second order. As an outcome of this analysis a critical parameter is obtained which is dependent on the deformation of the algebra and on the number of particles.

1. Introduction

In the last decade a great effort has been devoted to the development and understanding of deformed algebras, although in many cases their direct physical interpretation is incomplete or even completely lacking. In some cases, like the XXZ-model where the ferromagnetic/antiferromagnetic nature of a spin-$\frac{1}{2}$ chain of length N can be simulated through the introduction of a q-deformed algebra, or the rotational bands in deformed nuclei which can be fitted instead of using a variable moment of inertia (VMI-model) via a q-rotor Hamiltonian, the physical meaning of such a deformation is clearly established. From the original studies, which appeared in connection with problems related to solvable statistical mechanics models [1] and quantum inverse scattering theory [2], a solid development has emerged which encompasses nowadays various branches of mathematical problems related to physical applications, such as deformed superalgebras [3], knot theories [4], non-commutative geometries [5] and so on. In this context, the introduction of a q-deformed bosonic harmonic oscillator, derived in such a way to pass from a $su(2)$ symmetry, originally present in the non-deformed case, to a $su_q(2)$ one, gave origin to new commutation relations which have been extensively studied in several papers [6, 7], all these results being unambiguously obtained due to the underlying $sl_q(2)$ structure [8].

The many-body problem is another mainstream area in physics and, in all its complexity, it calls for the use of approximate methods or the development of simple solvable models which should entail most of the relevant physics combined with a technically simple treatment [9]. A long heritage of such models is available in the nuclear physics literature, among which the Lipkin model [10] has been extensively used as a laboratory to test approximate methods and to point out the main features of the many-body systems.

§ Present address: Universidade Federal de Santa Catarina, Departmento de Física, 88040-900, Florianópolis, S. Catarina, Brazil.

0305-4470/95/174915+09$19.50

Nowadays, an important problem is to understand how the basic characteristics and the general behaviour of many-body systems are modified when the underlying fermionic algebra is deformed. The use of q-deformed algebra in the description of some many-body systems has lead to the appearance of new features when compared to the non-deformed case. In this connection we mention some examples: (i) in the q-oscillator many-body problem [7] it was shown that, when promoting the symmetries of the standard oscillator system to q-symmetries, the spectrum of the system is found to exhibit interactions between the levels of the individual oscillators; (ii) the revivals phenomenon present in the Jaynes–Cummings model [11] disappears when the original $su(2)$ symmetry is deformed; (iii) an extensive study of a deformed collective Lipkin Hamiltonian was performed and the q-deformed second-order phase transition was found to be suppressed [12]. The second-order phase transition associated with the spherical symmetry breaking in the quasi-spin space [13] for this deformed model was also discussed in the q-coherent states framework [14].

In the present paper we return to the original fermionic Lipkin Hamiltonian and extend it to a new one written in terms of q-deformed fermionic operators. Our main goals in such a study are: (i) to try to get some idea on the influence of this q-deformation and (ii) to investigate if new physical phenomena comes out via the introduction of the deformed algebra. Similarly to the extraction of a collective Lipkin Hamiltonian in terms of $su(2)$ quasi-spin operators from the original fermionic one, we show here that such a construction in terms of $su_q(2)$ quasi-spin operators written now in terms of q-deformed fermionic operators, is still valid. This new Hamiltonian is very different from that discussed in [12, 14] in that the mean-field term embodies now the effects of the deformation of the algebra giving rise to a change in the one-body energy spectrum in a similar way to the q-oscillator many-body problem [7].

We study the only phase transitions in this q-deformed model, which are of second order, following Holzwarth [13], i.e. the spherical symmetry breaking in the quasi-spin space, with this new collective deformed Hamiltonian. q-coherent states are used to define θ and φ as collective variables in terms of which the phase transition is analysed through the behaviour of the variationally obtained ground-state energy.

This paper is organized as follows. In section 2 we lay the basis of the q-fermionic extension of the standard Lipkin model (SLM) and the new collective deformed Lipkin Hamiltonian is constructed. Section 3 contains the basic definitions of the q-coherent states and the derivation of the ground-state energy functional. Finally, in section 4 the main results and conclusions are presented.

2. The q-deformed Lipkin model

Since the standard Lipkin model has been widely studied in the literature [15], we will only present here its main features.

In the SLM a system of N fermions is distributed in two N-fold degenerated levels. These two levels are distinguished by a quantum number σ whose values $+1$ and -1 refer to the upper and lower levels respectively; they are separated by an energy gap ϵ. The degeneracy of each level is taken care of by a quantum number p with values ranging from 1 to N.

The SLM Hamiltonian is written as

$$H = \frac{\epsilon}{2}\sum_{p,\sigma}\sigma a^{\dagger}_{p,\sigma}a_{p,\sigma} + \frac{V}{2}\sum_{p,p',\sigma} a^{\dagger}_{p,\sigma}a^{\dagger}_{p',\sigma}a_{p',-\sigma}a_{p,-\sigma}. \tag{2.1}$$

The main advantage of this model, as was originally shown by Lipkin [10], is that it is

exactly soluble, its collective excitations being more clearly studied in the $su(2)$ quasi-spin formalism. As a result, a second-order phase transition is obtained from the calculated collective spectrum in the $N \to \infty$ limit [16].

Recently [12], the SLM has been studied in the q-deformed $su(2)$ quasi-spin formalism where q is the deformation parameter of the algebra. The usual $su(2)$ algebra is recovered when $q \to 1$. In this paper the phase transition was analysed in the q-deformed context and the main result of the analysis was the suppression of the phase transition as q increases. A problem akin to this was studied in another paper by one of the authors using deformed $su(2)$ coherent states in a variational approach [14]. On the other hand, a similar result was obtained in a study of the revivals which appear in the Jaynes–Cummings model [11], which are suppressed in the deformed case [17].

From a more fundamental point of view, the question on the possibility of constructing a q-deformed Lipkin Hamiltonian from the basic fermion operators is a very important one. The hint to answer this question is the study of a system of M bosonic harmonic oscillators developed by Floratos [7], where the full Hamiltonian is not just the sum of individual oscillators but rather a sum of terms involving coproducts, the construction being necessary in order to preserve the $U(M)$ symmetry when the algebra is deformed. Although we have not mathematically proved that the derived expressions satisfy a genuine fermionic coproduct, the adopted form is important to obtain the q-deformed quasi-spin operators, as will be seen later. Following the idea of Floratos, the deformed fermionic Lipkin Hamiltonian, with the deformation parameter expressed as $q = \exp\gamma$, is given by

$$H = \mathcal{H}_0 + \mathcal{H}_1 \tag{2.2}$$

with

$$\mathcal{H}_0 = \frac{\epsilon}{2}\sum_p e^{2\gamma\mathcal{A}_<(p)}\{\mathcal{H}_{p\uparrow}\cosh\gamma h_{p\downarrow} - \cosh\gamma h_{p\uparrow}\mathcal{H}_{p\downarrow}\}e^{-2\gamma\mathcal{A}_>(p)} \tag{2.3}$$

$$\mathcal{H}_1 = \frac{V}{2}\left[\left(\sum_p e^{\gamma\mathcal{A}_<(p)}a^\dagger_{p\uparrow}a_{p\downarrow}e^{-\gamma\mathcal{A}_>(p)}\right)^2 + \left(\sum_p e^{\gamma\mathcal{A}_<(p)}a^\dagger_{p\downarrow}a_{p\uparrow}e^{-\gamma\mathcal{A}_>(p)}\right)^2\right] \tag{2.4}$$

where

$$\mathcal{H}_{p\uparrow(\downarrow)} = \tfrac{1}{2}\left(a^\dagger_{p\uparrow(\downarrow)}a_{p\uparrow(\downarrow)} - a_{p\uparrow(\downarrow)}a^\dagger_{p\uparrow(\downarrow)}\right) \tag{2.5}$$

$$\mathcal{A}_<(p) = \tfrac{1}{2}\sum_{p'<p}(h_{p'\uparrow} - h_{p'\downarrow}) \tag{2.6}$$

$$\mathcal{A}_>(p) = \tfrac{1}{2}\sum_{p'>p}(h_{p'\uparrow} - h_{p'\downarrow}) \tag{2.7}$$

and

$$h_{p\uparrow(\downarrow)} = a^\dagger_{p\uparrow(\downarrow)}a_{p\uparrow(\downarrow)} - \tfrac{1}{2}. \tag{2.8}$$

In the above expressions the fermionic operators obey q-deformed anticommutation relations below [3, 18]; however, it is worth noting that the adopted q-deformed fermionic extension of the usual anticommutation relations are by no means unique in the literature [19].

$$a_{p\sigma}a^\dagger_{p\sigma} + qa^\dagger_{p\sigma}a_{p\sigma} = q^{\hat{n}_{p\sigma}} \tag{2.9}$$

$$\{a_{p\sigma}, a_{p'\sigma'}\} = \{a^\dagger_{p\sigma}, a^\dagger_{p'\sigma'}\} = 0 \qquad \forall p, p', \sigma, \sigma' \tag{2.10}$$

$$\{a_{p\sigma}, a^\dagger_{p'\sigma'}\} = 0 \qquad p \neq p' \tag{2.11}$$

$$\{a_{p\sigma}, a^\dagger_{p\sigma'}\} = 0 \qquad \sigma \neq \sigma' \tag{2.12}$$

$$[\hat{n}_{p\sigma}, a^{\dagger}_{p\sigma}] = a^{\dagger}_{p\sigma} \tag{2.13}$$

$$[\hat{n}_{p\sigma}, a_{p\sigma}] = -a_{p\sigma}. \tag{2.14}$$

The q-deformed number operator $\hat{n}_{p\sigma}$ in the above equations is equal to $(h_{p\sigma} + \frac{1}{2})$ only at the level of the physical representation. However, at the level of the algebra they are in general different.

Starting from equation (2.3) and using equations (2.9)–(2.14) it is straightforward but tedious to obtain

$$\mathcal{H}_0 = \frac{\epsilon}{4\sinh(\gamma/2)} \sinh\gamma \sum_p \left(h_{p\uparrow} - h_{p\downarrow}\right). \tag{2.15}$$

Until now we have been working with the deformed fermionic operators. The question now is to see if, as was done long ago in nuclear physics [20] for the non-deformed case, it is possible to construct a q-deformed quasi-spin algebra from the underlying q-deformed fermionic operators. Since our main interest is to study the collective excitations, in particular the phase transitions, we must construct the corresponding $su_q(2)$ quasi-spin Hamiltonian in order to recover the original simplicity of the SLM. We, therefore, introduce the operators

$$s^0_p \equiv \tfrac{1}{2}\left(h_{p\uparrow} - h_{p\downarrow}\right) \tag{2.16}$$

$$s^+_p \equiv a^{\dagger}_{p\uparrow} a_{p\downarrow} \tag{2.17}$$

$$s^-_p \equiv a^{\dagger}_{p\downarrow} a_{p\uparrow} \tag{2.18}$$

which satisfy the following commutation relations

$$[s^0_p, s^{\pm}_p] = \pm s^{\pm}_p \tag{2.19}$$

$$[s^+_p, s^-_p] = [2s^0_p]_q \tag{2.20}$$

where the bracket on the right-hand side of equation (2.20) is defined in the standard way

$$[x]_q = \frac{q^x - q^{-x}}{q - q^{-1}} = \frac{e^{\gamma x} - e^{-\gamma x}}{e^{\gamma} - e^{-\gamma}}. \tag{2.21}$$

Furthermore, we define the q-deformed quasi-spin operators

$$S_0 \equiv \sum_p s^0_p \tag{2.22}$$

$$S_{\pm} \equiv \sum_p e^{\gamma \sum_{p'<p} s^0_{p'}} s^{\pm}_p e^{-\gamma \sum_{p'>p} s^0_{p'}} = \sum_p e^{\gamma \mathcal{A}_<(p)} s^{\pm}_p e^{-\gamma \mathcal{A}_>(p)} \tag{2.23}$$

which satisfy the same commutation relations (2.19)–(2.20). It is important to emphasize the use of $h_{p\sigma}$ instead of $\hat{n}_{p\sigma}$, as usually performed in the literature in the bosonic case. As stated before, they are equivalent at the level of the representation.

The action of the S_0, $S_{\pm}$ operators on the deformed $|S, s\rangle$ basis [21] is given by

$$S_0|S, s\rangle = s|S, s\rangle \tag{2.24}$$

$$S_{\pm}|S, s\rangle = \sqrt{[S \mp s]_q [S \pm s + 1]_q}\,|S, s \pm 1\rangle \tag{2.25}$$

and, in particular, it is worth noting that for the Lipkin ground-state multiplet the basis states correspond to

$$|S, s\rangle = \left|\frac{N}{2}, s\right\rangle. \tag{2.26}$$

The q-deformed Lipkin Hamiltonian can then be rewritten in terms of S_0 and $S_\pm$ as

$$H = \frac{\epsilon}{4\sinh(\gamma/2)}\sinh(2\gamma S_0) + \frac{V}{2}(S_+^2 + S_-^2). \tag{2.27}$$

It is easy to verify that this expression goes back to the SLM Hamiltonian when $\gamma \to 0$ (or $q \to 1$), as do the commutation relations of the q-deformed quasi-spin operators.

We should point out here the difference between the Hamiltonian in equation (2.27) and the version of the Lipkin Hamiltonian used in previous papers [12, 14]. The difference lies in the mean-field term which now embodies q-deformation effects arising from a careful treatment of the q-deformation of the algebra already at the fermionic level.

3. The q-deformed Lipkin Hamiltonian in the $su_q(2)$ coherent states

Recently, in the works of Quesne and Jurčo [22] q-analogues of the $su(2)$ Perelomov coherent states [23] were defined for the $su_q(2)$ quantum algebra in terms of a q-exponential. Following [14] we define the q-analogue to the su (2) coherent state

$$|z\rangle \equiv \mathrm{e}_q^{\bar{z}S_-}|S, s\rangle \tag{3.1}$$

where z is a complex number ($\bar{z}$ is its complex conjugate) which for later convenience will be parametrized as

$$z = \tan\frac{\theta}{2}\mathrm{e}^{\mathrm{i}\phi} \tag{3.2}$$

where $\theta \in [0, \pi]$, $\phi \in [0, 2\pi]$ and the q-exponential is

$$\mathrm{e}_q^x = \sum_{n=0}^{\infty}\frac{x^n}{[n]_q!} \tag{3.3}$$

with $[n]_q! = [n]_q[n-1]_q \ldots [1]_q$. We would like to note that our definition for the $su_q(2)$ coherent state is based on the maximum weight, whereas in [22] the minimal one was used.

Defining the q-binomial coefficient

$$\begin{bmatrix} n \\ m \end{bmatrix}_q \equiv \frac{[n]_q!}{[n-m]_q![m]_q!} \tag{3.4}$$

equation (3.1) can be rewritten as

$$|z\rangle = \sum_{s=-S}^{S}\begin{bmatrix} 2S \\ S-s \end{bmatrix}_q^{1/2}\bar{z}^{S-s}|S, s\rangle \tag{3.5}$$

whose normalization is given by

$$\langle z|z\rangle = \prod_{k=0}^{N-1}\left[1 + \mathrm{e}^{\gamma(2k-N+1)}\right]. \tag{3.6}$$

We now use the coherent state (3.1) as a trial state for the q-deformed Lipkin Hamiltonian ground state. Thus, we get

$$\frac{\langle z|H|z\rangle}{\langle z|z\rangle} = \frac{\epsilon\langle z|\sinh(2\gamma S_0)|z\rangle}{4\sinh(\gamma/2)\langle z|z\rangle} + \frac{V\langle z|S_+^2 + S_-^2|z\rangle}{2\langle z|z\rangle} \tag{3.7}$$

where

$$\frac{\langle z|\sinh(2\gamma S_0)|z\rangle}{\sinh(\gamma/2)\langle z|z\rangle} = \frac{[N]_q}{[1/2]_q}\frac{\cos\theta}{\mathcal{D}(\gamma, \theta)} \tag{3.8}$$

$$\frac{\langle z|S_+^2 + S_-^2|z\rangle}{\langle z|z\rangle} = \frac{[N]_q[N-1]_q\sin^2\theta\cos 2\phi}{2\mathcal{D}(\gamma, \theta)} \tag{3.9}$$

and

$$\mathcal{D}(\gamma,\theta)=1+\sinh^2\left[\frac{\gamma}{2}(N-1)\right]\sin^2\theta. \tag{3.10}$$

We can normalize equation (3.7) as

$$E(\theta,\phi,\gamma,N)=\frac{\langle z|H|z\rangle}{\epsilon_q\langle z|z\rangle}=\frac{[N]_q}{2}\left\{\frac{\cos\theta}{\mathcal{D}(\gamma,\theta)}+\frac{\chi}{2}\frac{\sin^2\theta\cos 2\phi}{\mathcal{D}(\gamma,\theta)}\right\} \tag{3.11}$$

where

$$\epsilon_q=\frac{\epsilon}{2[1/2]_q}$$

is the q-deformed energy spacing and

$$\chi=\frac{V[N-1]_q}{\epsilon_q} \tag{3.12}$$

is an effective coupling strength.

4. Results and conclusions

Equation (3.11) is the expression for the variational energy from which we should extract the main information about the Lipkin model ground state, as described by the q-deformed coherent state. We should note that the energy depends on the deformation of the algebra and is proportional to $[N]_q$, whereas the terms enclosed by the curly brackets are functions of N and γ through the product $\gamma(N-1)$ and of the effective coupling strength χ.

In order to study the ground-state energy we must require the conditions

$$\frac{\partial E(\theta,\phi,\gamma,N)}{\partial\phi}=0 \tag{4.1}$$

$$\frac{\partial E(\theta,\phi,\gamma,N)}{\partial\theta}=0 \tag{4.2}$$

to be satisfied.

The first equation gives $\phi=\frac{\pi}{2}$ and $\frac{3\pi}{2}$ as global minima, the interesting physics lying on the interplay between θ and γN. The second equation exhibits two solutions with similar features as those obtained in the non-deformed Lipkin model, the first one being

$$\sin\theta=0 \tag{4.3}$$

completely equivalent to the standard case, while the second one

$$-1-\chi\cos\theta-2C\cos\theta\frac{(\cos\theta-\frac{1}{2}\chi\sin^2\theta)}{1+C\sin^2\theta}=0 \tag{4.4}$$

where

$$C=\sinh^2\left[\frac{\gamma}{2}(N-1)\right] \tag{4.5}$$

now embodies the effects of the deformation of the algebra. Equation (4.4) is quadratic in $\cos\theta$ giving rise only to second-order phase transitions.

Equation (4.4) allows us to calculate the critical value of the strength parameter χ characterizing the phase transition whose analytical expression is then

$$\chi_c=1+2\sinh^2\left[\frac{\gamma}{2}(N-1)\right]. \tag{4.6}$$

In the same fashion as discussed by Holzwarth [13], we would expect here the second-order phase transition, characterizing the spherical symmetry breaking in the quasi-spin space, to show up as the appearance of two symmetrical minima shifted from the origin and a maximum at the position of the old minimum. However, contrary to the standard case where $\chi_c = 1$, here the critical value of the coupling constant depends on the parameter $\gamma(N-1)$. This implies that now the phase transitions depend not only on the strength of the interaction but also on the deformation of the algebra and on the number of particles through the product $\gamma(N-1)$.

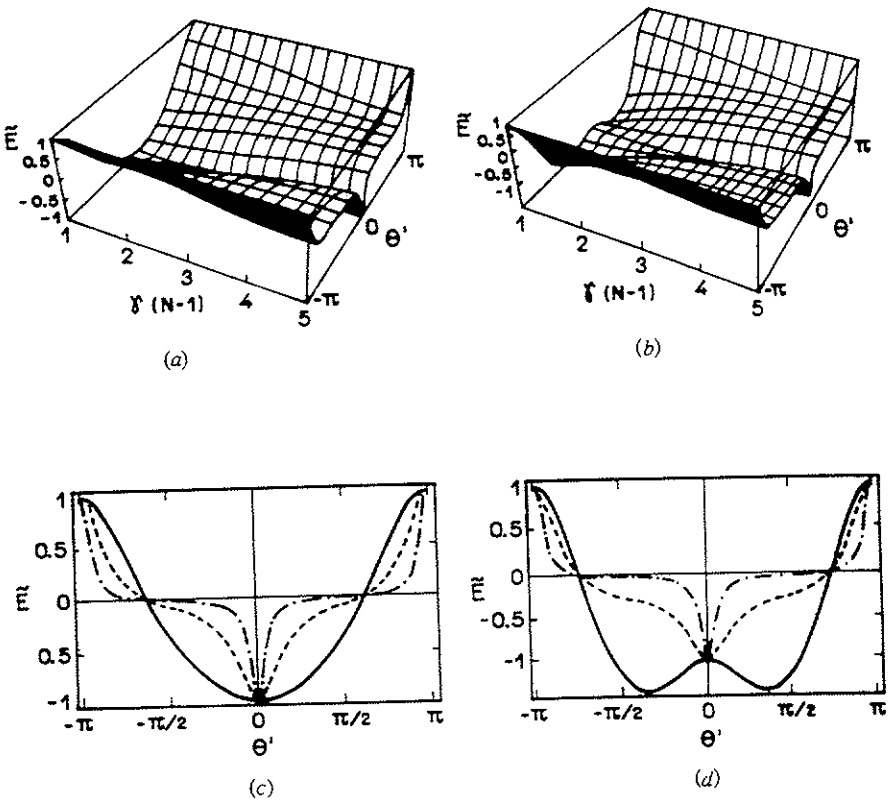

Figure 1. (*a*) and (*b*) show 3D views of the scaled energy surfaces ($\tilde{E} = 2E/[N]_q$) for $\chi = 1$ and 3 respectively, as a function of $\gamma(N-1)$ and of the order parameter $\theta' = \pi - \theta$. (*c*) and (*d*) show sections of the energy surfaces at $\gamma(N-1) = 1$ (full curve), 3 (dashed curve) and 5 (dot-dashed curve). The behaviour of $\tilde{E}$ for both global minima at $\varphi = \frac{\pi}{2}$ and $\frac{3\pi}{2}$ is shown together by extending the domain of θ' from $-\pi$ to π.

Figures 1(*a*) and (*b*) show scaled energy surfaces for different values of χ as a function of $\gamma(N-1)$ and the order parameter $\theta' = \pi - \theta$ [16], whereas figures 1(*c*) and (*d*) depict sections of the corresponding 3D-pictures for different values of $\gamma(N-1)$. There is a striking difference between the pictures on the left- and right-hand sides of figure 1, namely the number of minima. The reason for this behaviour in the first case is that χ_c, calculated by expression (4.6), is always greater than that for any value of $\gamma > 0$, as can be seen in figure 2. This in turn means that there will be no phase transition when one increases the deformation of the algebra for a fixed $\chi \leqslant 1$. Figures 1(*b*) and (*d*), however, present a gradual collapse of the two minima, characterizing the phase transition, in a new one at

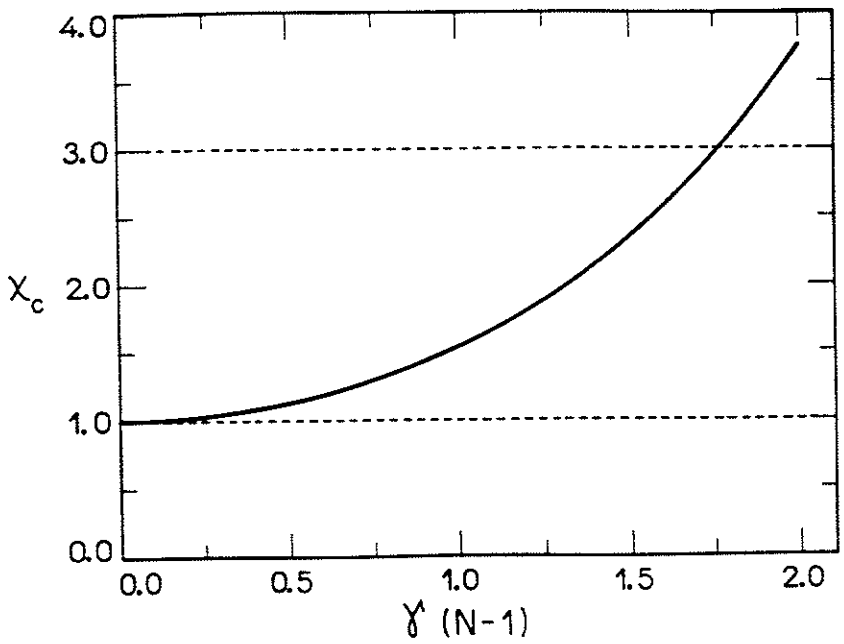

Figure 2. The critical value of χ as a function of $\gamma(N-1)$. The dashed curves indicate the region of existence of the phase transition.

$\theta' = 0$ as γ increases. For low values of $\gamma(N-1)$, $\chi = 3$ is greater than the value of χ_c, as can be seen from figure 2. In this range of $\gamma(N-1)$ we clearly identify the phase transition. However, for values of $\gamma(N-1)$ for which $\chi_c > 3$, no phase transition is allowed.

To summarize the main results of the present paper we would like initially to stress the importance of a careful treatment of the q-deformation, already at the fermionic level, in order to correctly take into account the effects in a many-body system. In the present case this gives rise to a q-dependent mean field as shown in equation (2.27). As a second aspect, we point out we have also obtained a critical value of χ, equation (4.6), which is a function of $\gamma(N-1)$. This means that a universal character can no longer be assigned to χ as a system-independent indicator of the phase transition in a q-deformed system.

Acknowledgments

The authors are grateful to J C Brunelli for helpful discussions. AE, DG, BMP and SSA acknowledge the support by Conselho Nacional de Desenvolvimento Cientí fico e Tecnológico (CNPq), Brazil.

References

[1] Baxter R J 1982 *Exactly Solved Models in Statistical Mechanics* (London: Academic)
[2] Sklyanin E, Takhatajan L and Fadeev L 1979 *Theor. Math. Phys.* **40** 194
[3] Chaichian M and Kulish P 1990 *Phys. Lett.* **234B** 72
[4] Kauffman L 1990 *Int. J. Mod. Phys.* A **5** 93
[5] Manin Y 1988 *Quantum Groups and Non-Commutative Geometry (Centre des Recherches Mathématiques)* (Montreal: Montreal University Press)
Connes A 1990 *Géometrie Non-Commutative* (Paris: Intereditions)

[6] Biedenharn L C 1989 *J. Phys. A: Math. Gen.* **22** L783
Macfarlane A J 1989 *J. Phys. A: Math. Gen.* **22** 4581
[7] Floratos E G 1991 *J. Phys. A: Math. Gen.* **24** 4739
[8] Chaichian M 1993 unpublished lecture notes, Instituto de Física Teórica, São Paulo, Brazil
[9] Ring P and Schuck P 1980 *The Nuclear Many-Body Problem* (New York: Springer)
[10] Lipkin H J, Meshkov N and Glick A J 1965 *Nucl. Phys.* **62** 188
[11] Buck B and Sukumar C V 1981 *Phys. Lett.* **81A** 132
Buzek V 1989 *Phys. Rev.* A **39** 3196
[12] Galetti D and Pimentel B M 1995 *Ann. Acad. Bras. Cien.* **67** 1
[13] Holzwarth G 1973 *Nucl. Phys.* A **207** 545
[14] Avancini S S and Brunelli J C 1993 *Phys. Lett.* **174A** 358
[15] Klein A and Marshalek E R 1991 *Rev. Mod. Phys.* **63** 375
[16] Gilmore R and Feng D H 1978 *Phys. Lett.* **76B** 26
Yaffe L 1982 *Rev. Mod. Phys.* **54** 482; 1983 *Phys. Today* **August** 50
[17] Chaichian M, Elinas D and Kulish P 1990 *Phys. Rev. Lett.* **65** 980
[18] Ng Y J 1990 *J. Phys. A: Math. Gen.* **23** 1203
[19] Frappat L, Sorba P and Sciarrino A 1991 *J. Phys. A: Math. Gen.* **24** L179
Viswanathan K S and Parthasarathy R 1992 *J. Phys. A: Math. Gen.* **25** L335
Bonatsos D and Daskaloyannis C 1993 *Phys. Lett.* **307B** 100
[20] Kerman A K 1961 *Ann. Phys., NY* **12** 300
[21] Jimbo M 1985 *Lett. Math. Phys.* **10** 63
[22] Quesne C 1991 *Phys. Lett.* **153A** 303
Jurčo B 1991 *Lett. Math. Phys.* **21** 51
[23] Arecchi F T, Courtens E, Gilmore R and Thomas H 1972 *Phys. Rev.* A **37** 2211
Perelomov M 1972 *Commun. Math. Phys.* **26** 222
Gilmore R 1974 *Rev. Mex. Fis.* **23** 143

Q-deformed algebras and many-body physics[1]

D. Galetti, J. T. Lunardi, B. M. Pimentel
Instituto de Física Teórica-UNESP
01405-900, São Paulo, SP - Brazil

C. L. Lima
Nuclear Theory and Elementary Particle Phenomenology Group
Instituto de Física-USP
05389-970, São Paulo, SP - Brazil

A review is presented of some applications of $q-$deformed algebras to many-body systems. The rotational and pairing nuclear problems will be discussed in the context of $q-$deformed algebras, before presenting a more microscopically based application of $q-$deformed concepts to many-fermion systems.

1. Introduction

In the last decade a great effort has been devoted to the development and understanding of deformed algebras, although their direct physical interpretation is sometimes incomplete or even completely lacking. In some cases like the XXZ-model, where the ferromagnetic/antiferromagnetic nature of a spin $\frac{1}{2}$ chain of length N can be simulated through the introduction of a q-deformed algebra [1], or the rotational bands in deformed nuclei and molecules which can be fitted via a q-rotor Hamiltonian [2-4], instead of using the variable moment of inertia (VMI-model), is the physical meaning of such a deformation established. From the original studies which appeared in connection with problems related to solvable statistical mechanics models [5] and quantum inverse scattering theory [6], a solid development has emerged which encompass nowadays various branches of mathematical problems related to physical applications, such as deformed superalgebras [7], knot theories [8], non-commutative geometries [9] and so on. In this context, the introduction of a q-deformed bosonic harmonic oscillator, derived in such a way to pass from a $su(2)$ symmetry, originally present in the non-deformed case, to a $su_q(2)$ one, gave

[1]Dedicated to Prof. Paulo Leal Ferreira on his 70th birthday. His scientific contribution to the development of Theoretical Physics, particularly in our country, will never be acknowledged enough.

origin to new commutation relations which have been extensively studied in several papers [10-12] being all these results unambiguously obtained due to the underlying $sl_q(2)$ structure [13].

The nucleus is a finite quantal many-baryon system. It provides a scenario where electromagnetic, weak and strong interactions play their role altogether. The nucleus may be, therefore, a natural place to look for manifestations of new symmetries and/or deviations from old ones.

A plethora of models have been developed to deal with the physics of such a complex system, some of them with more phenomenological foundations, for instance the nuclear collective model, being others based on the underlying fermionic structure of the nuclear many body system, like the mean-field plus residual interaction description of the nuclei.

The many-body problem in all its complexity calls for the use of approximate methods or the development of simple solvable models which should entail most of the relevant physics combined with a technically simple treatment [14]. A long heritage of such models is available in the nuclear physics literature, among which the Lipkin model [15] has been extensively used as a laboratory to test approximate methods and to point out the main features of the many-body systems.

From the point of view of $q-$deformed algebra applications to physical systems it is important to understand how the basic characteristics and the general behavior of many-body systems are modified when the underlying algebra is deformed. The use of q-deformed algebra in the description of some many-body systems has lead to the appearance of new features when compared to the non-deformed case. In this connection we mention some examples: a) in the q-oscillator many-body problem [12] it was shown that, when promoting the symmetries of the standard oscillator system to q-symmetries, the spectrum of the system is found to exhibit interactions between the levels of the individual oscillators, b) the revivals phenomenon present in the Jaynes-Cummings model [16] disappears when the original $su(2)$ symmetry is deformed, c) an extensive study of a deformed collective Lipkin Hamiltonian was performed and the q-deformed second order phase transition was found to be suppressed [17]. The second order phase transition associated to the spherical symmetry breaking in the quasi-spin space [18] for this deformed model was also discussed in the q-coherent states framework [19]. A recent paper [20] has shown, in the framework of the $q-$deformed Lipkin Hamiltonian, the importance of a careful treatment of the mean field, when dealing with $q-$deformed fermionic systems.

In this talk different aspects of the application of $q-$algebras to many-body physics will be presented. After a short review of the basic concepts of $q-$deformed algebras in section 2, "phenomenological" applications of $q-$ algebras in nuclear physics will be discussed in section 3. Section 4 will deal with $q-$deformed many fermion systems in the context of a q-fermionic extension of the standard Lipkin model (SLM). In this section the discussion will be concentrated on the phase transition behavior of fermionic $q-$deformed systems, both at zero and finite temperatures. Finally some conclusions will be drawn on section 5.

2. A brief review of $su_q(2)$ deformed algebras

The concept of deformed algebra emerged in the eighties and is still object of continuous developments in mathematics and physics. It was introduced in the context of exactly soluble statistical models, integrable systems in field theory, non-commutative geometry and other fields. Of particular interest are the developments by Biedenharn [10] and Macfarlane [11] on the $q-$analogues of the quantum harmonic oscillator. If the importance of the harmonic oscillator in many branches in physics will be reproduced in the context of $q-$algebras, it can be expected that its study may provide some guidance in this new field.

The quantum algebra $su_q(2)$ is a deformation of the Lie algebra of the $SU(2)$ group. Deformation in this context does not mean exactly what we may be acquainted with, for instance in a non spherical nucleus or a molecule, but rather deformation here is to be understood as modifications in the commutation relations among the generators of the algebra according to given, although not unique, prescriptions. A possible realization of the $su_q(2)$ quantum algebra in terms of three Hermitian operators J_+, J_- and J_0 is shown below along with the usual $su(2)$ algebra:

$$\boxed{\begin{array}{ccc} su(2) & & su_q(2) \\ [J_0, J_\pm] = \pm J_\pm & \rightarrow & [J_0, J_\pm] = \pm J_\pm \\ \\ [J_+, J_-] = 2J_0 & \rightarrow & [J_+, J_-] = [2J_0]_q \end{array}} \tag{2.1}$$

The new quantity $[x]_q$ appearing above is a $q-$number and it can be defined as,

$$[x]_q = \frac{q^x - q^{-x}}{q - q^{-1}} = \frac{\sinh \gamma x}{\sinh \gamma}, \tag{2.2}$$

where $q = e^\gamma$ may be a complex number. $Q-$numbers go to the usual numbers as $q \rightarrow 1$ (or $\gamma \rightarrow 0$), meaning that the well known commutation relations of the $su(2)$ algebra are recovered in this limit.

The quadratic Casimir operator of $su_q(2)$ given by,

$$C_q = J_+ J_- + [J_0]_q [J_0 - 1]_q, \tag{2.3}$$

still commutes with the generators of the algebra. Jimbo [21] has shown that, given Eqs.(2.1), exists a representation, for each j ($j = 0, 1/2, 1, ...,$) with basis $|jm\rangle$ ($-j \leq m \leq j$), such that,

$$J_0 |jm\rangle = m |jm\rangle \tag{2.4}$$

$$J_\pm |jm\rangle = \sqrt{[j \mp m]_q [j \pm m + 1]_q}\, |jm \pm 1\rangle . \tag{2.5}$$

The $su_q(2)$ irreducible representations D^j are obtained from the maximum weight states. The basis states $|jm\rangle$ are connected to the maximum weight states $|jj\rangle$ in the following way,

$$|jm\rangle = \sqrt{\frac{[j+m]_q!}{[2j]_q! [j-m]_q!}} (J_-)^{j-m} |jj\rangle , \tag{2.6}$$

where, $[n]_q! = [1]_q[2]_q....[n]_q$ and,

$$C_q\,|jm\rangle = [j]_q[j+1]_q\,|jm\rangle\,. \tag{2.7}$$

Analogously to the standard construction of irreducible representations of $su(2)$ due to Schwinger [22], Macfarlane proposed a way to write **J** in terms of the creation and destruction operators of a pair of independent $q-$deformed harmonic oscillator degrees of freedom [11]. $Q-$bosons can be defined through the commutation relations,

$$a_i a_i^\dagger - q a_i^\dagger a_i = q^{-N_i} \tag{2.8}$$

$$[N_i, a_i^\dagger] = a_i^\dagger \quad \text{and} \quad [N_i, a_i] = -a_i, \tag{2.9}$$

where $a_i^\dagger$ (a_i) are creation (annihilation) operators and N_i is the corresponding number operator. The whole $su_q(2)$ spectrum can now be described by two commuting oscillators,

$$|jm\rangle = \frac{(a_1^\dagger)^{j-m}}{\sqrt{[j-m]_q!}}\frac{(a_2^\dagger)^{j+m}}{\sqrt{[j+m]_q!}}\,|0\rangle\,. \tag{2.10}$$

In terms of $q-$bosons the generators of $su(2)$ can be written as,

$$J_+ = a_1^\dagger a_2, \quad J_- = a_2^\dagger a_1, \quad 2J_0 = N_1 - N_2. \tag{2.11}$$

We would like to call the reader's attention to the fact that the above way of $q-$deform the $su(2)$ algebra is by no means unique [23]. In fact, the lack of uniqueness in deriving $q-$deformed objects is a source of skepticism on the reliability of the application of $q-$algebras to physical systems. As a matter of fact, the unclear (if any) physical meaning of the $q-$deformation is another source of such a skeptical attitude. In the next section we will briefly review two examples where the physical meaning of the $q-$deformation seems to be established.

3. $Q-$deformed algebras applied to nuclear physics

This section will deal with some applications of $q-$deformation to nuclear systems. Two problems will be discussed: a) pairing in a single j shell , and b) the spectra of rotational nuclei. Both cases have a $su(2)$ structure and the $q-$deformation will be performed at the level of the generators of the algebra. We have called these two situations "phenomenological" because the $q-$deformation of the algebra is performed irrespectively of the underlying fermionic structure.

3.1. Pairing in a single j shell

Pairing plays an important role in the structure of nuclei. It is by far the most important part of the residual interaction around magic nuclei. Among the very many applications of pairing model to nuclei, the ^{40}Ca isotopes represent a particularly simple situation, since the $1f_{7/2}$ level is fairly isolated from the others and can therefore be considered as a single j shell.

In this case, the pairing Hamiltonian can be written,

$$H_{pairing} = -\frac{G}{4} \sum_{jm,j'm'} (-)^{j-m}(-)^{j'-m'} c^{\dagger}_{j'm'} c^{\dagger}_{j'-m'} c_{j-m} c_{jm}, \tag{3.1}$$

where $c^{\dagger}_{jm}(c_{jm})$ is the creation (annihilation) operator in the single j shell orbit. G is the pairing strength.

Due to the underlying $su(2)$ structure of the single j shell pairing Hamiltonian, it can be written in terms of the quasi-spin operators [14],

$$H_{pairing} = -GS_+S_- = -GS^2 - GS_0(S_0 - 1)), \tag{3.2}$$

where $S_+ = \sum_{m>0}(-)^{j+m} c^{\dagger}_{jm} c^{\dagger}_{j-m}$, $S_- = \sum_{m>0}(-)^{j+m} c_{j-m} c_{jm}$ and $S_0 = \frac{1}{2}(\sum_m c^{\dagger}_{jm} c_{jm} - \Omega)$ satisfy quasi-spin (angular momentum) commutation relations. $\Omega = \frac{1}{2}(2j+1)$ is the pair degeneracy. The eigenstates are labeled by the number of particles n and by the number of unpaired particles ν (seniority quantum number) giving rise to the eigenvalues,

$$E(n,\nu) = -\frac{G}{4}(n-\nu)(2\Omega - \nu - n + 2).$$

The $q-$deformation of the quasi-spin pairing Hamiltonian in Eq.(3.2) can be easily performed by using Eq.(2.3) and rewriting it in terms of the Casimir operators of $su_q(2)$,

$$H^q_{pairing} = -GC_q - G[S_0]_q[S_0 - 1]_q. \tag{3.3}$$

Like in the non-deformed case, n and ν label the eigenstates of $H^q_{pairing}$ and their eigenvalues are given by [24],

$$E_q(n,\nu) = -G\frac{(q^{\frac{1}{2}(n-\nu)} - q^{-\frac{1}{2}(n-\nu)})(q^{(\Omega-\frac{1}{2}(\nu+n)+1)} - q^{-(\Omega-\frac{1}{2}(\nu+n)+1)})}{(q-q^{-1})^2}. \tag{3.4}$$

Defining a state dependent parametrization for the deformation of the algebra, $q = \exp(\frac{1}{2}(n-\nu)\gamma')$, we obtain,

$$E_q(n,\nu) = -G\frac{\sinh[\frac{1}{2}(n-\nu)^2\gamma'] \sinh\{[\Omega - \frac{1}{2}(\nu+n)+1]\frac{1}{2}(n-\nu)\gamma'\}}{\sinh^2(\frac{1}{2}(n-\nu)\gamma')}. \tag{3.5}$$

Figure 3.1 shows the corresponding results for the ground state energies of the even-A Ca isotopes.

The results are rather good, even considering the, non usual, state dependent parametrization used. This can be understood if we Taylor expand a typical term appearing in $H^q_{pairing}$, namely,

$$\frac{q^{S_0} - q^{-S_0}}{q - q^{-1}} \approx S_0 + [(S_0-1)^2 + (S_0-3)^2 + ...](\delta q)^2. \tag{3.6}$$

Therefore, it seems that, by $q-$ deforming the $su(2)$ algebra, higher order terms of the residual interaction are taken into account in an effective way.

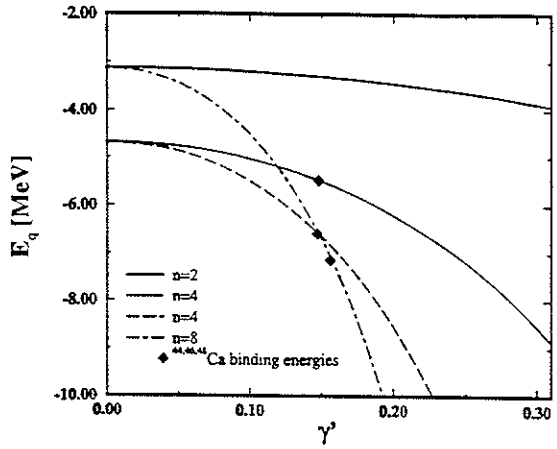

Fig. 3.1: This figure shows the binding energies of even A Ca isotopes as a function of the deformation parameter γ'. n=2,4,6,8 correspond to $^{42,44,46,48}Ca$ respectively. The diamonds are the experimental data for $^{44,46,48}Ca$. The pairing strength was adjusted to the ^{42}Ca binding energy.

3.2. The spectra of rotational nuclei

This case has some similarities with the pairing one. The $q-$deformed Hamiltonian for rotational nuclei can be written in terms of the usual one simply substituting the $su(2)$ Casimir operator by its deformed version:

$$\boxed{H_{rotor} = E_0 + \frac{1}{2I}J(J+1) \quad \rightarrow \quad H^q_{rotor} = E_0 + \frac{1}{2I}C_q,} \tag{3.7}$$

where E_0 is the band-head energy and I is the moment of inertia.

There are (at least) two different approaches:

1) q is a phase ($q = e^{i\gamma}$) and $C_q = J_+J_- + [J_0]_q[J_0 - 1]_q$. Rather good fits to the rotational spectra of nuclei and molecules are obtained.

Figure 3.2 presents the ^{236}U experimental transition energies along with fittings using the non-deformed and deformed rotor Hamiltonians. Three different values of the deformation parameter γ are presented and for $\gamma = 0.030$ the agreement is quite good. The reason for this success is simple: C_q is equivalent to an expansion in powers of $j(j+1)$:

$$E_j = E_0 + a(q)j(j+1) + b(q)[j(j+1)]^2 + \ldots .$$

Moreover, the coefficients $a(q), b(q), \ldots$ have alternating signs ($a > 0$) and magnitudes in agreement with phenomenology [3]. On the other side, looking at the corresponding transition probabilities (Fig. 3.3) [25], this success looks less spectacular: good agreement is obtained with $\gamma = 0.019$ whereas $\gamma = 0.030$ is completely off. This clearly should not be considered as a difficulty of the $q-$deformation scheme but rather it is an inherent difficulty in any attempt to get good descriptions of both spectra and wave functions.

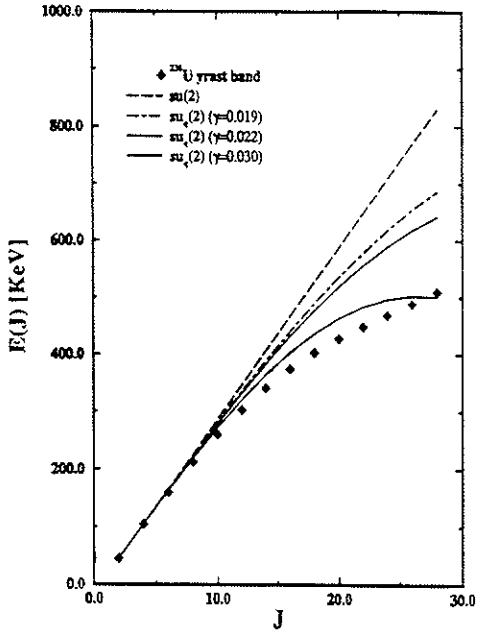

Fig. 3.2: Experimental transition energies $\Delta E(J) = E(J) - E(J-2)$ for the yrast states of ^{236}U are shown along with the $su(2)$ and $su_q(2)$ predictions calculated with three different values of the deformation parameter γ.

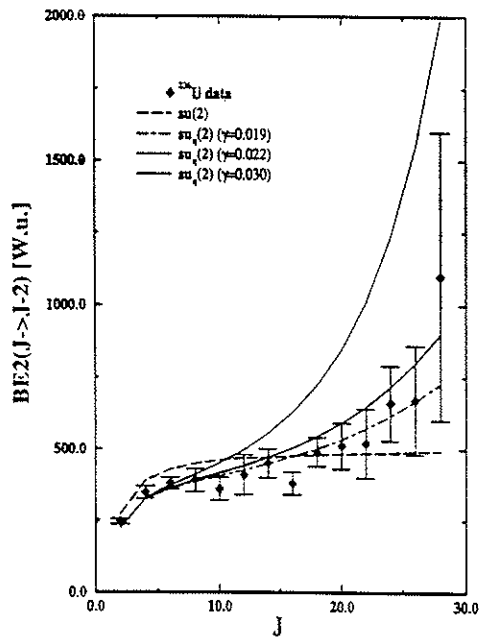

Fig. 3.3: The same as Fig. 3.2, but for the transition probabilities $BE2(J \rightarrow J-2)$.

We would like to call the readers' attention to a difficulty of this approach: if q is a phase, it is not clear how to calculate the norm of the q-deformed bosonic state. This can be considered as a minor problem since we are just fitting the data, however this may bring some doubts on the correctness of this deformation scheme, as applied to rotational nuclei.

2) q is real and the $q-$deformed Casimir is taken to be [26],

$$C_q = \frac{[4]_p}{2[2]_p} \frac{[2J+1]_p^2 [2J]_p [2J+2]_p}{[4J+2]_p^2},$$

($p = \sqrt{q}$). In this case, also impressive good fits to rotational spectra of nuclei and molecules can be obtained [2]. We would like to emphasize that this way of $q-$deforming the algebra is free from the normalization disease pointed out previously.

4. Phase transition in a $Q-$deformed Lipkin model

Along the years, the Lipkin Hamiltonian [15] has been a theoretical laboratory to test models in many-body physics. It is exactly soluble and is a "quasi-spin like" model. Its structural simplicity will again be useful in an attempt to understand the influence of the $q-$deformation on the behavior of physical systems. In the standard Lipkin model N fermions occupy two N-fold degenerate levels. The Hamiltonian of the SLM can be written as,

$$H_{Lipkin} = \frac{\epsilon}{2} \sum_{p,\sigma} \sigma a^\dagger_{p,\sigma} a_{p,\sigma} - \frac{V}{2} \sum_{p,p',\sigma} a^\dagger_{p,\sigma} a^\dagger_{p',\sigma} a_{p',-\sigma} a_{p,-\sigma}. \tag{4.1}$$

In the above expression p ranges from 1 to N and $\sigma = \pm 1$.

Galetti and Pimentel [17] studied the SLM in the deformed quasi-spin formalism to investigate the influence of the $q-$deformation in the phase transition. As a result they found the suppression of the phase transition with the increasing of q.

Along with this phenomenological approach, a question as emerged, namely, to understand how the general behavior of the many-body system is modified when the fermionic algebra is deformed.

In order to have some guidance we have looked at the bosonic case [12]:

> In a system of M bosonic harmonic oscillators, the full Hamiltonian is not just the sum of the individual oscillators, but rather it is a sum of terms involving coproducts if we want to preserve the symmetry of the algebra when deformed, namely, $su(M) \longrightarrow su_q(M)$.

For example, in the two-oscillator case:

$$N_i = a_i^\dagger a_i, \;\; h_i = N_i + \frac{1}{2}, \; H_i = \frac{1}{2}\left(\left[h_i + \frac{1}{2} \right]_q + \left[h_i - \frac{1}{2} \right]_q \right), \; i = 1, 2$$

we have,

normal	$q-$deformed
$[a_i, a_i^\dagger] = 1$	$a_i a_i^\dagger - q a_i^\dagger a_i = q^{-N_i}$
$H = h_1 + h_2$	$H^q = H_1 + H_2$
	$\hookrightarrow H^q = \dfrac{\sinh(\frac{1}{2}\gamma(h_1+h_2))}{2\sinh(\gamma/2)}$

A similar prescription applied to the $q-$deformed Lipkin Hamiltonian gives rise to:

$$H^q_{Lipkin} = \frac{\epsilon}{4\sinh\frac{\gamma}{2}}\sinh(2\gamma S_0) + \frac{V}{2}(S_+^2 + S_-^2), \tag{4.2}$$

where S_0, S_+ and S_- are the quasi-spin operators for the $q-$deformed Lipkin Hamiltonian. As a consequence, the mean field is also $q-$deformed [20].

With this new collective deformed Hamiltonian we study the only phase transitions in this $q-$deformed model, which are of second order, *a la* Holzwarth [18], *i.e.* the spherical symmetry breaking in the quasi-spin space.

Q-analogues [27] of the $su(2)$ Perelomov coherent states [28] are used to define θ and φ as collective variables. The phase transition is analyzed through the behavior of the variationally obtained ground state energy functional,

$$E(\theta,\phi,\gamma,N) = \frac{\langle z|\, H^q_{Lipkin}\,|z\rangle}{\epsilon_q\,\langle z|z\rangle} = \frac{[N]_q}{2}\left\{\frac{\cos\theta}{\mathcal{D}(\gamma,\theta)} + \frac{\chi}{2}\frac{\sin^2\theta\cos 2\phi}{\mathcal{D}(\gamma,\theta)}\right\} \tag{4.3}$$

where

$$\mathcal{D}(\gamma,\theta) = 1 + \sinh^2\left[\frac{\gamma}{2}(N-1)\right]\sin^2\theta. \tag{4.4}$$

In the above expressions, $\epsilon_q = \frac{\zeta}{2[1/2]_q}$ is the q-deformed energy spacing and $\chi = \frac{V[N-1]_q}{\epsilon_q}$ is an effective coupling strength.

From $E(\theta,\phi,\gamma,N)$ we extract the main information about the Lipkin model ground state, as described by the $q-$deformed coherent state. The energy depends on the deformation of the algebra and is proportional to $[N]_q$. The terms enclosed by the curly brackets in Eq.(4.3) are function of N and γ through the product $\gamma(N-1)$ and of the effective coupling strength χ.

In order to study the ground state energy we must require the conditions

$$\frac{\partial E(\theta,\phi,\gamma,N)}{\partial\phi} = 0 \tag{4.5}$$

$$\frac{\partial E(\theta,\phi,\gamma,N)}{\partial\theta} = 0 \tag{4.6}$$

to be satisfied.

From the above equations we can calculate the critical value of the coupling constant χ, which characterizes the phase transition. The frame below presents the differences between the non deformed case and the deformed one.

Standard case	$q-$deformed
$\chi_c = 1$	$\chi_c = 1 + 2\sinh^2\left[\frac{\gamma}{2}(N-1)\right]$

In the same fashion as discussed by Holzwarth [18], we would expect here the second order phase transition, characterizing the spherical symmetry breaking in the quasi-spin space, to show up as the appearance of two symmetrical minima shifted from the origin and a maximum at the position of the old minimum. In this $q-$deformed case, however, the phase transition depends **not only** on the strength of the interaction but **also on the deformation** of the algebra and **on the number of particles** through the product $\gamma(N-1)$ [20].

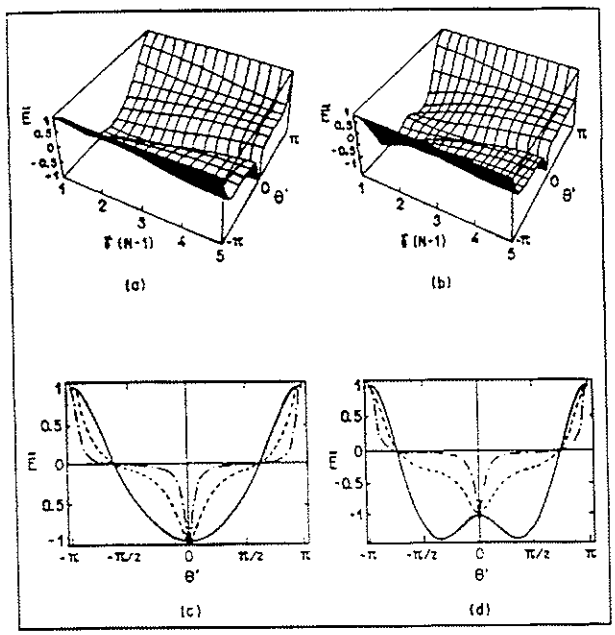

Fig. 4.1: Figures (a) and (b) show 3D views of the scaled energy surfaces ($\tilde{E} = 2E/[N]_q$) for $\chi = 1$ and 3 respectively, as function of $\gamma(N-1)$ and of the order parameter $\theta' = \pi - \theta$. Figures (c) and (d) show sections of the energy surfaces at $\gamma(N-1) = 1$ (full line), 3 (dashed line) and 5 (dot-dashed line). The behavior of $\tilde{E}$ for both global minima at $\varphi = \pi/2$ and $3\pi/2$ is shown together by extending the domain of θ' from -π to π.

Figures 4.1a and 4.1b show scaled energy surfaces for different values of χ as a function of $\gamma(N-1)$ and the order parameter $\theta' = \pi - \theta$ [29], whereas figures 4.1c and 4.1d depict sections of the corresponding 3D-pictures for different values of $\gamma(N-1)$. There is a striking difference between the pictures on lhs and rhs of Fig. 4.1, namely the number of minima. The reason for that behavior in the first case is that χ_c is always greater than one for any value of $\gamma > 0$, as can be seen in Fig. 4.2. This in turn means that there will be no phase transition when one increases the deformation of the algebra for a fixed $\chi \leq 1$.

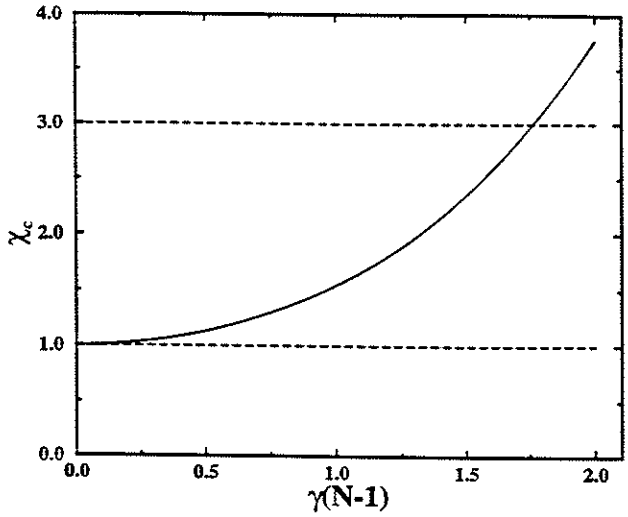

Fig. 4.2: The critical value of χ as function of $\gamma(N-1)$. The dashed lines indicate the region of existence of phase transition.

Figures 4.1b and 4.1d, however, present a gradual collapse of the two minima, characterizing the phase transition, in a new one at $\theta' = 0$ as γ increases. For low values of $\gamma(N-1)$, $\chi = 3$ is greater than the value of χ_c, as can be seen from Fig. 4.1. In this range of $\gamma(N-1)$ we clearly identify the phase transition. However for values of $\gamma(N-1)$ for which $\chi_c > 3$, no phase transition is allowed.

Recently, temperature was included in the above framework [30]. For each T a behavior similar to the one a $T = 0$ is obtained, at least before the value of q where the system collapses. $Q-$deformation has the effect of lowering the critical temperature.

5. Conclusions

The conclusions will be divided in two parts. In the first one, some general characteristics of the $q-$deformed algebras, as seen from some naïve applications to nuclear and molecular physics, will be pointed out. In the so called specific conclusions, the focus will be on characteristics of fermionic $q-$deformed many-body systems.

- General

  1. $q-$deformation perhaps may bring new physics.
  2. In some simple systems it is possible to attribute a physical meaning to the deformation parameter.
  3. However, it seems impossible to attribute a universal significance to it, particularly due to the different deformation schemes.
  4. $q-$deformation has one interesting aspect: it seems to incorporate in an effective way and in an elegant framework the interaction among the constituents of the system.

- **Specific**

  1. It is important a careful treatment of the q-deformation, already at the fermionic level, in order to take into account its effects correctly in a many-body system.
  2. $q-$deform a fermionic many-body system gives rise to a q-dependent mean field.
  3. The critical value of χ is a function of $\gamma(N-1)$. This means that no universal character can be anymore assigned to χ as a system independent indicator of the phase transition in a q-deformed system.
  4. Inclusion of temperature does not change the general behavior.

References

[1] V. Pasquier and H. Saleur, Nucl. Phys. **B330**, 523 (1990).

[2] S. Iwao, Prog. Theor. Phys. **83**, 363 (1990); R. H. Capps, Preprint Purdue University, PURD-TH-94-02 (1994).

[3] D. Bonatsos, E. N. Argyres, S. B. Drenska, P. P. Raychev, R. P. Roussev and Yu. F. Smirnov, Phys. Lett. **B251**, 477 (1990).

[4] E. Celeghini, R. Giachetti, E. Sorace and M. Tarlini, Phys. Lett. **B280**, 180 (1992).

[5] R. J. Baxter, *Exactly Solved Models in Statistical Mechanics* (Academic Press, London, 1982).

[6] E. Sklyanin, L. Takhatajan and L. Fadeev, Theor. Math. Phys. **40**, 194 (1979).

[7] M. Chaichian and P. Kulish, Phys. Lett. **B 234**, 72 (1990).

[8] L. Kauffman, Int. J. Mod. Phys. **A5**, 93 (1990).

[9] Y. Manin, *Quantum Groups and Non-Commutative Geometry, (Centre des Recherches Mathématiques*, Montreal University Press. Montreal, 1988); A. Connes, *Géometrie Non-Commutative* (Intereditions, Paris, 1990).

[10] L. C. Biedenharn, J. Phys. A: Math. Gen. **22**, L783 (1989).

[11] A. J. Macfarlane, J. Phys. A: Math. Gen. **22**, 4581 (1989).

[12] E. G. Floratos, J. Phys. A: Math. Gen. **24**, 4739 (1991).

[13] M. Chaichian, Lecture Notes, unpublished, Instituto de Física Teórica, 1993.

[14] P. Ring and P. Schuck, *The Nuclear Many-Body Problem* (Springer Verlag, New York, 1980).

[15] H. J. Lipkin, N. Meshkov and A. J. Glick, Nucl. Phys. **62**, 188 (1965).

[16] B. Buck and C. V. Sukumar, Phys. Lett. **A 81**, 132 (1981); V. Buzek, Phys. Rev. **A 39**, 3196 (1989).

[17] D. Galetti and B. M. Pimentel, Ann. Acad. Bras. Cien. **67**, 7 (1995).

[18] G. Holzwarth, Nucl. Phys. **A207**, 545 (1973).

[19] S. S. Avancini and J. C. Brunelli, Phys. Lett. **A 174**, 358 (1993).

[20] S. S. Avancini, A. Eiras, D. Galetti, B. M. Pimentel and C. L. Lima, J. Phys. A: Math. Gen. **28**, 4915 (1995).

[21] M. Jimbo, Lett. Math. Phys. **10**, 63 (1985).

[22] J. Schwinger, in *Quantum Theory of Angular Momentum* (eds. L. C. Biedenharn and H. van Dam, Academic Press, New York, 1965).

[23] For a review of the different deformation schemes see: D. Bonatsos and C. Daskaloyannis, Phys. Lett. **B 307**, 100 (1993).

[24] S. S. Sharma, Phys. Rev. **C46**, 404 (1992).

[25] D. Bonatsos, S. B. Drenska, P. P. Raychev, R. P. Roussev and Yu. F. Smirnov, J. Phys. G: Nucl. Part. Phys. **17**, L67 (1991).

[26] E. Witten, Nucl. Phys. **B 322**, 629 (1989); Commun. Math. Phys. **121**, 351 (1989).

[27] C. Quesne, Phys. Lett. **A 153**, 303 (1991); B. Jurčo, Lett. Math. Phys. **21**, 51 (1991).

[28] F. T. Arecchi, E. Courtens, R. Gilmore and H. Thomas, Phys. Rev. **A 37**, 2211 (1972); M. Perelomov, Commun. Math. Phys. **26**, 222 (1972); R. Gilmore, Rev. Mex. Fis. **23**, 143 (1974).

[29] R. Gilmore and D. H. Feng, Phys. Lett. **B 76**, 26 (1978); L. Yaffe, Rev. Mod. Phys. **54**, 482 (1982) and Phys. Today, August, 50 (1983).

[30] J. T. Lunardi, Msc. Thesis, Instituto de Física Teórica, São Paulo, 1995. To be published.

ELSEVIER

Physica A 242 (1997) 501–508

PHYSICA A

Q-deformed fermionic Lipkin model at finite temperature

D. Galetti[a,*], B.M. Pimentel[a], C.L. Lima[b], J.T. Lunardi[c]

[a] *Instituto de Física Teórica, Universidade Estadual Paulista, Rua Pamplona, 145, 01405-900, São Paulo, SP, Brazil*

[b] *Nuclear Theory and Elementary Particle Phenomenology Group, Instituto de Física, Universidade de São Paulo, C.P. 66318, 05389-970, São Paulo, SP, Brazil*

[c] *Departamento de Matemática e Estatística, Universidade Estadual de Ponta Grossa, Campus de Uvarana, Praça Santos Andrade s n, 84010-330 Ponta Grossa, PR, Brazil*

Received 21 October 1996; revised 18 February 1997

Abstract

The interplay between temperature and q-deformation in the phase transition properties of many-body systems is studied in the particular framework of the collective q-deformed fermionic Lipkin model. It is shown that in phase transitions occuring in many-fermion systems described by $su(2)_q$-like models are strongly influenced by the q-deformation.

PACS: 05.70.Fh; 03.65.Fd; 21.60.Fw
Keywords: Phase transition; q-algebras; Many-fermion systems

1. Introduction

Q-deformed algebras turned out to be a fertile area of research in the last few years. Many applications of q-deformation ideas can be found in the literature, in areas as different as optics or particle physics. A natural scenario for seeking a physical interpretation of the q-deformation parameter is the many-body physics. The multiple correlations among the constituents of the system may provide us with a framework where the physical effects of such a deformation may show up in an amplified way.

The many-body problem in all its complexity calls for the use of approximate methods or the development of simple solvable models which should entail most of the relevant physics combined with a technically simple treatment [1]. A long heritage of

* Corresponding author. E-mail: galetti@axp.ift.unesp.br.

PII S0378-4371(97)00250-1

such models is available in the nuclear physics literature, among which the Lipkin model [2] has been extensively used as a laboratory to test approximate methods and to point out the main features of the many-body systems.

From the point of view of q-deformed algebra applications to physical systems it is important to understand how the basic characteristics and the general behavior of many-body systems are modified when the underlying algebra is deformed. The use of q-deformed algebra in the description of some many-body systems has lead to the appearance of new features when compared to the non-deformed case. In this connection we mention some examples: (a) in the q-oscillator many-body problem [3] it was shown that, when promoting the symmetries of the standard oscillator system to q-symmetries, the spectrum of the system is found to exhibit interactions between the levels of the individual oscillators, (b) the revival phenomenon present in the Jaynes–Cummings model [4] disappears when the original $su(2)$ symmetry is deformed, (c) a good agreement with the experimental data was obtained through a κ-deformed Poincaré phenomenological fit to the rotational and radial excitations of mesons [5], (d) a purely $su(2)_q$-based mass formula for quarks and leptons was developed using an inequivalent representation [6], (e) phonons in the superfluid ^{4}He were shown to satisfy the Heisenberg q-deformed algebra [7], and (f) the chemical potential $\mu(T)$ has a linear dependence on T in addition to the usual behavior for a free q-deformed fermionic system [8].

Recently, the quasi-spin version of the Lipkin model has been treated by q-deforming the $su(2)$ algebra and the ground-state phase transition was discussed at $T=0$ by directly diagonalizing the energy matrix constructed out of the representation states $|jm\rangle$ [9]. A suppression of that phase transition was then found for $q>1$ [10]. Afterwards, a different treatment of the Lipkin model has been developed in which the q-deformation was performed already at the fermionic level. In this approach a new q-deformed collective Lipkin Hamiltonian was obtained which differs from that of the previous one by the presence of a q-deformed mean field term. The reason behind the care in treating the fermionic mean field of the many-body Hamiltonian is the necessity of preserving the symmetry of the original problem when the algebra is deformed. The $T=0$ ground-state phase transition was studied again by using a variational energy expression constructed out of q-deformed coherent states. As an outcome of the careful treatment of the fermionic degrees of freedom it emerged that for some values of q, the phase transition is not suppressed anymore [11]. In the present paper and still in the same spirit of a variational approach, we have included an explicit temperature dependence in the fermionic q-deformed Lipkin model, in order to study the interplay between temperature and deformation of the algebra. In this context, Gilmore and Feng [12] have treated the same problem for the $q=1$ case.

The present paper is organized as follows. In Section 2 we introduce the temperature dependence in the q-deformed Lipkin many-fermion model. Through the analysis of the free energy associated to this system, using q-deformed coherent states, we discuss the existence of phase transitions at finite temperature and its dependence with the q-deformation of the underlying algebra. In Section 3 we present our conclusions.

2. Q-deformed Lipkin model with temperature

The Lipkin model is a valuable tool to test specific methods to treat fermionic many-body systems. Besides, due to its $su(2)$ structure, it has been widely used in attempts to obtain a physical meaning to the q-deformation concept as applied to many-particle systems [10,11,13]. In Ref. [11] in contrast to [10,13] a careful treatment of the fermionic mean field was performed, which embodies q-deformation effects. There it has been shown that the q-deformed fermionic Lipkin Hamiltonian

$$H = \frac{\varepsilon}{4\sinh(\gamma/2)}\sinh(2\gamma S_0) + \frac{V}{2[N]_q}(S_-^2 + S_+^2)\,, \tag{2.1}$$

written in terms of $su_q(2)$ operators obeying the commutation relations

$$[S_0, S_\pm] = \pm S_\pm\,, \tag{2.2}$$

$$[S_+, S_-] = [2S_0]_q\,. \tag{2.3}$$

where

$$[x]_q = \frac{q^x - q^{-x}}{q - q^{-1}} = \frac{e^{\gamma x} - e^{-\gamma x}}{e^{\gamma} - e^{-\gamma}}\,. \tag{2.4}$$

undergoes a second-order phase transition, characterizing the spherical symmetry breaking in quasi-spin space. q-coherent states were used to define θ and φ as collective variables in terms of which the phase transition was analyzed through the behavior of the variationally obtained ground-state energy. As a result of that analysis the phase transitions not only depend on the strength of the interaction, V, but also on the deformation of the algebra and on the number of particles through the product $\gamma(N-1)$. The q-dependent critical value of the strength parameter χ characterizing the phase transition is

$$\chi_c = 1 + 2\sinh^2\left[\frac{\gamma}{2}(N-1)\right]\,. \tag{2.5}$$

meaning that a universal character can no longer be assigned to χ as a system-independent indicator of the phase transition in a q-deformed system.

In many-body systems undergoing phase transitions, temperature plays a role since it can restore the symmetry. The q-deformation also acts as a symmetry-restoring parameter [11]. It is therefore important to investigate the interplay of both effects in the q-deformed Lipkin model.

Let us consider again the q-deformed Lipkin Hamiltonian in order to calculate the free energy and study the phase transitions of the model. In this sense we must also select some test states so as to have a variational expression for the free energy which will be determined by a variational method. In this connection we will use the set of q-deformed coherent states already discussed in the literature [14,15] and defined by

$$|\widetilde{j,z}) = e_q^{zJ_+}\,|j,-j)$$

$$= \sum_{-j}^{j} \begin{pmatrix} 2j \\ j+m \end{pmatrix}_q^{1/2} z^{*(j+m)} |j,m\rangle \tag{2.6}$$

to write the free energy inequality

$$F \leqslant Tr(\hat{\rho}_{tr}\hat{H}) + \beta^{-1}\, Tr(\hat{\rho}_{tr} \ln \hat{\rho}_{tr}), \tag{2.7}$$

where $\hat{\rho}_{tr}$ is the trial density operator given by

$$\hat{\rho}_{tr} = Y^{-1}(N,j) \sum_{i=1}^{Y(N,j)} \frac{|\widetilde{j,z}\rangle_{ii}\langle\widetilde{j,z}|}{{}_i\langle\widetilde{j,z}|\widetilde{j,z}\rangle_i}. \tag{2.8}$$

$Y(N,j)$ is the multiplicity of the degenerate j-multiplet

$$Y(N,j) = \frac{N!\,(2j+1)}{(N/2+j+1)!\,(N/2-j)!}, \tag{2.9}$$

which is the same as in the standard Lipkin model because the q-deformation procedure does not change the number and labelling of the states [9]. The same reason guarantees that the q-deformed Lipkin Hamiltonian is block diagonal, being each block associated with a given j. Using the variational principle we obtain

$$F \leqslant \min_{j,\theta,\phi} \left(\frac{\langle j,\widetilde{\theta,\phi}|\hat{H}|j,\widetilde{\theta,\phi}\rangle}{\langle\widetilde{j,\theta,\phi}|j,\widetilde{\theta,\phi}\rangle} - \beta^{-1} \ln Y(N,j) \right) \tag{2.10}$$

which, by substituting the q-deformed Lipkin Hamiltonian, Eq. (2.1), gives rise to

$$F \leqslant \min_{j,\theta,\phi} (\varepsilon_q E_q(j,\theta,\phi) - \beta^{-1} \ln Y(N,j)), \tag{2.11}$$

where

$$\varepsilon_q = \frac{\varepsilon}{2[1/2]_q} \tag{2.12}$$

is a q-dependent single-particle spacing, and

$$E_q(j,\theta,\phi) = \frac{[2j]_q}{2} \left(-\frac{\cos\theta}{D(\gamma,\theta,j)} - \frac{\chi(j)}{2} \frac{\sin^2\theta\cos 2\phi}{D(\gamma,\theta,j)} \right). \tag{2.13}$$

In the above expression the q-dependent strength parameter now is

$$\chi(j) = \frac{|V|}{\varepsilon_q [N]_q} [2j-1]_q \tag{2.14}$$

and

$$D(\gamma,\theta,j) = 1 + \sinh^2\left[\frac{\gamma}{2}(2j-1)\right] \sin^2\theta. \tag{2.15}$$

Minimization on the parameters θ and ϕ gives rise to the extrema,

$$\phi = \tfrac{1}{2}\pi \text{ or } \tfrac{3}{2}\pi \qquad \theta = 0 \text{ or } \pi. \tag{2.16}$$

in the $V \geqslant 0$ case. New physics appears due to the interplay between the parameters θ, γ, N and j; the remaining analysis of the behavior of $E_q(j, \theta, \phi)$ around the extrema goes similarly as in Ref. [11]. However, there we were restricted to the analysis of the ground-state behavior, in which case j is fixed to $N/2$. Due to the temperature dependence of the second term of the free energy, j will not be fixed anymore to the ground-state multiplet, being therefore an additional parameter in the present extrema analysis. $\theta = \pi$ is still a maximum, but the condition at $\theta = 0$ is now j dependent:

$$-1 + \chi(j)\cos\theta - 2C\cos\theta\frac{(\cos\theta - \frac{1}{2}\chi(j)\sin^2\theta)}{1 + C\sin^2\theta} = 0\,, \tag{2.17}$$

where

$$C = \sinh^2\left[\frac{\gamma}{2}(2j-1)\right]\,, \tag{2.18}$$

being the solution a maximum or a minimum according to the inequality

$$\begin{aligned} &\text{maximum: } 2C - \chi(j) + 1 < 0\,,\\ &\text{minimum: } 2C - \chi(j) + 1 > 0\,. \end{aligned} \tag{2.19}$$

The solutions to Eq. (2.17) can be written as

$$\cos\theta = \frac{\chi(j)}{2C}\left(1 \pm \sqrt{1 - G^2(\gamma)}\right)\,, \tag{2.20}$$

where

$$G^2(\gamma) = \frac{4C(C+1)}{\chi^2(j)}\,. \tag{2.21}$$

These solutions must still obey the following conditions:

$$G(\gamma) \leqslant 1. \qquad 0 \leqslant |\cos\theta| \leqslant 1\,. \tag{2.22}$$

The first condition is related to the determination of $\gamma_{\max}$ given by the inequality

$$\varepsilon\sinh(\gamma N)\cosh(\gamma/2) - |V| \leqslant 0\,, \tag{2.23}$$

whereas the second one leads to the determination of critical j_c,

$$j_c = \frac{1}{2} + \gamma^{-1}\operatorname{arccoth}\left(\frac{1 + \sqrt{1 - G^2(\gamma)}}{G(\gamma)}\right)\,. \tag{2.24}$$

Once one is given j_c, one can readily obtain the corresponding χ_c by a direct substitution in Eq. (2.14),

$$\chi_c = \frac{\sinh[\gamma(2j_c - 1)]}{G(\gamma)}\,. \tag{2.25}$$

Table 1
The θ values at the extrema of the energy functional are shown for different values of j

j	Minimum	Maximum
$j<j_c$	$\theta=0$	$\theta=\pm\pi$
$j>j_c$	$\theta=\pm\theta_m$	$\theta=0,\pm\pi$

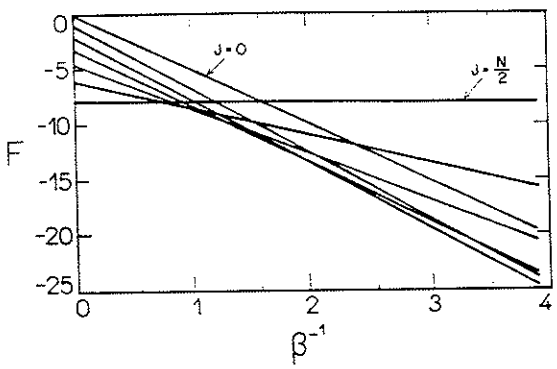

Fig. 1. This figure shows the behavior of a family of straight lines for j values running from $j=6$ to $j=0$ as a function of β^{-1}, for $N=12$, $V=2$, $\varepsilon=1$ and $q=1.116$. The free energy is the envelope formed by the lower frontier of these straight lines.

To summarize, $\gamma<\gamma_{\max}$ and $j>j_c$ are the necessary and sufficient conditions to the existence of the extremum θ_m given by

$$\cos\theta_m=\frac{\coth\gamma(j-\frac{1}{2})}{G(\gamma)}\left(1-\sqrt{1-G^2(\gamma)}\right), \tag{2.26}$$

leading to $\partial^2 E_q/\partial\theta^2|_{\theta=\theta_m}>0$, indicating that θ_m is a minimum.

Table 1 below presents the behavior of the energy extrema with respect to j_c.

Fig. 1 shows the free energy $F(\beta)$ as a function of $kT=1/\beta$. As in the non-deformed case, the free energy is given by the lower frontier of the family of straight lines, the main difference lying on the crossing points between the curves, which in the present case are shifted towards higher temperatures. The range of allowed values of j is given by $\sqrt{N}/2\leqslant j\leqslant N/2$, as in the non-deformed case.

When j_c exists, the crossing of the above-mentioned straight lines determines the phase transition temperature given by

$$\beta_c^{-1}=\frac{\min_{\theta,\phi}\varepsilon_q E_q(j_c,\theta,\phi)-\min_{\theta,\phi}\varepsilon_q E_q(j_c-1,\theta,\phi)}{\ln Y(N,j_c)-\ln Y(N,j_c-1)}. \tag{2.27}$$

Upon a substitution of the explicit expression of $E_q(j,\theta,\phi)$ we get

$$\beta_c^{-1}=\frac{\varepsilon_q\cosh(\gamma(2j_c-1))}{\ln Y(N,j_c)-\ln Y(N,j_c-1)}. \tag{2.28}$$

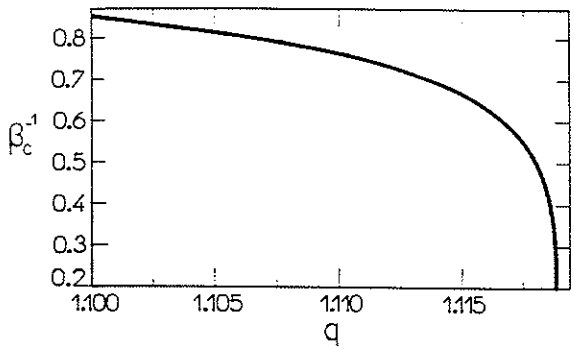

Fig. 2. The critical temperature β_c^{-1} is shown as a function of q, the deformation parameter of the algebra, for $N=12$, $V=2$, $\varepsilon=1$.

Fig. 2 shows the behavior of β_c^{-1} as a function of $q=\exp(\gamma)$ in the same physical situation as Fig. 1.

3. Conclusions

It has already been seen previously [11] that the critical value of the coupling constant χ_c is number and q-deformation dependent at $T=0$. With the introduction of the temperature, as performed in the present work, we could think that no new effect would appear, since the only temperature-dependent contribution to the free energy, $\beta^{-1}\ln Y(N,j)$, does not contain any q dependence, $Y(N,j)$ being just a level degeneracy counter. However, the temperature-dependent effects are embodied through j_c, the temperature-dependent critical j given by Eq. (2.24). Similarly, the interplay between temperature and q-deformation has also appeared in a q-bosonic description of the Bose condensation, where the critical temperature increases with the deformation parameter [16].

As shown in Fig. 2, the critical temperature presents strong dependence on the deformation of the algebra. The critical temperature decreases with increasing of the q-deformation. This means that phase transitions occurring in interacting many-fermion systems described by $su_q(2)$-like models are in fact strongly influenced by the q-deformation, indicating that any physical conclusions regarding the phase transition behavior must be taken with care, if the q-deformed concept has indeed any physical meaning.

Acknowledgements

This work was supported in part by Conselho Nacional de Desenvolvimento Cientifico e Tecnológico (CNPq), Brazil.

References

[1] P. Ring, P. Schuck, The Nuclear Many-Body Problem, Springer, New York, 1980.
[2] H.J. Lipkin, N. Meshkov, A.J. Glick, Nucl. Phys. 62 (1965) 188.
[3] E.G. Floratos, J. Phys. A: Math. Gen. 24 (1991) 4739.
[4] M. Chaichian, P. Kulish, Phys. Lett. B 234 (1990) 72.
[5] J. Day, M. Day, P.L. Ferreira, L. Tomio, Phys. Lett B 365 (1996) 157.
[6] B.E. Palladino, P.L. Ferreira, Quark and lepton masses from deformed su(2), contributed paper to the XVII Encontro Nacional de Fisica de Particulas e Campos, Serra Negra, S.P., Brazil, 1996.
[7] M.R. Monteiro, L.M.C.S. Rodrigues, S. Wulck, Phys. Rev. Lett. 76 (1996) 1098.
[8] M.R. Ubriaco, Phys. Lett. A 219 (1996) 205.
[9] M. Jimbo, Lett. Math. Phys. 10 (1985) 63.
[10] D. Galetti, B.M. Pimentel, An. Acad. Bras. Ci. 67 (1995) 7.
[11] S.S. Avancini, A. Eiras, D. Galetti, B.M. Pimentel, C.L. Lima, J. Phys. A: Math. Gen. 28 (1995) 4915.
[12] D.H. Feng, R. Gilmore, L.M. Narducci, Phys. Rev. C 19 (1979) 1119.
[13] S.S. Avancini, F.F. de Souza Cruz, D [illegible]ezes, M.M. Watanabe de Moraes, J. Phys. A: Math. Gen. 27 (1994) 831.
[14] C. Quesne, Phys. Lett. A 153 (1991) 303; B. Jurčo, Lett. Math. Phys. 21 (1991) 51.
[15] S.S. Avancini, J.C. Brunelli, Phys. Lett. A 174 (1993) 358.
[16] M. R-Monteiro, I. Roditi, L.M.C.S. Rodrigues, Int. J. Mod. Phys. B 8 (1994) 3281.

ELSEVIER

23 October 1997

PHYSICS LETTERS B

Physics Letters B 412 (1997) 7–13

On a q-covariant form of the BCS approximation

Leandro Tripodi [1], Celso L. Lima [2]

Nuclear Theory and Elementary Particle Phenomenology Group, Instituto de Física, Universidade de São Paulo, CP66318, 05389-970 São Paulo, SP, Brazil

Received 7 April 1997; revised 4 August 1997
Editor: W. Haxton

Abstract

A new form of the BCS approximation for a pure pairing force in terms of $SU_q(N)$-covariant fermion operators is presented. A set of quantum BCS equations is derived, as well as a q-analog to the gap equation. The quantum occupation probabilities and gap are shown to depend explicitly on the quantum parameter. © 1997 Elsevier Science B.V.

PACS: 21.60-n; 03.65.Fd

Keywords: Quantum groups; Many-body physics; BCS

In the last few years, q-deformed algebraic methods have been of much interest in many-body physics [1–9]. In the framework of the q-deformed quasi-spin algebra, the phenomenology of nuclear rotational states [1–4], the pairing problem for a single j-shell [5] and the Lipkin-Meshkov-Glick model [8,9], to quote some, were studied (for a brief review on these topics, see [10]); a recent application of this formalism to boson expansion methods can be found in Ref. [11]. Nonetheless, the q-fermionic theory used in previous works, following [12–15], is a generalization – or *deformation* – of the usual one, compatible with the standard Drinfel'd-Jimbo quantization of $\mathcal{U}(su(2))$ rather than strictly covariant under some linear quantum group transformations [16–18]. This fact originated some confusion, mainly with respect to the language adopted in the literature, but we hope that concepts here will be clearly defined.

Recently, Ubriaco [19] has studied thermodynamical properties of a free quantum group fermionic system with two "flavors". In particular, it was given there a $SU_q(N)$-covariant representation of the fermionic algebra for arbitrary N in terms of ordinary creation and annihilation operators. This enables one to attempt the construction of a quantum group invariant second quantized Hamiltonian for an arbitrary fermionic system. In this paper we propose a construction of the Bardeen-Cooper-Schrieffer (BCS) many-body formalism [20,21] for a pure pairing force in which the usual fermions are replaced by quantum group covariant ones satisfying

[1] Supported by Conselho Nacional de Desenvolvimento Tecnológico (CNPq). E-mail address: tripodi@linpel.if.usp.br.
[2] Corresponding author. E-mail address: cllima@if.usp.br.

PII S0370-2693(97)01056-3

appropriate anticommutation relations for a $SU_q(N)$-fermionic algebra. Our main purposes are: 1) to study, in a simple case, the effects of introducing q-covariance in a many fermion system, 2) to introduce a many-body model based on quantum group covariance rather than in q -deformed fermionic symmetry and 3) to obtain the first results concerning with the application of the BCS framework in the $q \neq 1$ realm. In what follows, we write the quantum invariant pairing Hamiltonian and BCS vacuum wavefunction and apply the standard variational process to the this wavefunction obtaining the q-analog to the BCS and gap equations.

We will work in the usual spherical basis $\{j, -j \leq m \leq j\}$ and use the BCS phases for convenience (we are allowed to use BCS phases regardless of quantum group angular momentum coupling coefficients because the coupling between $|j_1 j_2 m_1 m_2\rangle$ and $|j_1 j_2 IM\rangle$ states is unique and independent of q, see Ref. [22]). In this basis, the usual BCS vacuum wavefunction is written in terms of particle operators as [21]:

$$|\mathrm{BCS}\rangle = \prod_{jm>0} \left[u_j + v_j c^{\dagger}_{jm} c^{\dagger}_{j-m}\right] |0\rangle, \tag{1}$$

where the u_j and v_j are variational coefficients, c_{jm} and $c^{\dagger}_{jm}$ are the usual particle fermion operators satisfying $\{c_{jm}, c^{\dagger}_{j'm'}\} = \delta_{jj'}\delta_{mm'}$ with all other anticommutators vanishing and $|0\rangle$ is the bare vacuum state. We assume that we can rewrite the wavefunction (1) as a quantum group invariant one in the following fashion:

$$|\mathrm{BCS}\rangle_q = \prod_{jm>0} \left[u^q_j + v^q_j C^{\dagger}_{jm} C^{\dagger}_{j-m}\right] |0\rangle_q, \tag{2}$$

where the operators C_{jm} and $C^{\dagger}_{jm}$ play the role of creation and annihilation operators for $SU_q(2j+1)$-fermions within the j-shell with angular momentum projection m and the q-bare vacuum ket is a vector in the product Fock space defined through $C_{jm}|0\rangle_q = 0$. The superscripts on the occupation probabilities mean that these quantities may now depend upon the quantum parameter q. Now, the q-fermion operators C_{jm} and $C^{\dagger}_{jm}$ are required to satisfy an algebra covariant under quantum group transformations: we clearly want this algebra to act on physical vectors, that is, we want it to have a representation in the direct product Fock space generated by the eigenstates $|n_{j=1/2}, n_{j=3/2}, \ldots\rangle = \prod_{jm} \otimes |n_j\rangle$ of the operator $N = \sum_{jm} c^{\dagger}_{jm} c_{jm}$ (we use n_j as a shorthand for n_{jm}, $n_j = \{n_{jm}\}$). If we put the quantum group operators in one-to-one correspondence with differentials in the quantum plane, then a q-fermionic algebra explicitly invariant under linear $SU_q(2j+1)$ transformations can be cast in the form (we assume real q and consider $q > 0$) [18,23]:

$$C_{jk} C_{jl} + q \mathscr{R}_{lkmn} C_{jm} C_{jn} = 0; \tag{3}$$

$$C_{jk} C^{\dagger}_{jl} + q^{-1} \mathscr{R}_{kmnl} C^{\dagger}_{jm} C_{jn} = \delta_{kl} \tag{4}$$

(sum over repeated m,n indices), where $-j \leq \mu \leq j$, $\mu = k,l,m,n$ with the matrix $\mathscr{R}_{klmn} = \delta_{lm}\delta_{kn}[1 + (q-1)\delta_{kl})] + \delta_{km}\delta_{ln}\theta(m-k)(q-q^{-1})$, with the usual theta function $\theta(x-y)$ ($\mathscr{R} = PR$, where P is the permutation matrix and R is the R-matrix of $GL_q(2j+1)$). (It is easy to check that in the classical limit $q = 1$ these expressions become the usual $SU(2j+1)$-invariant anticommutation relations for fermions). For a given j, a representation of this algebra can be given by [19]:

$$C_{jm} = c_{jm} \prod_{i=m+1}^{j} \left(1 + \left(q^{-1} - 1\right) c^{\dagger}_{ji} c_{ji}\right); \tag{5}$$

$$C^{\dagger}_{jm} = c^{\dagger}_{jm} \prod_{i=m+1}^{j} \left(1 + \left(q^{-1} - 1\right) c^{\dagger}_{ji} c_{ji}\right). \tag{6}$$

The q-fermions for various j orbits are given by $C = \prod_j \otimes \mathscr{A}_j$, where $\mathscr{A}_j$ is the algebra (3), (4). The products in (5) and (6) can be written as:

$$\begin{aligned} M_{jm} &\doteq \prod_{i=m+1}^{j} \left(1 + (q^{-1} - 1)c_{ji}^{\dagger}c_{ji}\right) \\ &= 1 + \sum_{i_1=m+1}^{j} (q^{-1} - 1)c_{ji_1}^{\dagger}c_{ji_1} \\ &\quad + \sum_{i_2>i_1=m+1}^{j} (q^{-1} - 1)^2 c_{ji_1}^{\dagger}c_{ji_1}c_{ji_2}^{\dagger}c_{ji_2} + \ldots + (q^{-1} - 1)^{j-m} c_{jm+1}^{\dagger}c_{jm+1}\cdots c_{jj}^{\dagger}c_{jj}. \end{aligned} \tag{7}$$

It is easy to see that the c_{jm} and $c_{jm}^{\dagger}$ commute with M_{jm}. We may interpret the action of this operator on a given state as taking into account, in some effective way, not only the mean-field strength but also two-body and higher order contributions (a similar interpretation has already appeared in the literature when the consequences of q-deformation were concerned). Let us now assume that we can expand in a convergent manner the q-bare vacuum as:

$$|0\rangle_q \equiv \sum \ldots \sum_{n_j=0}^{2j+1} \ldots \sum \ldots \xi(q, n_{j=1/2}, n_{j=3/2}, \ldots) \left| n_{j=1/2}, n_{j=3/2}, \ldots \right\rangle, \tag{8}$$

where the coefficients should satisfy $\xi(q = 1,0,0,\ldots) = 1$ and $\xi(q = 1,\ldots,0,0,n_j \neq 0,0,0,\ldots) = 0$. Acting on the vacuum state with the operator C_{jm}, we obtain:

$$\begin{aligned} C_{jm}|0\rangle_q &= \sum \ldots \sum_{n_{j'}=0}^{2j'+1} \ldots \sum \ldots \xi(q, n_{j'=1/2}, n_{j'=3/2}, \ldots) m_{jm}(n_{j'=1/2}, n_{j'=3/2}, \ldots) \\ &\quad \times c_{jm} \left| n_{j'=1/2}, n_{j'=3/2}, \ldots \right\rangle = 0, \end{aligned} \tag{9}$$

with $m_{jm} \geq 1$ the eigenvalue of M_{jm} (which can be immediately inferred from (7)). We should note that all states with occupation number n_{jm} originally equal to zero are automatically excluded from the sum; therefore, since all the state kets are orthogonal, all the coefficients corresponding to states with n_{jm} originally equal to one must vanish. But j and m are arbitrary, which implies that:

$$|0\rangle_q = \alpha e^{i\theta}|0\rangle. \tag{10}$$

Here the factor $\alpha e^{i\theta}$ is undefined, and we choose $\alpha^2 = 1$ independently of q. (Note that, due to $M_{jm}|0\rangle = |0\rangle$, $C_{jm}|0\rangle = 0$; with this it is shown the uniqueness of a ray in the product Fock space which is annihilated by the operator C_{jm}.) Thence, the BCS q-covariant vacuum ket reads:

$$|\mathrm{BCS}\rangle_q = \prod_{jm} \left[u_j^q + v_j^q C_{jm}^{\dagger} C_{j-m}^{\dagger}\right]|0\rangle = \prod_{jm} \left[u_j^q + v_j^q c_{jm}^{\dagger} c_{j-m}^{\dagger} M_{jm} M_{j-m}\right]|0\rangle = \prod_{jm} \left[u_j^q + v_j^q c_{jm}^{\dagger} c_{j-m}^{\dagger}\right]|0\rangle. \tag{11}$$

(The superscripts will hereafter be omitted in v_j^q and u_j^q.) We now turn to the expression of the q-Hamiltonian. We are interested in a pure pairing Hamiltonian, whose $q = 1$ version we write as [21]:

$$H = \sum_{jm} \epsilon_j c_{jm}^{\dagger} c_{jm} - G \sum_{jj'm_1m_2} c_{jm_1}^{\dagger} c_{j-m_1}^{\dagger} c_{j'-m_2} c_{j'm_2}. \tag{12}$$

where G is the pairing strength and the ϵ_j are the single-particle energies; here we understand that the indices m_1 and m_2 are greater than zero. We write a q-Hamiltonian following expression (12) in the form:

$$H_q \doteq \sum_{jm} \epsilon_j c_{jm}^{\dagger} c_{jm} (M_{jm})^2 - G \sum_{jj'm_1m_2} c_{jm_1}^{\dagger} c_{j-m_1}^{\dagger} M_{jm_1} M_{j-m_1} c_{j'-m_2} M_{j'-m_2} c_{j'm_2} M_{j'm_2}. \tag{13}$$

One can observe that the "mean-field" term in (13) already contains explicit interaction among different levels (see also Eq. (16) of Ref. [19]). Using expression (7), and anticommutation properties of ordinary fermion operators, one can perform straightforwardly the calculation of the mean-value of (13) between $|\mathrm{BCS}\rangle_q$ states. The result is:

$$
\begin{aligned}
{}_q\langle \mathrm{BCS}|H_q|\mathrm{BCS}\rangle_q = & \sum_j \epsilon_j v_j^2 \times \frac{(1/q)^{4\Omega_j}-1}{(1/q)^2-1} - G\sum_{j\neq j'} v_j v_{j'} u_j u_{j'} \times (1/q)^{2j+2j'} \times \Omega_j \Omega_{j'} \\
& - \frac{G}{2}\sum_{jm>0} v_j^2 u_j^2 \left[(1/q)^{3j-m}\zeta_{2j-m} + (1/q)^{2j}\zeta_{1jm}\zeta_{1j-m}\right] \times \Omega_j ,
\end{aligned} \tag{14}
$$

where

$$
\begin{aligned}
\zeta_{njm} \doteq & 1 + (q^{-1}-1)(j-m-n) + (q^{-1}-1)^2\left[\frac{(j-m)(j-m-1)}{2!} - nj - nm - n\right] \\
& + \ldots + (q^{-1}-1)^{j-m-1}[(j-m) - n(m+3)(m+2)\ldots(j-m-3) - n(-m-1) \\
& \times (m+2)(m+1)\ldots(j-m-2) - \ldots]
\end{aligned} \tag{15}
$$

and Ω_j is the pair degeneracy of the j-shell. The coefficients of each power of $(q^{-1}-1)$ in ζ obviously have to be either positive or zero. The variational q-Hamiltonian is $\tilde{H}' = \tilde{H} - \lambda_q \sum_j 2\Omega_j v_j^2$. Performing a naive variation with respect to the Lagrange multiplier λ_q one obtains:

$$
\lambda_q = \frac{d_q\langle \mathrm{BCS}|H_q|\mathrm{BCS}\rangle_q}{d\sum_j 2\Omega_j v_j^2} . \tag{16}
$$

which means that λ_q works as the chemical potential in the frame of the q-energy $E_q = {}_q\langle \mathrm{BCS}|H_q|\mathrm{BCS}\rangle_q$. One may now calculate the variation with respect to the occupation probabilities:

$$
\delta_q\langle \mathrm{BCS}|H_q - \lambda_q \sum_j 2\Omega_j v_j^2|\mathrm{BCS}\rangle_q = \left(\frac{\partial}{\partial v_j} + \frac{u_j}{v_j}\frac{\partial}{\partial u_j}\right)_q \langle \mathrm{BCS}|H_q - \lambda_q \sum_j 2\Omega_j v_j^2|\mathrm{BCS}\rangle_q , \tag{17}
$$

which one then imposes to vanish for some fixed q. The resulting q-BCS equations are:

$$
u_j v_j \left(\epsilon_j \times \left(\frac{(1/q)^{4\Omega_j}-1}{\left[(1/q)^2-1\right]\Omega_j}\right) - 2\lambda_q\right) + \left(u_j^2 - v_j^2\right)\Delta_j^q = 0 , \tag{18}
$$

where

$$
\Delta_j^q \doteq G\left[\sum_{j'\neq j} u_{j'} v_{j'} (1/q)^{2j+2j'}\Omega_{j'} + \frac{u_j v_j}{2}\sum_{m>0}(1/q)^{3j-m}\zeta_{2j-m} + (1/q)^{2j}\zeta_{1jm}\zeta_{1j-m}\right] \tag{19}
$$

is the quantum gap parameter (which, in opposition to the standard pure pairing case, depends upon the shell label j). It is easy to verify that when $q=1$, the quantum equations (18) are the BCS equations:

$$
2u_j v_j(\epsilon_j - \lambda) + \left(u_j^2 - v_j^2\right)\Delta = 0 \tag{20}
$$

for the nuclear pairing problem, with the non-quantum gap parameter $\Delta = G\sum_j u_j v_j \Omega_j$. The solution of Eqs. (18) for the variational parameters u_j and v_j is:

$$\left.\begin{matrix} u_j^2 \\ v_j^2 \end{matrix}\right\} = \frac{1}{2}\left[1 \pm \frac{\left(\epsilon_j \times \left(\frac{(1/q)^{4\Omega_j}-1}{2\left[(1/q)^2-1\right]\Omega_j}\right) - \lambda_q\right)}{\sqrt{\left(\epsilon_j \times \left(\frac{(1/q)^{4\Omega_j}-1}{2\left[(1/q)^2-1\right]\Omega_j}\right) - \lambda_q\right)^2 + \left(\Delta_j^q\right)^2}}\right]. \tag{21}$$

The quantum gap equation is obtained in an analog way as for the standard case by substitution of (21) into (19):

$$\Delta_j^q = \frac{G}{2}\left[\sum_{j'\neq j}(1/q)^{2j'+2j}\Omega_{j'}\frac{\Delta_{j'}^q}{\sqrt{\left(\epsilon_{j'} \times \left(\frac{(1/q)^{4\Omega_{j'}}-1}{2\left[(1/q)^2-1\right]\Omega_{j'}}\right) - \lambda_q\right)^2 + \left(\Delta_{j'}^q\right)^2}}\right.$$

$$\left. + \frac{\Delta_j^q}{\sqrt{\left(\epsilon_j \times \left(\frac{(1/q)^{4\Omega_j}-1}{2\left[(1/q)^2-1\right]\Omega_j}\right) - \lambda_q\right)^2 + \left(\Delta_j^q\right)^2}}\sum_{m>0}(1/q)^{3j-m}\zeta_{2j-m} + (1/q)^{2j}\zeta_{1jm}\zeta_{1j-m}\right]. \tag{22}$$

For the case of a single j-shell, the quantum gap parameter assumes the form:

$$\Delta_j^q = \left[\frac{G^2}{4}\left(\sum_{m>0}(1/q)^{3j-m}\zeta_{2j-m} + (1/q)^{2j}\zeta_{1jm}\zeta_{1j-m}\right)^2 - \left(\epsilon_j \times \left(\frac{(1/q)^{4\Omega_j}-1}{2\left[(1/q)^2-1\right]\Omega_j}\right) - \lambda_q\right)^2\right]^{1/2}. \tag{23}$$

The qualitative behavior of Δ_j^q is, as one can see, independent of the shell label. A 3D plot shows the dependence of the curve $v_j^2 \times \epsilon_j$ upon the parameter q, for a $j = \frac{3}{2}$ shell (Fig. 1).

In summary, we presented a quantum group form of the BCS method for the case of a pure pairing force, following the $SU_q(N)$-covariant representation of the fermionic algebra given by Ubriaco in Ref. [19]. The quantum bare vacuum was shown to be identical (apart from a multiplicative constant) to the product Fock space vacuum. The q-analogues to the BCS equations (18) were derived along with the quantum gap equation (22). The quantum gap (19) was shown to depend explicitly on the deformation parameter: we found that the quantum gap is reduced as the deformation increases, as if the system collapsed into its ground-state and, conversely, that it goes to infinity as q tends to zero making the system unexcitable. A 3D plot was made to illustrate the dependence of the occupation probabilities v_j^2 versus the single-particle energies on the quantum parameter. One can check this dependence is qualitatively in agreement with the remark in the first paragraph below Eq. (19) in Ref. [19]. The study of introduction of q-covariance may be interesting in other many-body systems, in special in toy models such as the Moszkowski and the Lipkin-Meshkov-Glick ones, studied

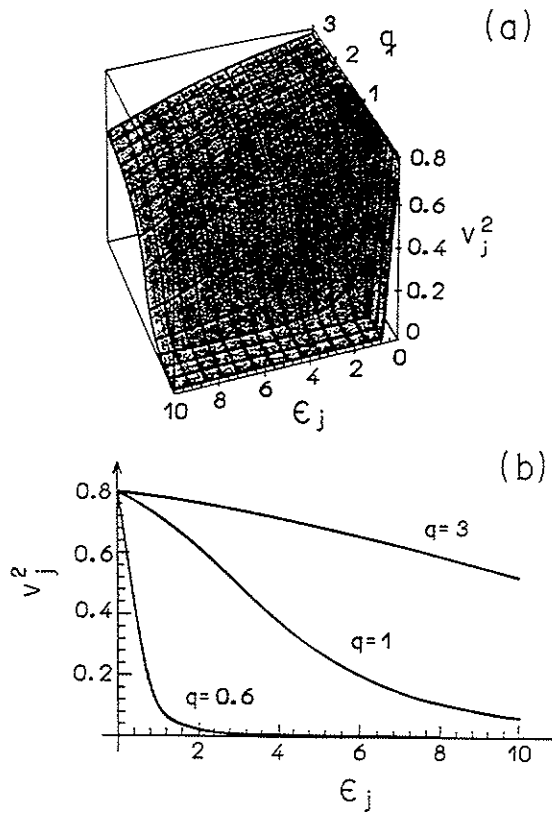

Fig. 1. Quantum occupation probabilities v_j^2 as a function of the single-particle energy ϵ_j and of the quantum parameter q for $j = 3/2$. Fig. 1a is a 3D view whereas Fig. 1b presents the behavior for three different values of q.

previously (in the deformed algebraic approach) in [6,7] and [8,9]. A q-analog of two-level pairing is under study and we hope to address it in a future publication.

Acknowledgements

C.L.L. thanks D. Galetti and B.M. Pimentel for their continuous interest and discussions. L.T. thanks M. Kyotoku, J.C. Alves Barata and E. Baldini Neto for valuable help. The authors are grateful to B.M. Pimentel for the critical reading of the manuscript.

References

[1] P.P. Raychev, R.P. Roussev, Yu.F. Smirnov, J. Phys G: Nucl. Part. Phys. 16 (1990) L137.
[2] S. Iwao, Prog. Theor. Phys. 83 (1990) 363.
[3] D. Bonatsos, E.N. Argyres, S.B. Drenska, P.P. Raychev, R.P. Roussev, Yu.F. Smirnov, Phys. Lett. B 251 (1990) 477.
[4] R. Barbier, J. Meyer, M. Kibler, Int. Jour. Mod. Phys. E 4 (1995) 385.
[5] S.S. Sharma, Phys. Rev. C 46 (1992) 904.
[6] D. Bonatsos, L. Brito, D.P. de Menezes, J. Phys. A: Math. Gen. 26 (1993) 895.
[7] C. da Providência, L. Brito, J. da Providência, D. Bonatsos, D.P. de Menezes, J. Phys. G: Nucl. Part. Phys. 20 (1994) 1209.

[8] D. Galetti, B.M. Pimentel, An. Acad. Bras. Ciên. 67 (1995) 1.
[9] S.S. Avancini, A. Eiras, D. Galetti, B.M. Pimentel, C.L. Lima, J. Phys. A: Math. Gen. 28 (1995) 4915.
[10] D. Galetti, J.T. Lunardi, B.M. Pimentel, C.L. Lima, in: Proceedings of the Theoretical Physics Symposium in honor of P.L. Ferreira, Eds. V.C. Aguilera-Navarro, D. Galetti, B.M. Pimentel, L. Tomio (IFT ed., São Paulo, 1995).
[11] S.S. Avancini, F.F. de S. Cruz, J.R. Marinelli, D.P. de Menezes, M.M.W. de Moraes, J. Phys. A: Math. Gen. 29 (1996) 5559.
[12] L.C. Biedenharn, J. Phys. A: Math. Gen. 22 (1989) L783.
[13] A.J. MacFarlane, J. Phys. A: Math. Gen. 22 (1989) 4581.
[14] C.P. Sun, H.C. Fu, J. Phys. A: Math. Gen. 22 (1989) L873.
[15] E.G. Floratos, J. Phys. A: Math. Gen. 24 (1991) 4739.
[16] H.D. Döbner, J.D. Hennig, W. Lücke, in: Quantum Groups, Proceedings of the 8th. International Workshop on Mathematical Physics, Eds. H.D. Döbner, W. Lücke, Springer Lect. Notes in Phys. 370 (1990), in particular Sections 5.2, 5.3, and 6.2, and references therein.
[17] Yu.I. Manin, Quantum Groups and Non-Commutative Geometry, Preprint CRM-Université de Montréal (1988).
[18] J. Wess, B. Zumino, Nucl. Phys. B (Proc. Suppl.) 18B (1990) 302.
[19] M.R. Ubriaco, Phys. Lett. A 219 (1996) 205.
[20] J. Bardeen, L.N. Cooper, J. Schrieffer, Phys. Rev. 108 (1957) 1175.
[21] J.M. Eisenberg, W. Greiner, Nuclear Theory, Vol. III (North-Holland, Amsterdam, 1976), Chap. 9.
[22] L.C. Biedenharn, in: Quantum Groups, Proceedings of the 8th. International Workshop on Mathematical Physics, Eds. H.D. Döbner, W. Lücke, Springer Lect. Notes in Phys. 370 (1990), Section 3.
[23] M.R. Ubriaco, Mod. Phys. Lett. A 8 23 (1993) 2213.

ELSEVIER

18 February 1999

PHYSICS LETTERS B

Physics Letters B 448 (1999) 1–5

Effect of q-deformation in the NJL gap equation

V.S. Timóteo, C.L. Lima [1]

Nuclear Theory and Elementary Particle Phenomenology Group, Instituto de Física, Universidade de São Paulo, CP 66318, 05315-970 São Paulo, SP, Brazil

Received 4 September 1998; revised 10 December 1998
Editor: W. Haxton

Abstract

We obtain a q-deformed algebra version of the Nambu–Jona-Lasinio model gap equation. In this framework we discuss some hadronic properties such as the dynamical mass generated for the quarks, the pion decay constant and the phase transition present in this model. © 1999 Published by Elsevier Science B.V. All rights reserved.

PACS: 11.30.Rd; 03.65.Fd; 12.40.-y
Keywords: Deformed algebras; Hadronic physics; Effective models

The concept of symmetry is of fundamental importance in physics; the breaking of a symmetry and its associated phase transition are universal phenomena appearing in many branches in physics, such as nuclear and solid state physics, although the broken symmetries and the physical systems involved are quite different. Y. Nambu was the first to realize this universal aspect of dynamical symmetry breaking [1]. The Nambu-Jona-Lasinio (NJL) model is very adequate to study the breaking of chiral symmetry and the generation of a dynamical mass for the quarks due to the appearance of condensates.

On another side, in the last few years the study of q-deformed algebras turned out to be a fertile area of research. The use of q-deformed algebra in the description of some many-body systems has lead to the appearance of new features when compared to the non-deformed case [2]. In particular, it seems to be a very elegant framework to describe perturbations from some underlying symmetry structure. From the many applications of q-deformation ideas existing in the literature, ranging from optics to particle physics, we would like to pinpoint three of them: the investigation of the behavior of the second order phase transition in a q-deformed Lipkin model [3], the good agreement with the experimental data obtained through a κ-deformed Poincaré phenomenological fit to the dynamical mass and rotational and radial excitations of mesons [4], and the purely $su_q(2)$-based mass formula for quarks and leptons developed by using an inequivalent representation [5].

It sounds therefore reasonable to study the influence of the q-deformation on the mass generation mechanism due to the breaking of chiral symmetry. To be definite, in this work we intend to investigate the effects of the q-deformation on the phase transi-

[1] E-mail: cllima@if.usp.br

PII: S0370-2693(98)01590-1

tion of the NJL model, stimulated by an analogy with q-deformed Lipkin model, where the phase transition is smoothed down when the Lipkin Hamiltonian is deformed [3].

Recently, the thermodynamical properties of a free quantum group fermionic system with two "flavors" were studied [6]. In particular, it was given there a $su_q(N)$-covariant representation of the fermionic algebra for arbitrary N in terms of ordinary creation and annihilation operators. The $su_q(2)$-covariant algebra is given by the following relations

$$\left\{\psi_1,\bar{\psi}_1\right\} = 1-\left(1-q^{-2}\right)\bar{\psi}_2\psi_2, \quad \left\{\psi_2,\bar{\psi}_2\right\} = 1, \tag{1}$$

$$\psi_1\psi_2 = -q\psi_2\psi_1, \quad \bar{\psi}_1\psi_2 = -q\psi_2\bar{\psi}_1, \tag{2}$$

$$\left\{\psi_1,\psi_1\right\} = 0, \quad \left\{\psi_2,\psi_2\right\} = 0. \tag{3}$$

The usual $su(2)$ covariant fermionic algebra is recovered when $q=1$. Later, the pure nuclear pairing force version of the Bardeen-Cooper-Schrieffer (BCS) many-body formalism [7] was extended in such a way to replace the usual fermions by quantum group covariant ones satisfying appropriate anticommutation relations for a $su_q(N)$-fermionic algebra [8]. Using the $su_q(2j+1)$-covariant representation of the fermionic algebra, a q-covariant form of the BCS approximation was constructed and the q-analog to the BCS equations along with the quantum gap equation was derived. The quantum gap was shown to depend explicitly on the deformation parameter and it is reduced as the deformation increases.

The Nambu–Jona-Lasinio model was first introduced to describe the nucleon-nucleon interaction via a four-fermion contact interaction. Later, the model was extended to quark degrees of freedom becoming an effective model for quantum chromodynamics (QCD).

The Lagrangian of the NJL model is given by

$$\mathscr{L}_{\mathrm{NJL}} = \bar{\psi}\, i\gamma^{\mu}\partial_{\mu}\psi + \mathscr{L}_{\mathrm{int}}, \tag{4}$$

$$\mathscr{L}_{\mathrm{int}} = G\left[\left(\bar{\psi}\psi\right)^2 + \left(\bar{\psi}\, i\gamma_5\tau\psi\right)^2\right]. \tag{5}$$

Linearizing the above interaction in a mean field approach, the last term does not contribute if the vacuum is parity and Lorentz invariant. The Lagrangian with the linearized interaction is then

$$\mathscr{L}_{\mathrm{NJL}} = \bar{\psi}\, i\gamma^{\mu}\partial_{\mu}\psi + 2G\langle\bar{\psi}\psi\rangle\bar{\psi}\psi. \tag{6}$$

Regarding this Lagrangian as a Dirac Lagrangian for massive quarks we obtain a dynamical mass for the quarks

$$m = -2G\langle\bar{\psi}\psi\rangle, \tag{7}$$

where $\langle\bar{\psi}\psi\rangle$ is the vacuum expectation value of the scalar density $\bar{\psi}\psi$, representing the quark condensates. Eq. (7) describes how the dynamical mass is generated with the appearance of the quark condensates. The quarks are massless if the condensate vanishes.

We now turn to the q-deformation of the NJL gap equation. Following [6,8] we write the creation and annihilation operators of the $su_q(2j+1)$ fermionic algebra as,

$$A_{jm} = a_{jm}\prod_{i=m+1}\left(1+Qa_{ji}^{\dagger}a_{ji}\right), \tag{8}$$

$$A_{jm}^{\dagger} = a_{jm}^{\dagger}\prod_{i=m+1}\left(1+Qa_{ji}^{\dagger}a_{ji}\right), \tag{9}$$

where $Q=q^{-1}-1$, $j=1/2$ and $m=\pm 1/2$. The first consequence of the above deformation is that only the operators corresponding to $m=-\frac{1}{2}$ are modified. Since in the NJL model we deal with quarks (anti-quarks) creation and annihilation operators, this feature is important because only negative helicity quarks (anti-quarks) operators will be deformed. Explicitly, we have

$$A_- = a_-\left(1+Qa_+^{\dagger}a_+\right), \quad A_-^{\dagger} = a_-^{\dagger}\left(1+Qa_+^{\dagger}a_+\right), \tag{10}$$

$$A_+ = a_+, \quad A_+^{\dagger} = a_+^{\dagger}, \tag{11}$$

where $+$ $(-)$ stands for the positive (negative) helicity. In a sense, we are embedding the chiral symmetry breaking effects in the operators' definition.

We are now in position a to obtain the deformed gap equation by introducing a BCS-like vacuum and proceeding similarly to the standard Bogoliubov-Valatin approach [9]. The q-deformed BCS vacuum reads

$$|NJL\rangle = \prod_{p,s=\pm 1}\left[\cos\theta(p) + s\sin\theta(p)\,B^{\dagger}(p,s)\,D^{\dagger}(-p,s)\right]|0\rangle \tag{12}$$

and the quark fields are expressed in terms of q-deformed creation and annihilation operators as

$$\psi_q(x,0) = \sum_s \int \frac{d^3p}{(2\pi)^3}\left[B(p,s)u(p,s)e^{ip\cdot x} + D^\dagger(p,s)v(p,s)e^{-ip\cdot x}\right]. \quad (13)$$

The q-deformed quark and anti-quark creation and annihilation operators B, $B^\dagger$, D, and $D^\dagger$, are expressed in terms of the non-deformed ones according to Eqs. (10) and (11)

$$B_- = b_-\left(1 + Qb_+^\dagger b_+\right), \quad B_-^\dagger = b_-^\dagger\left(1 + Qb_+^\dagger b_+\right), \quad (14)$$

$$D_- = d_-\left(1 + Qd_+^\dagger d_+\right), \quad D_-^\dagger = d_-^\dagger\left(1 + Qd_+^\dagger d_+\right), \quad (15)$$

$$B_+ = b_+, \quad B_+^\dagger = b_+^\dagger, \quad (16)$$

$$D_+ = d_+, \quad D_+^\dagger = d_+^\dagger, \quad (17)$$

(in the above equations we simplified the notation: $B(p,s) \to B_s$, $b(p,s) \to b_s$, etc.). We would like to stress that, as discussed in Ref. [8], the deformed vacuum differs from the non-deformed one only by a phase and, therefore, the effects of the deformation comes solely from the modified field operators. Additionally, the q-deformed NJL Lagrangian, constructed using ψ_q instead of ψ, is invariant under the quantum group $SU_q(2)$ transformations. This can be seen by using the two-dimensional representation of the $SU_q(2)$ unitary transformation given in Ref. [6].

The deformed gap equation is

$$m = -2G\langle\bar{\psi}\psi\rangle_q, \quad (18)$$

where $\langle\bar{\psi}\psi\rangle_q$ is the q-deformed condensate calculated using the BCS-like vacuum, Eq. (12), and Eq. (13),

$$\langle\bar{\psi}\psi\rangle_q = \langle NJL|\bar{\psi}_q\psi_q|NJL\rangle = \langle\bar{\psi}\psi\rangle + \langle NJL|\mathscr{O}|NJL\rangle, \quad (19)$$

where $\langle\bar{\psi}\psi\rangle$ is the non-deformed condensate and $\langle NJL|\mathscr{O}|NJL\rangle$ represents all non-vanishing matrix elements arising from the q-deformation of the quark fields. The contribution of these q-deformed matrix elements is

$$\langle NJL|\mathscr{O}|NJL\rangle = Q\int \frac{d^3p}{(2\pi)^3}\left[\sin 2\theta(p) - \sin 2\theta(p)\cos 2\theta(p)\right]. \quad (20)$$

The calculation of the deformed condensate will be performed in a similar way as in the usual case [10]. It requires also a regularization procedure since the NJL interaction is not perturbatively renormalizable. For reasons of simplicity a non-covariant trimomentum cutoff is applied arising

$$\langle\bar{\psi}\psi\rangle_q = -\frac{3m}{\pi^2}\left[\left(1 - \frac{Q}{2}\right)\int_0^\Lambda dp\,\frac{p^2}{\sqrt{p^2+m^2}} + \frac{Q}{2}\int_0^\Lambda dp\,\frac{p^3}{p^2+m^2}\right] \quad (21)$$

for each quark flavor. At this point we see that the dynamical mass is again given by a self-consistent equation since the condensate depends also on the mass. Inserting Eq. (21) into Eq. (18) we obtain the deformed NJL gap equation

$$m = \frac{2Gm}{\pi^2}\left[\left(1 - \frac{Q}{2}\right)\int_0^\Lambda dp\,\frac{p^2}{\sqrt{p^2+m^2}} + \frac{Q}{2}\int_0^\Lambda dp\,\frac{p^3}{p^2+m^2}\right]. \quad (22)$$

It is easy to see that for $Q = 0$ ($q = 1$), we recover the NJL gap equation in its more familiar form

$$m = \frac{2Gm}{\pi^2}\int_0^\Lambda dp\,\frac{p^2}{\sqrt{p^2+m^2}} + m_0, \quad (23)$$

where m_0 appears only if we consider the current quark mass term $\mathscr{L}_{\text{mass}} = -m_0\bar{\psi}\psi$ in the NJL Lagrangian Eq. (4).

The pion decay constant is calculated from the vacuum to one pion axial vector current matrix element, which, in the simple 3D non-covariant cutoff we are using [9], is given by

$$f_\pi^2 = \int_0^\Lambda \frac{d^3p}{(2\pi)^3}\,\frac{1}{\left(p^2+m^2\right)^{3/2}}, \quad (24)$$

for each quark color. The deformed calculation of f_π is performed directly by substituting the dynamical mass in Eq. (24) from the one obtained in Eq. (22), instead of deforming the axial current in the calcula-

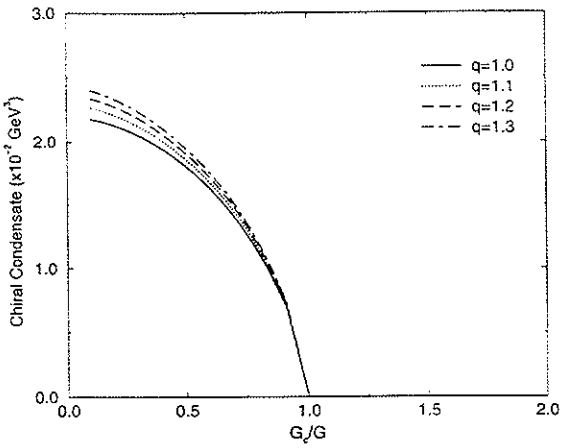

Fig. 1. Behavior of the phase transition for different values of q. The non-deformed situation corresponds to $q = 1$. In all curves $\Lambda = 600$ MeV and $m_0 = 0$.

tion of its matrix element of between the vacuum and the one pion state.

As in the non-deformed case, the q-gap equation has non-trivial solutions when the coupling G exceeds a critical value G_{crit} related to the cutoff. Fig. 1 depicts the sharp phase transition at $G = G_{\text{crit}}$ separating the Wigner-Weyl and Nambu-Goldstone phases, corresponding to different realizations of chiral symmetry.

Fig. 1 also shows the deformed condensate values as a function of q. We can see the enhancement of the condensate's value, due to presence of the q-deformation. The dynamical mass is accordingly modified through the deformed gap equation (22), as can be seen in Table 1, along with the corresponding values of the pion decay constant, f_π. The behavior of the condensate around the critical coupling, G_c, is similar for both deformed and non-deformed cases, meaning that the adopted procedure to q-deform the underlying $su(2)$ algebra in a two flavor NJL model does not change the behavior of the phase transition around G_c. Table 2 presents the behavior of the coupling constant for two typical dynamical mass values for different q's. The analysis of this table shows that the coupling constant G decreases with q, for a given value of the dynamical mass, meaning that to acquire a given mass we need a weaker coupling when the algebra is deformed. This indicates that the deformation of the $su(2)$ algebra incorporates effects the NJL interaction which are propagated to the physical quantities such as the condensate, the dynamical mass and the pion decay constant. The formalism developed in Refs. [6,8] allow q-values smaller than one (which corresponds to $Q > 0$). It is worth to mention that in this case the q-deformation effect goes in the opposite direction, namely, the condensate value and the dynamical mass decrease for $q < 1$.

To summarize, the main objective of this work was to analyze the influence of the q-deformation in the NJL model. We studied the deformation of the underlying $su(2)$ algebra in a two flavor version of the model and investigated an important feature of the $su(2)$ chiral symmetry breaking, namely the dynamical mass generation, through the incorporation of helicity non-conserving terms directly in the fermionic operators. The main effect of the q-deformation is to effectively enhance the coupling strength of the NJL four fermion interaction, leading to an increasing in the value of the quark condensate. The dynamical mass, which is related to the presence of the condensate, is correspondingly increased. We also looked closely at the behavior of the phase transition around the critical point, which is still sharp, meaning that the new contributions arising from the deformation of the condensate do not play the role of explicit chiral symmetry breaking terms [10].

Table 1
Mass and f_π for different values of q, for $\Lambda = 600$ MeV, $G_c = 4.57$ GeV^{-2}, and $G = 6.53$ GeV^{-2}. The condensate was calculated for two flavors and three colors

	$q = 1.0$	$q = 1.1$	$q = 1.2$	$q = 1.3$
Mass [MeV]	365	375	384	392
f_π [MeV]	92.0	92.4	92.9	93.3

Table 2
Behavior of the coupling constant G at given values of the dynamical mass for different values of q. Cutoff and critical coupling are the same as in Table 1

Mass [MeV]	$q = 1.0$	$q = 1.1$	$q = 1.2$	$q = 1.3$
300	6.04	5.98	5.94	5.90
350	6.42	6.35	6.28	6.23

Acknowledgements

The authors are grateful to D. Galetti and B. M. Pimentel for helpful discussions. V. S. T. would like to acknowledge Fundação de Amparo à Pesquisa do Estado de São Paulo (FAPESP) for financial support and M. Malheiro for very helpful discussions concerning the q-deformation in the NJL model.

References

[1] Y. Nambu, G. Jona-Lasinio, Physical Review 122 (1961) 345.
[2] For a review on some aspects of q-deformed algebras applications see: D. Galetti, J.T. Lunardi, B.M. Pimentel, C.L. Lima, in: V.C. Aguillera-Navarro, D. Galetti, B.M. Pimentel, L. Tomio (Eds.), Topics in Theoretical Physics, Proc. Theoretical Symposium in honor of Paulo Leal Ferreira, pp. 227–239, IFT, 1995, and references therein.
[3] D. Galetti, B.M. Pimentel, An. Acad. Bras. Ci. 67 (1995) 7; S.S. Avancini, A. Eiras, D. Galetti, B.M. Pimentel, C.L. Lima, J. Phys. A: Math. Gen. 28 (1995) 4915; D. Galetti, J.T. Lunardi, B.M. Pimentel, C.L. Lima, Physica A 242 (1997) 501.
[4] J. Dey, M. Dey, P.L. Ferreira, L. Tomio, Phys. Lett. B 365 (1996) 157; A. Delfino, J. Dey, M. Malheiro, Phys. Lett. B 348 (1995) 417.
[5] F. Iachello, in: P. Drayer and, J. Janecke (Eds.), Group Theory and Special Symmetries in Nuclear Physics, Proc. International Symposium in Honor of K.T. Hecht, pp. 211–218, World Scientific, Singapore, 1992; B.E. Palladino, P.L. Ferreira, Nuovo Cimento A 110 (1997) 303.
[6] M. Ubriaco, Phys. Lett. A 219 (1996) 205.
[7] P. Ring, P. Schuck, The Nuclear Many-Body Problem, Springer Verlag, New York, 1980.
[8] L. Tripodi, C.L. Lima, Phys. Lett. B 412 (1997) 7.
[9] S.P. Klevansky, Reviews of Modern Physics 64 (1992) 649.
[10] U. Vogl, W. Weise, Prog. Part. Nucl. Phys. 27 (1991) 195.